

LOUGHBOROUGH
UNIVERSITY OF TECHNOLOGY
LIBRARY

AUTHOR

HAWLEY, B. J.

COPY NO.

061508/02

VOL NO.

CLASS MARK

ARCHIVE
COPY

FOR REFERENCE ONLY

THE EFFECT OF 4-SUBSTITUTION
ON SOME PROPERTIES OF THE
O-H BOND IN 1-NAPHTHOLS

by

BERNARD JOEL HAWLEY

A DOCTORAL THESIS SUBMITTED IN PARTIAL FULFILMENT
OF THE REQUIREMENTS FOR THE AWARD OF

DOCTOR OF PHILOSOPHY

OF THE LOUGHBOROUGH UNIVERSITY OF TECHNOLOGY

SUPERVISORS:

PROFESSOR R.F. PHILLIPS, DEPARTMENT OF CHEMISTRY,
LOUGHBOROUGH UNIVERSITY.

DOCTOR D.A. IBBITSON, DEPARTMENT OF CHEMISTRY,
DERBY COLLEGE OF ART & TECHNOLOGY.

DERBY COLLEGE OF
ART AND TECHNOLOGY

MARCH
1974

© BY BERNARD JOEL HAWLEY, 1974

Loughborough University
of Technology Library

Date 30 MAY 1974

Class

Acc.

No.

061508/02

SUMMARY

The effects of 4-substitution on some of those properties of the OH bond in 1-naphthols which reflect its hydrogen bonding tendency have been studied. The properties investigated were the near infrared OH stretching frequencies in cyclohexane and dioxan solutions, the association constant of complex formation with dioxan and the affinity of adsorption at an activated alumina/solution interface.

A series of 4-substituted-1-naphthols has been prepared and comparisons in behaviour with 4-substituted phenols have been made throughout.

Investigation of the solution phase included measurements of the OH stretching frequencies in both cyclohexane and dioxan solution. The frequency shift, $\Delta\nu$, upon change of solvent has been found to vary linearly with appropriate Hammett σ substituent constants derived from a series of 4-substituted-1-naphthoic acids and reported in the literature.

Absorbance measurements made in the ultraviolet have been used in calculating hydrogen bonding association constants of the naphthols to dioxan in cyclohexane solution at both 25°C and 35°C. The enthalpy changes on association, ΔH^\ominus , have been determined from the temperature coefficients of the association constants and although variation was small a continuous decrease was shown with increasing σ value. Free energy changes, ΔG^\ominus , and entropy changes, ΔS^\ominus , have also been estimated and show similar trends. Enthalpy changes, rather than entropy changes, seemed to be responsible for the magnitude of the free energy changes.

Studies at the alumina-solution interface have included a characterisation of the adsorbent surface by low temperature argon adsorption, vapour phase adsorptions of cyclohexane and dioxan and quantitative dehydration experiments. The adsorption characteristics of 1-naphthol from various solvents have been investigated and those of 4-substituted-1-naphthols from dioxan. The results have been analysed by application of a thermodynamic equation derived by Everett on the basis of an ideal adsorption system: Although parameters calculated from the equation once again showed correlation with σ values, in those systems where adsorption of solvent was extensive large departures from ideality have been found and Everetts model proved inappropriate.

CONTENTS

<u>INTRODUCTION</u>	<u>Page</u>
(A) THE ASSESSMENT OF ELECTRONIC EFFECTS IN ORGANIC MOLECULES	3
(B) INTERACTIONS IN THE LIQUID PHASE	15
(C) INTERACTIONS AT THE SOLID-SOLUTION INTERFACE	30
(D) THERMODYNAMICS OF ADSORPTION AT THE SOLID-SOLUTION INTERFACE	42
(E) THE PRESENT INVESTIGATION	56
 <u>EXPERIMENTAL</u>	
(A) ASSOCIATION IN SOLUTION	
1. Group Stretching Frequency in the Infrared	58
2. Association Constants	61
(B) ADSORPTION STUDIES	
1. Adsorption at the Gas-solid Interface :	
Characterisation of the Alumina	80
(a) Structure	81
(b) Surface Area	93
2. Adsorption at the Solution-solid Interface	
(a) Adsorption of 1-Naphthol	120
(b) Adsorption of 4-Substituted-1- Naphthols	133

DISCUSSION OF RESULTS

(A)	ASSOCIATION IN SOLUTION	142
1.	The Association Constant	148
2.	Changes in Thermodynamic Functions upon Association	155
(B)	ADSORPTION ON ALUMINA	
1.	The Sorbent	160
2.	Adsorption of Organic Vapours	168
3.	Adsorption at the Solution-solid Interface	172
(a)	The Adsorption of 1-Naphthol from Various Solvents	177
(b)	The Adsorption of 4-Substituted-1- Naphthols from Dioxan Solution	193

APPENDIX

PREPARATION AND PURIFICATION OF SOLVENTS AND SOLUTES	201
---	-----

<u>REFERENCES</u>	207
-------------------	-----

ACKNOWLEDGEMENTS

I am indebted to Professor R.F. Phillips, my Supervisor at the Loughborough University of Technology, for his support in presenting this work and for the interest he has always shown.

Thanks are also due to Mr. M.S.J. Twiselton, Head of the Department of Chemistry and Materials Science at Derby College of Art and Technology, for providing research facilities and to the Governors of the Derby College for their award of a Research Assistantship.

I would like to thank Mrs. Ann Marshall for her patient decyphering and consummate typing of the MS.

Finally, I wish to acknowledge my debt and gratitude to Dr. D.A. Ibbitson, my Supervisor at Derby, for his suggestion of the topic, for his counsel and encouragement throughout the course of the investigation and for the benefit of his invaluable experience in preparing this thesis.

B.J.H.

DERBY
MARCH, 1974

DECLARATION

The experimental work described in this thesis is original and has been carried out by the author in the chemical laboratories of the Derby College of Art and Technology.

INTRODUCTION

In this study of various properties of the OH group in 4-substituted-1-naphthols, solute-solvent interactions in the liquid phase are discussed and then the consequences of presenting such a binary solution to an alumina surface. Finally, the thermodynamics of the solution-solid interface are considered. But before patterns of behaviour can be collated and inferences drawn, some overall procedure for comparison of reactivities has to be established and the first part of the Introduction presents the parameter employed for this purpose in the Discussion of Results.

(A) THE ASSESSMENT OF ELECTRONIC EFFECTS IN ORGANIC MOLECULES

Careful scrutiny of the chemical properties of organic molecules reveals regular patterns of behaviour, and a study of these has led to the recognition of general electronic effects in organic systems. Such principles as the inductive and mesomeric effects can be usefully applied to predict the chemical properties of a compound, although when different effects are opposed in the same molecule the problem of predominance of one effect over another may well fail to be resolved by qualitative discussion. It would thus be invaluable to have a quantitative assessment of these effects, or of their resultant effect, whence the extent and speed of a compound's interaction with its chemical environment (i. e. its reactivity) could be accounted for and even predicted. Further, real deviations from expected behaviour might indicate the incursion of factors previously not recognised or changes in reaction mechanism.

Before a meaningful study of real systems can be commenced it is necessary to establish a framework of reference by consideration of theoretical concepts. It is reasonable to postulate that the reactivity of a substance in a particular environment is related to the thermodynamic free energy change for the reaction in question, or, more conveniently, the standard free energy change. A discussion on reactivity may be centred on three variables: (a) the substrate structure, (b) the reagent structure, and (c) the reaction medium.

A substrate may be considered to be composed of a reactive group (i. e. the reaction 'site') Q, an influential substituent group X and an inert, non-influential linking group R. When a reaction of such a substrate (X-R-Q) is postulated the calculated standard free energy change, ΔG^\ominus , for the desired reaction indicates whether the reaction is spontaneous or not (sign) and is a measure of the tendency of the process to occur (magnitude). Thus the ΔG value for the prevailing conditions could be taken as a measure of reactivity.

All reactions may be regarded as equilibria, albeit many are heavily weighted ones, and in general a reaction may be represented:



and could be assigned a standard free energy change $\Delta G^{A\ominus}$. It is proposed that the reactivity of the substrate be considered a function of the free energy change which in turn will be a function of a number of variables:

$$\Delta G^{A\ominus} = f(x, y, z, \dots) \quad (2)$$

where x, y, z, ... are independent variables.

In general, as X changes

$$\begin{aligned} d(\Delta G^{A\ominus}) = & \left(\frac{\partial \Delta G^{A\ominus}}{\partial x} \right)_{y, z, \dots} \cdot dx + \left(\frac{\partial \Delta G^{A\ominus}}{\partial y} \right)_{x, z, \dots} \cdot dy + \\ & \left(\frac{\partial \Delta G^{A\ominus}}{\partial z} \right)_{x, y, \dots} \cdot dz \dots \dots \dots \end{aligned} \quad (3)$$

If one variable only, x, varies (y, z, ... remaining constant),

then

$$d(\Delta G^{A\ominus}) = \left(\frac{\partial \Delta G^{A\ominus}}{\partial x} \right)_{y, z, \dots} \cdot dx \quad (4)$$

Further, if x varies with X and $\Delta G^{A\ominus}$ is a linear function of x so that

$$\left(\frac{\partial \Delta G^{A\ominus}}{\partial x}\right)_{y,z,\dots} = \text{constant and } \left(\frac{\partial^2 \Delta G^{A\ominus}}{\partial x^2}\right)_{y,z,\dots} = 0,$$

then Equation (4) can be integrated:

$$\int_{\Delta G_1^{A\ominus}}^{\Delta G_2^{A\ominus}} d(\Delta G^{A\ominus}) = \int_{x_1}^{x_2} \left(\frac{\partial \Delta G^{A\ominus}}{\partial x}\right)_{y,z,\dots} \cdot dx \quad (5)$$

where the variable x has the value x_1 for substituent X_1 and the standard free energy change $\Delta G_1^{A\ominus}$ and the variable x has the value x_2 for substituent X_2 and the standard free energy change $\Delta G_2^{A\ominus}$.

Equation (5) can thus be written

$$\Delta G_2^{A\ominus} - \Delta G_1^{A\ominus} = \left(\frac{\partial \Delta G^{A\ominus}}{\partial x}\right)_{y,z,\dots} \cdot (x_2 - x_1) \quad (6)$$

The left-hand side of Equation (6) is a measure of the change in 'reactivity' upon replacing X_1 by X_2 and can be made more useful by substituting

$$\Delta G^{A\ominus} = -RT^A \ln K^A$$

where K^A is the equilibrium constant for reaction (1) above.

$$\text{Then } \Delta G_2^{A\ominus} - \Delta G_1^{A\ominus} = -RT^A \left[\ln K_2^A - \ln K_1^A \right] \quad (7)$$

and substituting in Equation (6) gives

$$-RT^A \ln \left(\frac{K_2^A}{K_1^A} \right) = \left(\frac{\partial \Delta G^{A\ominus}}{\partial x}\right)_{y,z,\dots} \cdot (x_2 - x_1) \quad (8)$$

Unfortunately, Equation (8) contains three inaccessible quantities on the right-hand side, but it does enable $(x_2 - x_1)$ to be defined:

$$(x_2 - x_1) = - \frac{RT^A \ln(K_2^A / K_1^A)}{\left(\frac{\partial \Delta G^A}{\partial x}\right)_{y,z,\dots}} \quad (9)$$

To make further progress a new reaction series ('B') must now be considered with new equilibrium constants (K^B) and standard free energy changes ($\Delta G^{B\ominus}$) but employing the same series of substituents X_1, X_2, \dots etc. :-



Again, an equation similar to Equation (6) can be derived:

$$\Delta G_2^{B\ominus} - \Delta G_1^{B\ominus} = \left(\frac{\partial \Delta G^{B\ominus}}{\partial x}\right)_{y,z,\dots} \cdot (x_2 - x_1) \quad (11)$$

assuming that x_1 and x_2 are solely determined by X_1 and X_2 .

Equation (8) now becomes

$$-RT^B \ln \left(\frac{K_2^B}{K_1^B}\right) = \left(\frac{\partial \Delta G^{B\ominus}}{\partial x}\right)_{y,z,\dots} \cdot (x_2 - x_1) \quad (12)$$

Substituting for the unknown $(x_2 - x_1)$ from Equation (9) Equation (12) becomes

$$\begin{aligned} -RT^B \ln \left[\frac{K_2^B}{K_1^B}\right] &= \frac{\left(\frac{\partial \Delta G^{B\ominus}}{\partial x}\right)_{y,z,\dots}}{\left(\frac{\partial \Delta G^A}{\partial x}\right)_{y,z,\dots}} \times \\ &\left[-RT^A \ln \left(\frac{K_2^A}{K_1^A}\right)\right] \end{aligned} \quad (13)$$

and upon rearranging Equation (13) becomes

$$\log \left(\frac{K_2^B}{K_1^B}\right) = \frac{T^A \cdot \left(\frac{\partial \Delta G^{B\ominus}}{\partial x}\right)_{y,z,\dots}}{T^B \cdot \left(\frac{\partial \Delta G^A}{\partial x}\right)_{y,z,\dots}} \times \log \left(\frac{K_2^A}{K_1^A}\right) \quad (14)$$

To give practical significance to Equation (14) the second arbitrary standard must be introduced. Since x_1 and x_2 cannot be defined in absolute terms, reactions of X_1 RQ, X_2 RQ, X_3 RQ etc. with reagent A (as in reaction (1)) are adopted as a standard reference reaction series. Further, to overcome the difficulty in quantifying the partial differentials, x_1 and x_2 it is convenient to define a 'relative reactivity' thus:

$$\text{relative reactivity of } X_2\text{RQ} = \log\left(\frac{K_2^A}{K_1^A}\right) \quad (15)$$

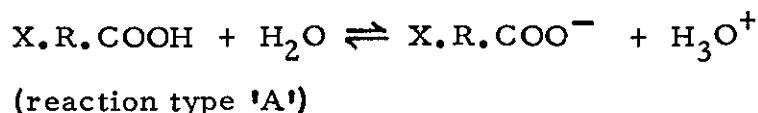
thus effectively making substituent X_1 a standard reference substituent.

$$\begin{aligned} \text{Equation (14) may now be expressed more simply :-} \\ \text{(Relative reactivity of } X_2\text{R}^1\text{Q}^1 \text{ in reaction type B)} \\ = \text{a constant X (relative reactivity of } X_2\text{RQ} \\ \text{in standard reaction A)} \end{aligned} \quad (16)$$

It will be noted that the constant is independent of the magnitude of x and that the relative reactivity of X_2 RQ in series A is independent of series B, since, from Equation (9),

$$\log\left(\frac{K_2^A}{K_1^A}\right) = \frac{-(x_2 - x_1)\left(\frac{\partial \Delta G^A}{\partial x}\right)_{y,z,\dots}}{2.303 RT^A}$$

Hammett^{1,2} investigated free energy relationships for families of aromatic organic compounds and took as a standard reaction series the dissociation of aromatic organic acids in water:



and discovered that plots corresponding to $\log K_2^B$, $\log K_3^B$ etc. against $\log K_2^A$, $\log K_3^A$ etc. were linear. This led him to put forward the empirical relationship known as the Hammett Equation:

$$\log \left(\frac{K}{K_0} \right) = \rho \sigma \quad (17)$$

where K was an equilibrium constant for a substituted compound,
 K_0 for the unsubstituted compound (i. e. $X_1 \equiv H$),
 ρ was a variable dependent upon the type of reaction series
only,

σ was a variable dependent upon the substituent only.

Comparison of the empirical Hammett equation (17) with
Equation (14) shows close similarities but it should be noted that a
number of conditions were made in deriving Equation (14) and these
are also likely to be binding on empirical relationships such as
Hammett's, viz:

- (a) the effect that a substituent, X , has upon the reactivity
(and therefore free energy change) of a substrate
molecule can be represented quantitatively by a
variable x acting via an unspecified mechanism.
- (b) when a substituent is changed in a substrate molecule
the change in free energy in a particular reaction is
brought about by a change in x only, and in no other
variable
- (c) a linear free energy relationship with x exists, that is

$$\Delta G^\ddagger = \alpha \cdot x + \beta \quad \text{where } \alpha \text{ and } \beta \text{ are constants,}$$

so that $\frac{\partial \Delta G^\ddagger}{\partial x} = \alpha$ and $\frac{\partial^2 \Delta G^\ddagger}{\partial x^2} = 0$.

With regard to these points it must be emphasized that it is
not yet possible to estimate the effects of substituents by a priori
quantum mechanical calculations, Empirical parameters must be
admitted to describe the effects of substituents and the corresponding

response of a reaction centre, and such simplified approaches will inevitably prove inexact. For example, the form of the Hammett equation clearly requires that there be no direct interaction (i. e. mutual conjugation³) between the reaction centre and the substituent; such interactions if they occur will produce variable effects in different substituents so that their relative efficacy can no longer be expressed in terms of single fixed σ constants. A possible solution is to add a second term to the Hammett equation i. e.

$$\log\left(\frac{K}{K_0}\right) = \rho\sigma + \rho^1\sigma^1 \quad (18)$$

where ρ^1 is a new constant measuring the sensitivity of the reaction centre to mutual conjugation and σ^1 is a corresponding measure of the conjugative power of the substituent. Relations of this type have been proposed⁴ but they suffer from the disadvantage of requiring even more parameters than the original approach and as the number of parameters multiplies their physical meaning rapidly dwindles into obscurity.

The basic interactions between a substituent and an adjacent substrate are of two kinds : inductive and mesomeric. Since these effects cannot yet be calculated theoretically two empirical factors must be accepted for each substituent and a further two are needed for each reaction centre to allow for its general response to polarisation of the substrate by the substituent and for its special response to mutual conjugation; this approach already demands a large number of empirical parameters which must be kept to a minimum if the treatment of substituents is to be meaningful.

Taft et al^{5,6} have tried to subdivide the effects of substituents in benzene nuclei into inductive and mesomeric parts by

making arbitrary assumptions concerning the relative efficiency of transmission of electronic effects to the positions meta and para to the substituent. However, they could draw no valid conclusions about the manner in which substituent effects were transmitted across a molecule and their treatment could not be extended to other molecules, e.g. naphthalene, without introducing numerous additional parameters.

There are at least five distinct processes by which substituents can affect a distant reaction centre. Three of these are initiated by the polarity of the bond linking the substituent to the substrate (i. e. the primary inductive effect) and two by the resonance interactions between them (i. e. the mesomeric and electro-meric effects):

- (a) the electric dipole field of the polar substituent-substrate bond can influence the reaction centre across space (the 'field effect'),
- (b) the primary inductive effect can be transmitted to the reaction centre by successive polarisation of intervening σ -bonds (σ - inductive effect),
- (c) the electrostatic charge set up at a conjugated atom adjacent to the substituent may polarise the corresponding π - electron system (the inducto-electromeric⁷ or π - inductive⁸ effect); the resulting charges set up on the π - electron system can influence the reaction centre either by a field effect or by secondary polarisation of intervening σ -bonds,
- (d) the π - electron system can also be polarised by resonance interactions with the substituent (the mesomeric effect),

- (e) there may be mutual conjugation³ between the substituent and the reaction centre through an intervening conjugated system (the electromeric effect).

Whilst the variation of each effect with distance can be estimated, at least to a first approximation, the absolute importance of the various effects in any given case cannot be estimated theoretically. It is therefore essential to have extensive data for the effects of substituents in a variety of ring systems, the substituents being at varying distances from the reaction centre: reports of data of this kind in the literature are unfortunately scarce.

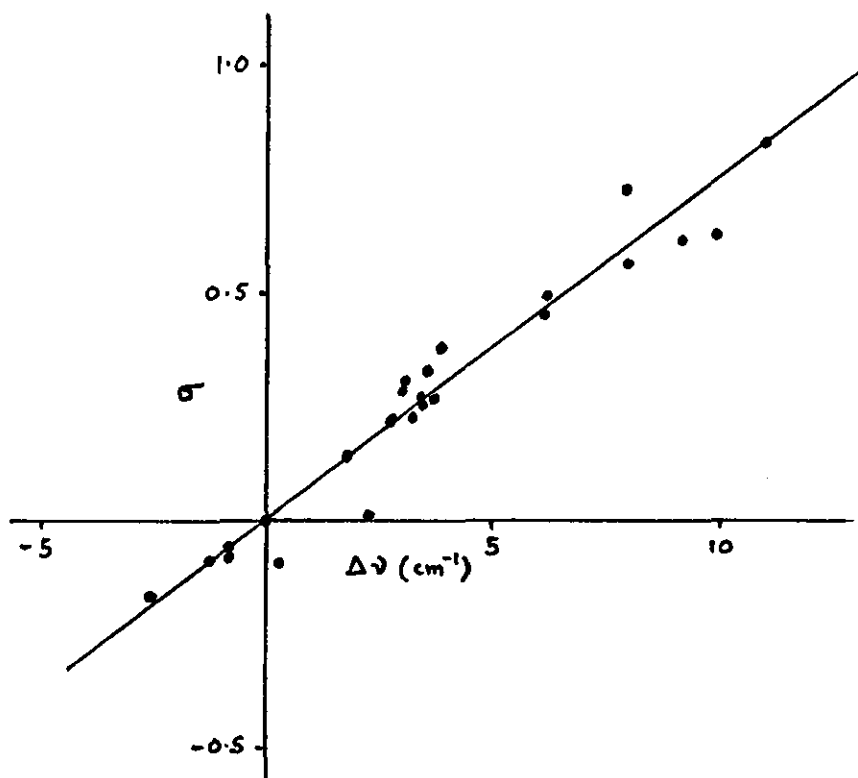
Dewar and Grisdale⁹ have carried out an investigation of substituent effects in the naphthalene aromatic system. Their standard substituent was hydrogen and their standard reaction was the dissociation of substituted 1-naphthoic acids in a partially aqueous medium. They measured pK values in 50:50 v/v ethanol/water solvent and the value for the reaction parameter, ρ , was taken as that assigned for the benzoic acids in the same solvent mixture (1522)¹⁰. Experimental σ values for naphthalene derivatives are compared with those for the corresponding benzene analogues in Table 1.

TABLE 1 : EXPERIMENTAL σ CONSTANTS

<u>4-Substituent</u>	<u>Benzene Deriv.</u> ¹⁰	<u>1-Naphthalene Deriv.</u> ⁹
NO ₂	0.778	0.86
CN	0.628	0.79
Br	0.232	0.30
Cl	0.227	0.26
H	0	0
CH ₃	-0.170	-0.14
C(CH ₃) ₃	-0.197	/

Dewar and Grisdale proceeded to measure shifts in the infrared carbonyl stretching frequencies of the methyl esters of substituted 1-naphthoic acids and a plot of these ($\Delta\nu$) against appropriate values of σ for the position and nature of the substituent is shown in Fig. 1.⁹

Fig. 1



From their work the authors conclude that of the five effects described earlier only the field, the π - inductive and the mesomeric effects make a recognisable contribution to the overall substituent effect and attempt to quantify them by relationships of the kind shown in Equations (19) and (20).

$$\sigma_{ij} = F/r_{ij} + Mq_{ij} \quad (19)$$

$$\text{or } \sigma_{ij} = F^1/r_{ij} - M^1\pi_{ij} \quad (20)$$

where σ_{ij} : the substituent constant for a substituent at carbon atom i and reaction centre at j,

F or F^1 : a measure of the field set up by the substituent,

M or M^1 : a measure of the combined π - inductive and mesomeric effect of the substituent,

r_{ij} : the distance between carbon atoms i and j,

π_{ij} : the atom-atom polarisability of atoms i and j,

q_{ij} : the formal charge at position j produced by attaching the group $-\text{CH}_2^-$ at position i.

F, M or F^1, M^1 can be found for a given substituent from σ_{meta} and σ_{para} for benzene derivatives and σ constants for any other system can then be calculated from Equation (19) or (20). The quantities q_{ij} can be calculated by the method of Longuet-Higgins¹¹ who tabulated values for a number of systems and values for atom-atom polarisabilities for all the common ring systems have been estimated.¹² Some calculated σ values are shown in Table 2 and may be compared with experimental values in Table 1.

TABLE 2 : σ Constants Calculated by FM (F^1M^1)
Methods for Naphthalene Derivatives

Substituent	σ_{41} (FM)	$\sigma_{41}^{(F^1M^1)}$
NO ₂	0.84	0.84
CN	0.73	0.72
Br	0.19	0.19
Cl	0.19	0.20
CH ₃	-0.21	-0.21

The above treatment is limited to examples where mutual conjugation is unimportant and to reactions where the substrate to which the substituent is attached undergoes no drastic reorganisation. These are the conditions prevailing in this study and must be met if the Hammett equation is to hold good. Failing this, the more general equation

$$\log (K/K_0) = \rho\sigma + \rho^1\sigma^1 \quad (18)$$

must be used in which ρ^1 and σ^1 are measures of the response of the reaction centre and substituent to mutual conjugation.

In the above treatment σ^1 would be given approximately by

$$\sigma_{ij}^1 = E_{q_{ij}} \quad \text{or} \quad \sigma_{ij} = E^1\pi_{ij}$$

where the electromeric parameters E and E^1 could be determined empirically from data for benzene compounds.

(B) INTERACTIONS IN THE LIQUID PHASE

That the extremes of perfect chaos and perfect order lend themselves to relatively simple mathematical expression is demonstrated by the respectably advanced theories of gases and crystals. The liquid phase, however, portraying a peculiar and shifting compromise between order and disorder has yielded less readily to a quantitative description. The cohesive forces are sufficiently strong to support a condensed state but not strong enough to preclude a considerable translational energy of the individual molecules, introducing disorder without completely sacrificing a regularity of structure. The forces between particles in the liquid phase are ultimately electrostatic in origin and where no discrete ions are involved (as in this study) may result from :

- permanent dipole - permanent dipole interactions,
- permanent dipole - induced dipole interactions, and
- induced dipole - induced dipole interactions

collectively known as van der Waals forces.

In a dilute binary solution interactions occur between solvent molecules and between solvent and solute molecules and in nature may be related to dispersion, charge transfer, hydrogen bonding effects etc. Since the dominant effect in the circumstances encountered in this study is hydrogen bonding discussion is largely restricted to this phenomenon.

The Solvent Effect

It is widely recognised that properties of solutions are dependent upon the nature of the solvent and so an impartial

assessment of its influence is an invaluable aid. One of the most satisfactory parameters representing solvent reactivity is the E_T function of Dimroch, Reichardt, Siepmann and Bohlmann.¹³ This parameter is determined experimentally from the position of the absorption band of solutions of pyridinium N-phenolbetaine in the visible region of the spectrum and is given by

$$E_T \text{ (kJ mol}^{-1}\text{)} = 1.195 \times 10^5 / \lambda_{\text{max}}$$

where λ_{max} is the wavelength of maximum absorption in nm. The stronger the stabilising effect of the solvent on the ionic ground state of the standard dye compared with that of the less polar excited state, the higher the energy of the electron transition and the lower the wavelength of the absorption band. Thus increasing E_T value represents increasing interaction between the solvent and the standard compound, pyridinium N-phenolbetaine, and so provides a measure of solvent reactivity.

Other spectroscopic measures of solvent reactivity reported recently are the $\Delta\nu_D$ and $\Delta\nu_A$ functions. Kagiya et al¹⁴ have measured the infrared frequency of the O-D or C=O vibrational bands of monodeuteriomethanol or acetophenone, respectively, in various solvents. Taking benzene as a standard they have used the frequency shift as a measure of electron-donating power, $\Delta\nu_D$, and electron-accepting power, $\Delta\nu_A$, respectively, of a given solvent. For an homologous series Kagiya found that the electron-donating power as measured by $\Delta\nu_D$ decreased with an increase in the ionisation potential in the gaseous phase or with an increase in the pK_b value in the liquid phase. Similar correlations were obtained when considering $\Delta\nu_A$.

Solute-Solvent Interactions in Solution

Since the initial work of Benesi and Hildebrand¹⁵ on donor-acceptor interactions in solution, there has been considerable theoretical and experimental interest in the nature of these and other non-ionic complexes. Mulliken¹⁶ considered that such complexes arise from a Lewis acid-base type of interaction, the bond between the components of the complex resulting from partial transfer of a π electron from the base to an orbital of the acid. He termed the compounds formed from this type of transfer 'charge transfer complexes'.

Slight overlap of orbitals of adjacent molecules is of general occurrence giving rise to very weak interactions, but if one of the atoms involved is a hydrogen atom attached to a strongly electronegative atom in the same molecule and the other atom is a strongly electronegative atom in a different molecule then owing to the unique size and disposition of the hydrogen atom the interaction is now of unusual strength and is well characterised as a weak chemical bond : the hydrogen bond. In this study hydrogen bonds of the type O-H.....O are exclusively investigated and the following have been suggested as contributory structures :¹⁷

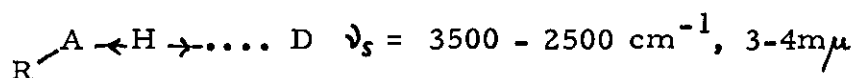
- (1) $\text{—O—H} \quad \text{O}=\text{}$ covalent, no charge transfer
- (2) $\text{—O}^- \quad \text{H}^+ \quad \text{O}=\text{}$ ionic, no charge transfer
- (3) $\text{—O}^+ \quad \text{H}^- \quad \text{O}=\text{}$ ionic, no charge transfer
- (4) $\text{—O}^- \quad \text{H—}\overset{+}{\text{O}}=\text{}$ charge transfer, long H-O bond
- (5) $\text{—O—}\overset{-}{\text{H}}\text{—}\overset{+}{\text{O}}=\text{}$ charge transfer, O-O bonding

A hydrogen bond of the type A-H.....D exists when (a) there is evidence of bond formation and (b) there is evidence that this bond

specifically involves the hydrogen atom already bonded to A. In fulfilment of condition (a) all the methods for detecting chemical bonds have been cited as providing evidence for hydrogen bonds: cryoscopic, vapour pressure, vapour density measurements are typical. Demonstration of condition (b) usually depends upon spectroscopic and diffraction data. Hydrogen bonding is accompanied by some or all of the following measurable effects:

(1) Changes occur in the vibrational spectra of A-H and D:

(a) the frequency of the A-H stretching mode decreases

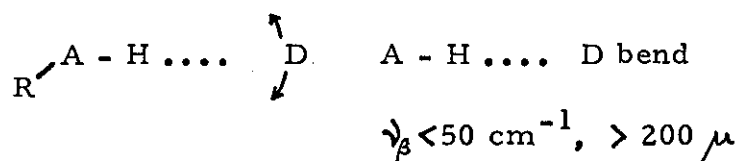
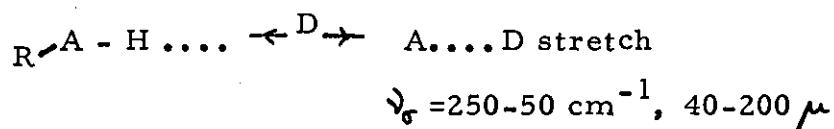


(b) the band width of the A-H stretching mode increases

(c) the intensity of the A-H stretching mode increases

(d) the frequencies of the A-H deformation modes increase

(e) there are new low frequency modes associated with stretching and bending of the hydrogen-bond itself



(2) the proton magnetic resonance moves towards lower field,

(3) the A D distance is short compared to the sum of the van der Waals radii,

(4) electronic transitions of either the acid or the base may be shifted,

(5) the molecular mass is larger than the formula mass, as shown by cryoscopic, vapour pressure and vapour density data.

(6) changes in various properties indicate association : dielectric behaviour, solubility, heat of mixing, molar volume, viscosity etc.

Of these effects the infrared intensity (1)(c) and the proton magnetic resonance (2) are probably the most sensitive to hydrogen-bond formation whereas the infrared frequency is probably the most easily measured and for the purposes of this thesis only values of $\Delta\nu$, are considered.

If a complex AD is formed by interaction of an electron acceptor A (e. g. a naphthol) with an electron donor (e. g. dioxan) which specifically involves the formation of a hydrogen bond, the association equilibrium constant, K, is a measure of the tendency for the formation of the hydrogen bond and is related to the standard free energy change, ΔG^\ominus , of the process by

$$\Delta G^\ominus = - RT \ln K.$$

This standard free energy of association will represent a balance between the tendency to minimise the enthalpy change and to maximise the probability or disorder of the system, expressed thermodynamically by

$$\Delta G^\ominus = \Delta H^\ominus - T \Delta S^\ominus$$

where ΔH^\ominus and ΔS^\ominus are the standard enthalpy and entropy changes, respectively, on association at constant pressure. The standard enthalpy change ΔH^\ominus can be calculated from the temperature coefficient of the logarithm of the association constant, K, and is a direct measure of the strength of the hydrogen bond.

Although infrared spectroscopy has been widely used to investigate the properties of hydrogen bonded systems, ultraviolet spectroscopy has also provided useful information concerning the

strength of hydrogen bonding in these systems. Changes in the ultraviolet spectrum of a molecule occurring as a result of hydrogen bond formation enable calculation of the equilibrium concentrations of complex and hence the association constant.

The ultraviolet spectrum of a molecule is altered by the formation of a hydrogen bond if the chromophoric portion of the molecule is perturbed by the bond. Changes in electronic transitions of acidic or basic substances on hydrogen bonding in solution are associated with shifts in the frequency of the band maximum. The shifts may be either to lower frequency (longer wavelength - red shift) or to higher frequency (shorter wavelength - blue shift) and usually there is no pronounced change of the absorption coefficient.

It is commonly accepted¹⁸ that $n \rightarrow \pi^*$ transitions which involve the excitation of non-bonding electrons into the lowest unoccupied π state in a molecule always cause a frequency shift towards shorter wavelengths on hydrogen bond formation. The $\pi \rightarrow \pi^*$ transitions which correspond to the excitation of π - bonding electrons to the lowest antibonding π orbital usually cause a frequency shift towards longer wavelengths.

Pimentel¹⁹ has suggested that, in general, the effect of hydrogen bonding on the ultraviolet spectrum overrides the effects of solvent polarisation, dipole-dipole interactions and dipole polarisation forces which have been discussed by Bayliss and McRae.²⁰

Brealey and Kasha²¹ investigated the change in position of the $n \rightarrow \pi^*$ ultraviolet absorption band of a number of bases such as pyridine N-oxide and benzophenone on changing from a hydrocarbon to a hydroxylic solvent. The large blue shift observed was shown to

be due to hydrogen bonding of the n-electrons of the base by the hydroxylic solvent causing stabilisation of the ground state compared to the excited state of the molecule.

Nagakura and Baba²² studied the ultraviolet absorption spectra of aniline, phenol and anisole in various hydrocarbon and ether - type solvents. The frequency shift was found to be anomalously large for aniline and phenol dissolved in the ether - type solvents and they concluded that hydrogen bonding occurred between the solute and solvent molecules.

Quantitatively ultraviolet spectroscopy has been used by many workers to determine the association equilibrium constant of complex formation in solution e. g. Benesi and Hildebrand,¹⁵ Ketelaar et al,²³ Nagakura et al^{24, 25, 26} and Keefer and Andrews.^{27, 28}

Rose and Drago²⁹ devised a general method for rigorously treating spectrophotometric data for any donor-acceptor system. The general equation for the equilibrium in the liquid phase is :



where D is an electron pair donor and A an electron pair acceptor.

The expression for the molar equilibrium constant, K_c , is

$$K_c = \frac{e^{c_{DA}}}{(c_D - e^{c_{DA}})(c_A - e^{c_{DA}})} \quad (21)$$

where c_D and c_A are the initial concentrations of D and A respectively, $e^{c_{DA}}$ is the equilibrium concentration of the complex, DA. If the donor molecule does not absorb in the region of spectral measurement and if additivity of absorbances is assumed, then for a cell of unit path length and at constant wavelength

$$A = \epsilon_{DA} \cdot e^{c_{DA}} + \epsilon_A \cdot e^{c_A} \quad (22)$$

where A is the total absorbance of the solution,

ϵ_{DA} is the extinction coefficient of the complex,

ϵ_A is the extinction coefficient of the electron pair acceptor, and

e^c_A is the equilibrium concentration of the electron pair acceptor.

$$\text{Also } c_A = e^c_{DA} + e^c_A \quad (23)$$

Expanding equation (21) gives :

$$K_c = \frac{e^c_{DA}}{(c_D \cdot c_A + e^c_{DA}{}^2 - e^c_{DA} \cdot c_D - e^c_{DA} \cdot c_A)} \quad (24)$$

Eliminating e^c_A between (22) and (23) :

$$A = e^c_{DA} (\epsilon_{DA} - \epsilon_A) + \epsilon_A \cdot c_A$$

If A^0 corresponds to the absorbance of A alone at its initial concentration, c_A , at the same wavelength and in the absence of D , then :

$$A^0 = \epsilon_A \cdot c_A \text{ and}$$

$$A = e^c_{DA} (\epsilon_{DA} - \epsilon_A) + A^0 \quad (25)$$

Rearranging (25) gives

$$e^c_{DA} = \frac{(A - A^0)}{(\epsilon_{DA} - \epsilon_A)}$$

Substituting this value of e^c_{DA} in equation (24) gives :

$$K_c^{-1} = \frac{c_D \cdot c_A (\epsilon_{DA} - \epsilon_A)}{(A - A^0)} - c_D + \frac{(A - A^0)}{(\epsilon_{DA} - \epsilon_A)} - c_A \quad (26)$$

Equation (26) may be solved for the association equilibrium constant K_c if a series of absorbances, A , corresponding to solutions containing different equilibrium amounts of complex and acceptor are known. Accordingly, the absorbances, A , are measured experimentally at a selected wavelength for a series of solutions in

an inert solvent containing a constant initial amount of acceptor with varying amounts of donor. If the experimental conditions are chosen such that c_D is very much larger than c_A , then

$$\frac{(A-A^0)}{(\epsilon_{DA} - \epsilon_A)} - c_A \text{ may be neglected in comparison with}$$

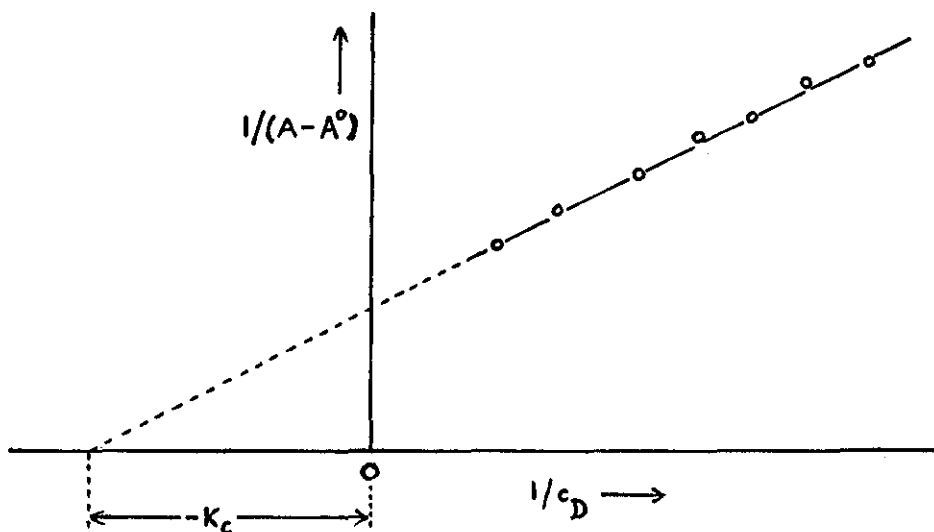
$$\frac{c_D \cdot c_A (\epsilon_{DA} - \epsilon_A)}{(A-A^0)} - c_D \text{ and equation (26) reduces to}$$

$$K_c^{-1} = \frac{c_D \cdot c_A (\epsilon_{DA} - \epsilon_A)}{(A-A^0)} - c_D \quad \text{or}$$

$$\frac{c_A}{(A-A^0)} = \frac{1}{K_c (\epsilon_{DA} - \epsilon_A)} \cdot \frac{1}{c_D} + \frac{1}{(\epsilon_{DA} - \epsilon_A)} \quad (27)$$

Equation (27) has been used by Nagakura et al^{24, 30, 31} to evaluate association constants of complex formation since a linear plot of $1/(A-A^0)$ against $1/c_D$ extrapolated to $1/(A-A^0) = 0$ gives the association equilibrium constant as $K_c = -(1/c_D)$ extrapolated (Fig. 2).

Fig. 2 : A Nagakura Plot



In an earlier study³² the author investigated the effect of 4-substitution on the hydrogen bonding tendency to dioxan of a series of 4-substituted phenols in cyclohexane solution. The association equilibrium constants, K_c , were calculated from ultraviolet spectroscopic data as outlined above and the results (obtained at two temperatures) are recorded in Table 3.

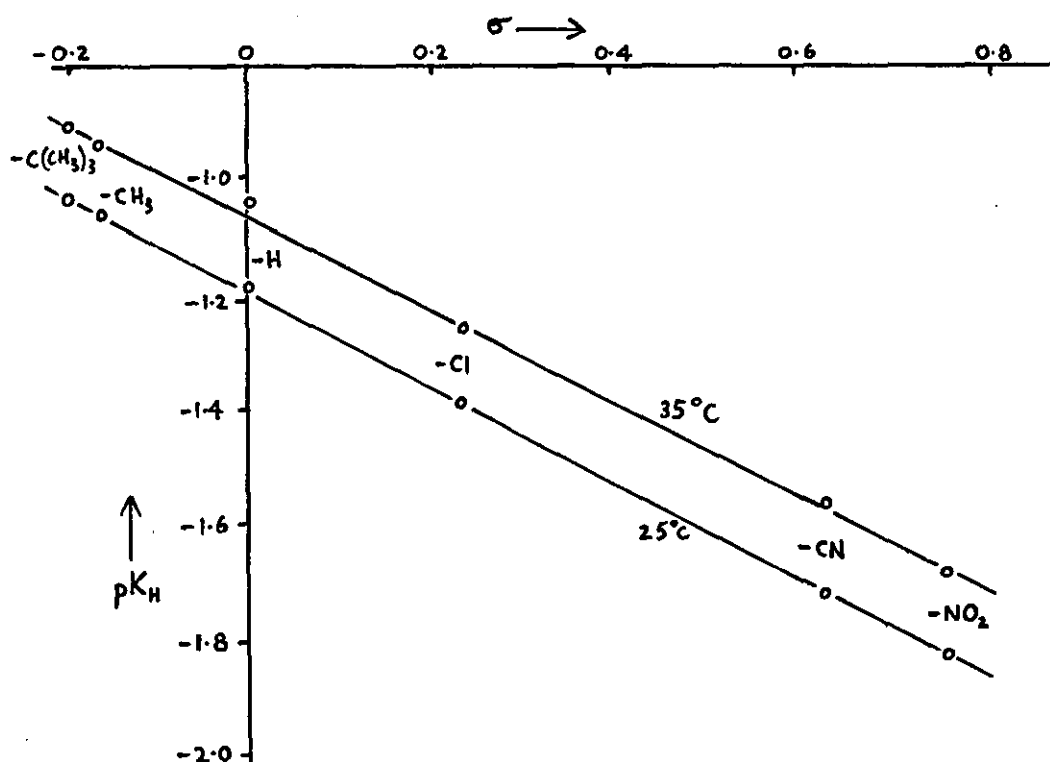
The value of K_c , and therefore the strength of the hydrogen bond, was found to vary congruously with the nature of the 4-substituent; electron donating groups (continued overleaf)

TABLE 3

Phenols

<u>Substituent</u>	<u>K_c</u>		<u>pK_c</u>		<u>σ</u>
	<u>25°C</u>	<u>35°C</u>	<u>25°C</u>	<u>35°C</u>	
4-C(CH ₃) ₃	10.42	8.50	-1.02	-0.93	-0.20
4-CH ₃	10.94	8.81	-1.04	-0.95	-0.17
-H	15.21	10.79	-1.18	-1.03	0
4-Cl	24.43	18.28	-1.39	-1.26	0.23
4-CN	50.20	37.22	-1.70	-1.57	0.63
4-NO ₂	66.83	49.00	-1.83	-1.69	0.78

Fig. 3 : Association of Phenols to Dioxan in Cyclohexane Solution



caused a decrease and electron withdrawing groups an increase in K_c over that observed for the parent compound, phenol. The Hammett substituent parameter, σ ,³³ was taken as a measure of the electron donating or withdrawing power of the 4-substituent and a linear relationship was demonstrated between pK_c (i. e. $-\log_{10} K_c$) and σ (see Fig. 3) suggesting that the latter reflects the effect of the 4-substituent on the strength of the hydrogen bond formed by the phenolic OH group with an oxygen atom of the dioxan.

A similar investigation has been carried out by Vallance³⁴ for a series of 4-substituted anilines and the calculated association constants are reproduced in Table 3.

A linear correlation was again obtained between pK_c and Hammett substituent constant, σ , (see Fig. 4) and comparison with the author's results found for phenols indicates a greater hydrogen bonding affinity in solution of phenols than anilines for dioxan. These affinities

TABLE 3

Anilines

<u>Substituent</u>	<u>K_c</u>		<u>pK_c</u>		<u>σ</u>
	<u>25°C</u>	<u>35°C</u>	<u>25°C</u>	<u>35°C</u>	
4-OCH ₃	0.45	0.36	0.35	0.44	-0.27
4-CH ₃	0.51	0.44	0.29	0.36	-0.17
-H	0.59	0.53	0.23	0.28	0
4-Cl	0.84	0.66	0.08	0.18	0.23
4-Br	0.86	0.64	0.07	0.19	0.23
4-CH ₃ CO	1.09	0.88	-0.04	0.06	0.52
4-CN	1.20	1.00	-0.08	0.00	0.63

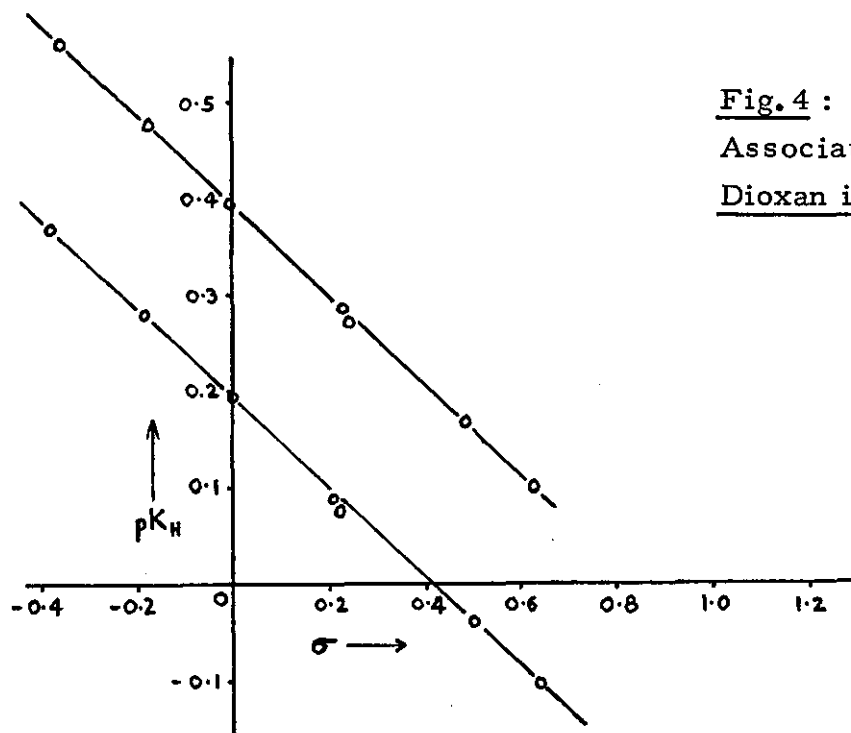


Fig. 4 :
Association of Anilines to
Dioxan in Cyclohexane Solution

may be compared more precisely by calculating the enthalpies of hydrogen bond formation in solution for the respective complexes.

Application of the van't Hoff equation (Equation 28)

$$\frac{d \ln K}{dT} = \frac{\Delta H^{\ominus}}{RT^2} \quad (28)$$

where K is an equilibrium constant,

ΔH^{\ominus} is the standard enthalpy change for the process,

R is the universal gas constant,

T is the absolute temperature,

to association data enables enthalpy values to be found provided it is assumed that ΔH^{\ominus} remains constant over the temperature range considered. An integrated form of the van't Hoff equation :

$$\log \left(\frac{K_2}{K_1} \right) = \frac{\Delta H^{\ominus}}{2.303R} \cdot \frac{(T_2 - T_1)}{T_1 T_2} \quad (29)$$

where K_1 is the equilibrium constant at T_1 ,

and K_2 is the equilibrium constant at T_2 ,

enables ΔH^{\ominus} values to be assessed from association data at two different temperatures.

From the data of Vallance and the author (Tables 3 and 4) ΔH^{\ominus} values have been found but the scatter tends to obscure any significant variation. Accordingly, the data was reprocessed: regression lines for plots of $\log K_c$ against σ at each temperature were calculated using the method of least squares and smoothed K_c values introduced into Equation (29). The regression lines are quoted below and the calculated enthalpies in Table 5.

$$\begin{aligned} \text{Phenols} \quad \text{at } 25^{\circ}\text{C} : \log K_c &= 0.828\sigma + 1.184 \\ &\text{at } 35^{\circ}\text{C} : \log K_c = 0.728\sigma + 1.082 \\ \text{Anilines} \quad \text{at } 25^{\circ}\text{C} : \log K_c &= 0.480\sigma - 0.218 \\ &\text{at } 35^{\circ}\text{C} : \log K_c = 0.441\sigma - 0.282 \end{aligned}$$

The relatively small magnitude of ΔH^{\ominus} for the 4-substituted anilines compared to the corresponding values for phenols indicates the weaker nature of the hydrogen bonding encountered in the aniline series. This is further demonstrated by the slope of 1.76 in the plot of $\log K_c$ for the 4-substituted phenols against $\log K_c$ for the corresponding anilines, see Fig. 5. The graph shows the expected linear relationship and its temperature independence.

TABLE 5.

<u>Substituent</u>	<u>ΔH^{\ominus} anilines (kJ mol⁻¹)</u>	<u>ΔH^{\ominus} phenols (kJ mol⁻¹)</u>
4 - OCH ₃	- 9.45	-
4 - CH ₃	- 10.11	- 16.58
- H	- 11.28	- 18.00
4 - Cl	- 12.82	- 19.84
4 - Br	- 12.86	-
4 - COCH ₃	- 14.80	-
4 - CN	- 15.58	- 23.55
4 - NO ₂	-	- 24.30

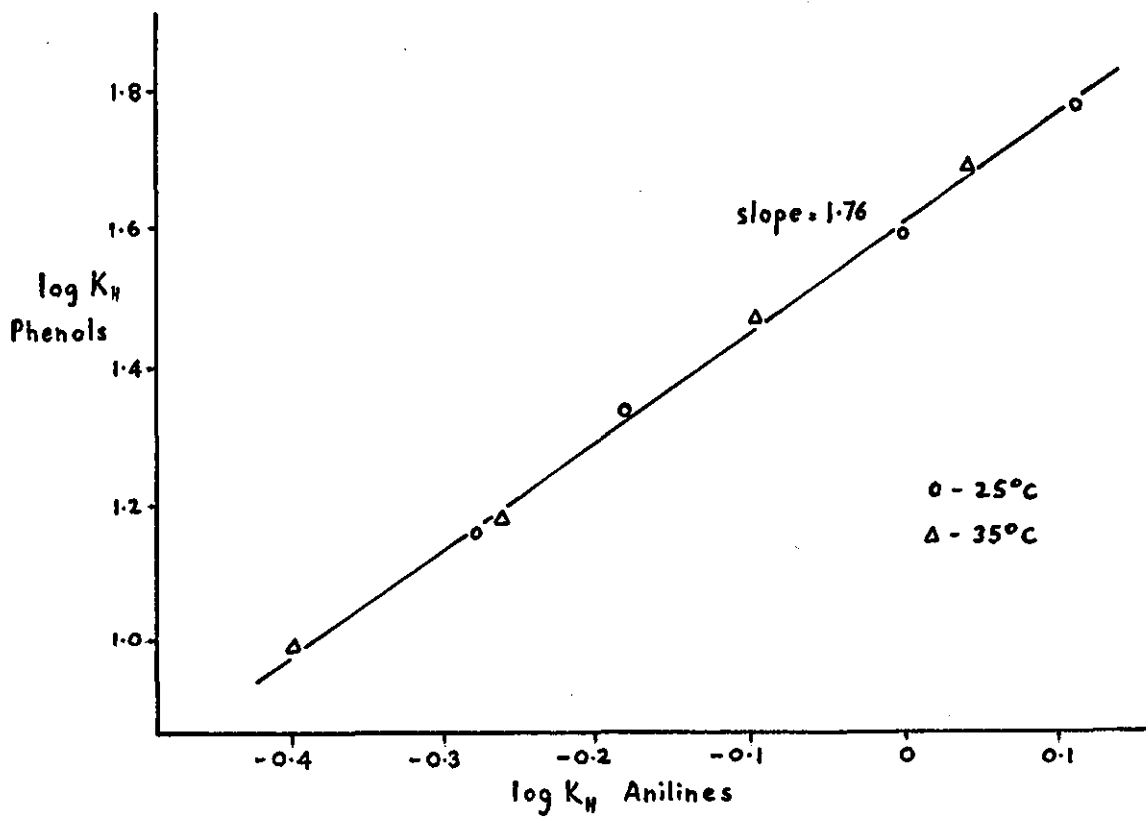


Fig. 5 : Hydrogen Bonding Constants of Anilines and Phenols

(C) INTERACTIONS AT THE SOLID-SOLUTION INTERFACE

The ability of charcoal to take up gases and remove coloured solutes from solution was reported by many early workers (C.W. Scheele, 1773; Abbe F. Fontana, 1777; T. Lowitz, 1785) and many later observations have confirmed the property of fine powders which enables them to take up substances from solution.

The term 'adsorption' (Kayser, 1881) strictly refers to the existence of a higher concentration of any particular component at the surface of a liquid or solid phase than is present in the bulk, as opposed to 'absorption' which implies more or less uniform penetration. As these two effects frequently overlap the more general term 'sorption' is widely employed.

The nature of the sorption process may be regarded in this way : the units of a crystal lattice may be considered as being surrounded by a field of force and although there is little residual attraction within the crystal, where each unit is situated symmetrically with respect to the electrical forces of cohesion, the unsaturated character or the intensity of this field assumes large values in the space adjacent to the crystal surface. The surface of a crystal may thus be regarded as unsaturated and the existence of a definite surface energy is due to this unsaturation.

Since the surface of a crystal consists of a regular lattice of orderly distributed units (ions or atoms) the surface adhesional forces may be regarded as being distributed over the centres of these lattice units, although in all probability these points represent maxima in a continuous field. Owing to the solid possessing a residual field of

force there will be a tendency for the thermodynamic free energy of any surface to decrease and it is this tendency which is ultimately responsible for the phenomenon of sorption. In addition to the diminution in free energy of the system when sorption occurs it is natural to suppose that as a result of the enhanced configurational restriction imposed on the molecule sorbed on the solid surface a decrease in entropy will result. By application to the sorption process of the equation

$$\Delta G^\ominus = \Delta H^\ominus - T \Delta S^\ominus$$

in which ΔG^\ominus , ΔS^\ominus and ΔH^\ominus represent the standard changes in free energy, entropy and enthalpy, respectively, associated with a change of state of a system at temperature T, it is apparent that since both ΔG^\ominus and ΔS^\ominus are both negative numerically then ΔH^\ominus will also be negative numerically, i. e. sorption is an exothermic process.

When there is convincing evidence that the adsorbate molecule has formed a chemical bond with the adsorbent surface 'chemisorption' has occurred, but when the mode of attachment is less well defined the effect is designated 'physical adsorption'. It is sometimes difficult to locate the boundary between these two types of adsorption and indeed a correct description may be time dependent. As the systems studied in the experimental part of this thesis relate specifically to physical adsorption, discussion will be restricted to this type of adsorption, and further, to metal oxide surfaces.

In the case of adsorption from solution, preferential adsorption of one component or the other of a binary solution over part or all of the concentration range studied often occurs. For example, alcohols are adsorbed in preference to benzene onto an oxide surface

over the whole of the concentration range,^{35, 36, 37} the interaction between the lower alcohols and the surface being most probably hydrogen bonding. Again, methyl acetate is preferentially adsorbed from benzene by silica and alumina surfaces,³⁸ and this can be attributed to specific interaction of the polar centre of the ester molecule with the polar groups which cover the solid surface. The preferential adsorption of one component over the whole of the concentration range in the above examples suggests that the surface adsorption sites are homogeneously polar. However, some heterogeneity of oxide surfaces generally arises from the presence of both oxide and hydroxyl groups and as these are both highly polar, their respective discriminations between pairs of adsorbates is not always easy to detect.

The type of orientation that the adsorbed molecule assumes at the adsorbent surface can provide information about the nature of the interaction between the adsorbate and the metal oxide surface.

Monocarboxylic acids are adsorbed from organic solvents onto silica³⁹ with their major axes parallel to the solid surface. Adsorption on alumina, however, occurs with the major axis of the adsorbed acid molecule perpendicular to the surface. On alumina the adsorbed molecules do not form a close packed monolayer, implying adsorption onto specific sites such as oxygen atoms or ions. Thus while the adsorbate-adsorbent interaction in the case of silica is insufficient to cause rupture of the hydrogen bonds in the dimeric acid molecule, the stronger attraction on alumina results in bond breakage and adsorption of monomeric acid molecules onto specific sites on the surface.

Specific adsorption on silica is thought to be due mainly to hydrogen bonding between the surface hydroxyl groups of the adsorbent and the electron donor groups of the adsorbate.^{40, 41} In this connection, Cusamo and Low⁴² have recently studied the adsorption of a variety of substituted benzenes on to porous glass. They concluded that the π - OH interaction could be explained in terms of the charge transfer model developed by Mulliken⁴³ and later modified by Puramik.⁴⁴ For a π - OH interaction the model involved the formation of an asymmetrically bonded surface complex, an electron entering the antibonding orbital of the surface hydroxyl, interaction occurring between that orbital and the aromatic π - system along one of the C-C directions. Application of the charge transfer theory led to relationships between the shift of the hydroxyl absorption frequency, $\Delta \nu_{OH}$, and the ionisation potential of the adsorbate, and also between $\Delta \nu_{OH}$ and the change in the hydroxyl absorption intensity brought about by the adsorbate - OH interaction.

Various workers have studied the adsorptive properties of alumina and have concluded that the process of adsorption is brought about by :

- (i) conventional electrostatic processes,⁴⁵
- (ii) hydrogen bonding with the alumina surface acting either as a proton donor⁴⁶ or proton acceptor,⁴⁷
- (iii) charge transfer complex formation with the alumina surface acting as either an electron donor or acceptor,⁴⁸
- (iv) ionisation of the adsorbate upon adsorption.⁴⁹

Possible surface sites for adsorption on γ - alumina, such as that used in the sorption work of this study, include hydroxyl groups, oxide ions or exposed aluminium ions.

The surface of the alumina used in this investigation is known to be completely hydroxylated implying the absence of oxide sites or aluminium ions. Previous work carried out on this alumina has shown hydrogen bonding to be the essential mechanism of adsorption for a variety of adsorbates. Ibbitson, Jackson, McCarthy and Stone⁵⁰ studied the adsorption of substituted azo compounds from benzene by alumina and found that replacement of the hydrogen of the hydroxyl group in 4-hydroxy-1-azo benzene resulted in negligible adsorption of 4-methoxy-1-azo benzene. Replacement of both hydrogen atoms in 4-amino-1-azo benzene by methyl groups produced a similar result. For the adsorption of phenols from cyclohexane, Eric, Goode and Ibbitson⁵¹ showed that phenol molecules were adsorbed perpendicularly to the surface, the most probable mechanism of adsorption being hydrogen bonding of the phenolic hydroxyl group to the hydroxyl groups present on the alumina surface.

More recently, Vallance³⁴ has studied the adsorption of 4-substituted anilines from cyclohexane solution at the alumina interface, and has concluded that hydrogen bonding is the predominant interaction. Defining an arbitrary 'index of adsorption' Vallance was able to show that the adsorption tendency of the 4-substituted anilines for the alumina surface was reflected in the changes in the electrical character of the NH_2 group owing to the presence of the 4-substituent.

Finally, the author in his earlier work³² on the sorption of 4-substituted phenols from cyclohexane and dioxan solution onto alumina came to the conclusion that four factors were important in explaining the sorption saturation values: (a) sorption of the solvent, (b) spacing of sorption sites on the surface, (c) orientation of the adsorbed molecules and (d) the polar character of the 4-substituent. He concluded that sorption from cyclohexane solution resulted in a close packed monolayer of phenol molecules : the affinity of the non-polar cyclohexane for the surface, even though fully hydroxylated, was so low that the solvent was excluded from the surface at monolayer coverage. However, dioxan, being able to hydrogen bond effectively with the surface hydroxyl groups, provided strong competition at the surface and reduced the moles of phenol sorbed by more than half, although hydrogen bonding between phenols and dioxan in solution would also contribute to this effect. Overall, the forces on the surface seemed to be the dominant ones since the phenols were not adsorbed as 1:1 complexes, but bonds between phenol and dioxan molecules were broken and the phenol molecules sorbed as discrete entities. Interaction with the surface was through hydrogen bonding and the phenol molecules assumed a vertical orientation on localised sites. The contribution of the 4-substituent to the electrical state of the phenol molecules was reflected by the sorption saturation values but only in the presence of a solvent which could compete effectively for surface adsorption sites.

The Adsorption Isotherm

(1) The Composite Isotherm.

Experimental adsorption data appropriate to the solid-solution interface is usually presented in the form of an adsorption isotherm, in which the change in mole fraction on adsorption of one of the components in a binary solution is plotted against the equilibrium mole fraction of that component in the liquid phase. An equation expressing the change in mole fraction of component 1 in the binary mobile phase on adsorption in terms of the adsorption of both components is derived below.

Consider a system of two components 1 and 2, the total number of moles being n_o . When placed in contact with m grams of solid adsorbent the mole fraction of component 1 decreases by Δx_1^l . This change in concentration is a result of the transfer of n_1^s moles of component 1 and n_2^s moles of component 2, giving mole fractions x_1^l and x_2^l respectively (initial mole fractions being represented by $(x_1^l)_o$ and $(x_2^l)_o$). By simple algebra it can be shown that

$$\frac{n_o \Delta x_1^l}{m} = n_1^s \cdot x_2^l - n_2^s \cdot x_1^l \quad (30)$$

The composite isotherm representing adsorption of both components 1 and 2 is obtained by plotting $n_o \Delta x_1^l / m$ against x_1^l . Sometimes the isotherm is expressed in terms of $(x_1^s - x_1^l)$ where x_1^s is the mole fraction of component 1 in the adsorbed layer. This form emphasises the preferential adsorption of one component and it can be readily shown that

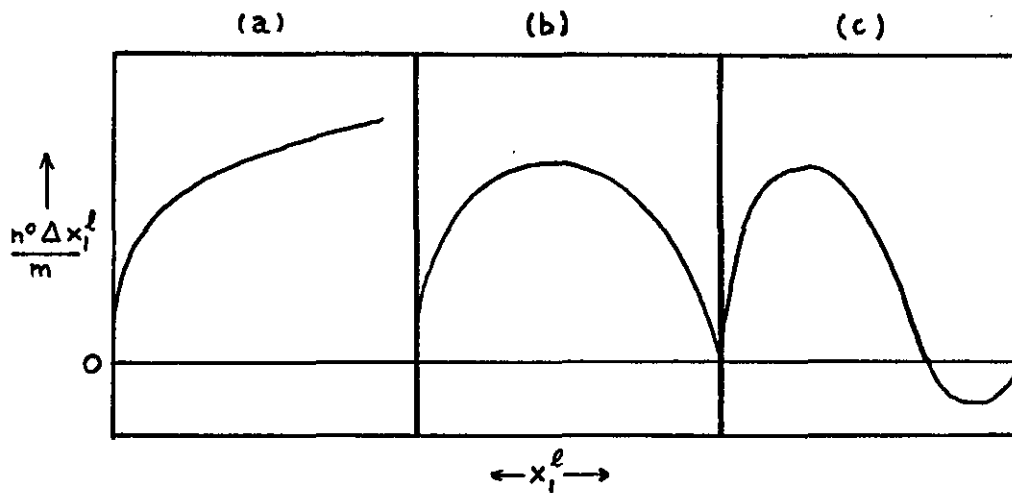
$$x_1^s - x_1^l = \frac{1}{n^s} \cdot \frac{n_o \Delta x_1^l}{m} \quad (31)$$

where n^s is the total number of moles in the adsorbed layer on unit mass of solid.

The main types of isotherm experimentally realised are shown in Fig. 6⁵², isotherm (a) representing adsorption from dilute solution.

In the case of adsorption from a dilute solution of component 1 in component 2 or when component 1 has

Fig. 6 : The Main Types of Isotherms



limited solubility in component 2, then

$$x_1^l \ll x_2^l \approx 1.$$

Both n_1^s and n_2^s are small and thus $n_2^s x_1^l$ is small and Equation (3) reduces to

$$\frac{n_o \Delta x_1^l}{m} \approx n_1^s \quad (32)$$

indicating that the composite isotherm is almost identical with the isotherm representing adsorption of component 1 alone.

(2) The Individual Isotherms.

As Equation (30) contains two unknowns, n_1^s and n_2^s , a further independent relationship between these two quantities is required before the composite isotherm can be resolved into its individual components.

If it is assumed that the solid surface is completely covered by the adsorbed layer whatever the composition of the liquid phase and that the layer is unimolecular,⁵³ then

$$n_1^s A_1 + n_2^s A_2 = A \quad (33)$$

where A_1 , A_2 are the partial molar areas occupied at the surface by the two components, 1 and 2 respectively, and A is the surface area of unit weight of solid.

Kipling and Tester⁵⁴ suggested the alternative form of this expression :

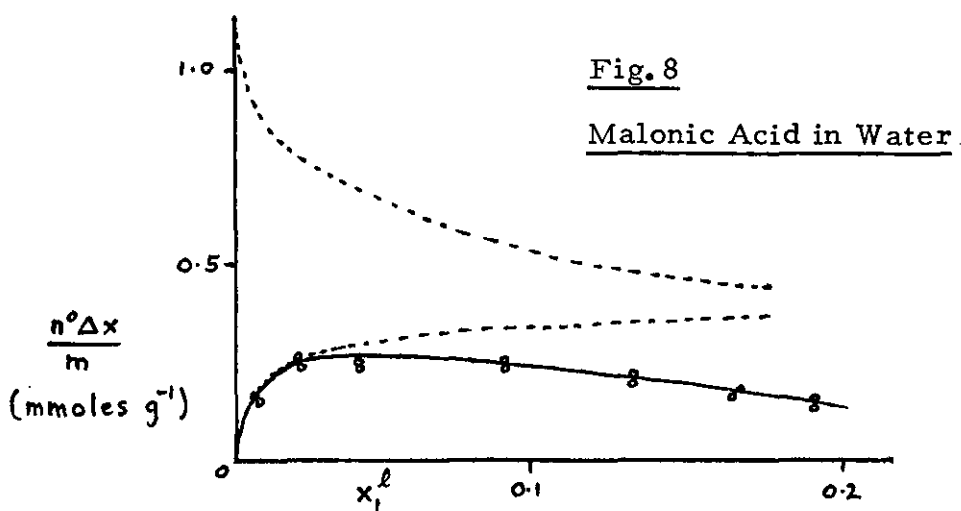
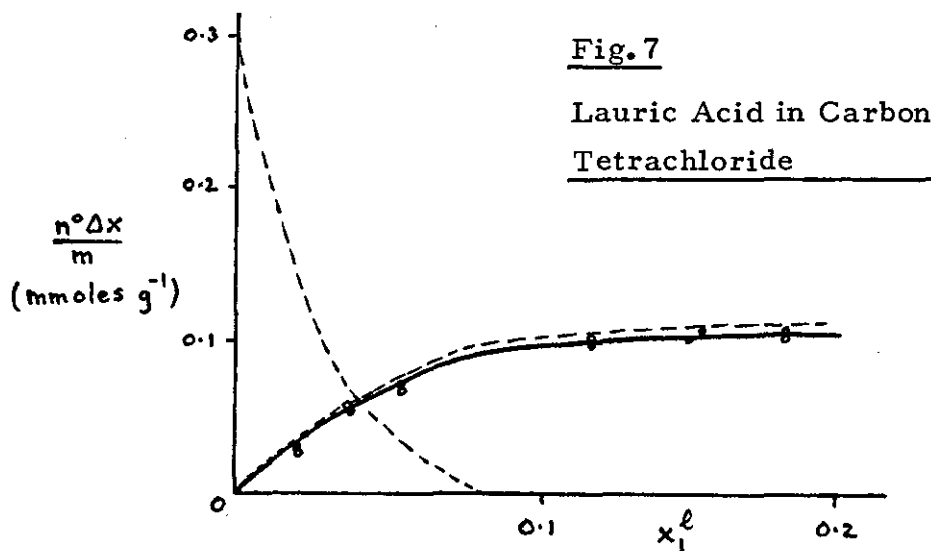
$$\frac{n_1^s}{(n_1^s)_m} + \frac{n_2^s}{(n_2^s)_m} = 1 \quad (34)$$

where $(n_1^s)_m$ and $(n_2^s)_m$ are the number of moles of the individual components required to cover the surface area of unit mass of adsorbent completely with a monolayer. These latter quantities can be determined by vapour phase adsorption of the individual components.

Examples of calculated individual isotherms are shown in Figs. 7 and 8, one being for an aqueous and the other for a non-aqueous system.⁵⁵ In both instances the sorption of the solvent is very high for dilute solutions because the solvent molecules are considerably smaller than those of the solute and a greater number of moles is required to cover a given area.

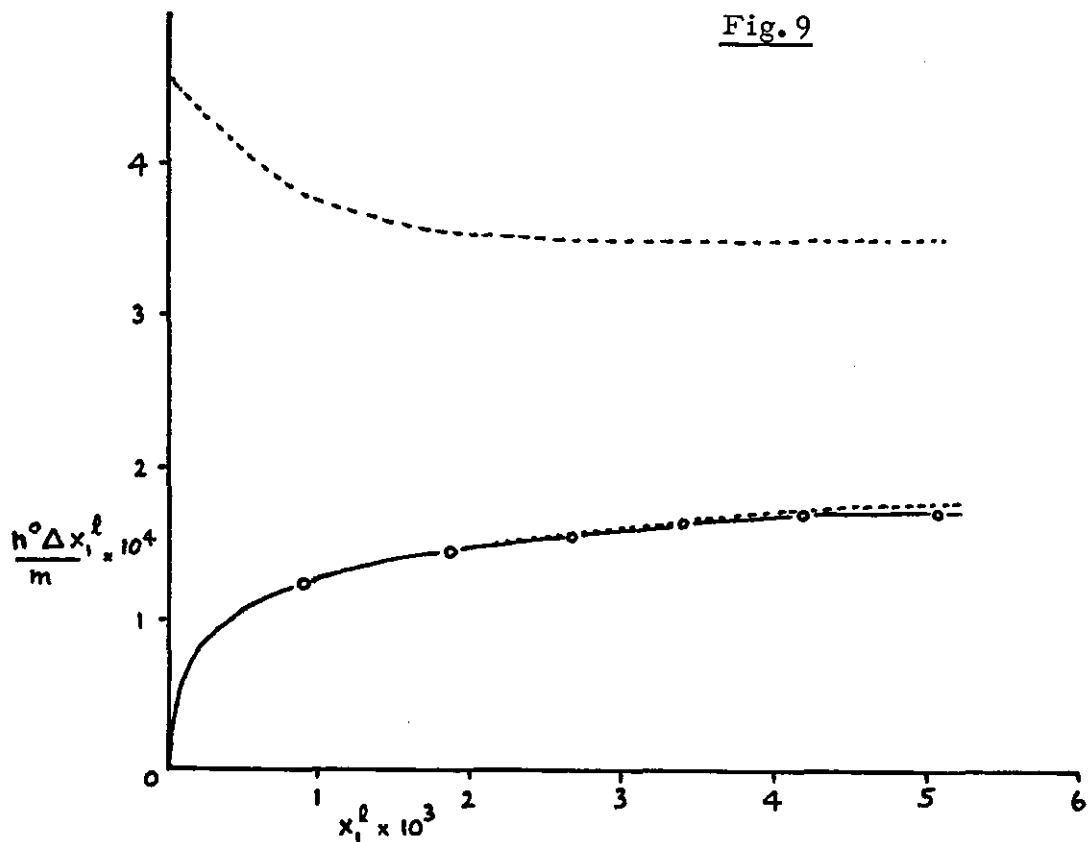
In Fig.7 it is seen that the individual isotherm for the sorption of the solute lies close to the composite isotherm. For many systems there is even less separation, the reason lying in the form of Equation (30). As the limiting solubility usually occurs at a low value of the mole fraction all realisable values of x_1^l are small. Consequently, even if n_2^s is large, $n_2^s x_1^l$ is small compared to $n^o \Delta x_1^l / m$ and since $(1-x_1^l)$ approximates to unity $n^o \Delta x_1^l / m \approx n_1^s$ in this case.

In Fig.8 the composite and individual isotherms for malonic



Composite Isotherms (full lines) and Individual Isotherms (broken lines) for Adsorption on Graphon.

Fig. 9



Composite Isotherms (full line) and Individual Isotherms (broken lines) for Adsorption of Phenol from Dioxan on Alumina.

acid diverge markedly as the mole fraction of the acid increases, the principle cause being the relatively high value of n_2^s at high values of x_1^l .

Fig. 9 shows the individual isotherms for the sorption of phenol from dioxan onto alumina calculated from the author's earlier results.³² Once again, the low mole fractions of the phenol ensure minimal separation of the composite and individual isotherms. The data from the sorptions of naphthols onto alumina reported in this thesis yield exactly parallel results upon similar analysis.

If adsorption at the solid-solution interface is multi-molecular, then Equation (34) becomes

$$\frac{n_1^s}{(n_1^s)_m} + \frac{n_2^s}{(n_2^s)_m} > 1.$$

Applications of Equation (34) to adsorption on rutile from solutions of long chain alcohols and hydrocarbons led Day and Parfitt⁵⁶ to conclude that multilayer adsorption of the parallel-orientated hydrocarbon molecules occurred in the spaces between the perpendicularly orientated adsorbed alcohol molecules to an extent dependent upon the length of the alcohol molecule. Use of a value of $(n_2^s)_m$ representing the number of moles of hydrocarbon occupying the same volume as that of a monolayer of alcohol molecules in a perpendicular orientation gave a value of 0.96 in Equation (34) for the n-octanol/n-heptane system. This work emphasises the need to consider each system individually in order to decide whether the assumption of monolayer coverage of the adsorbent surface is justified.

(D) THERMODYNAMICS OF ADSORPTION AT THE SOLID-
SOLUTION INTERFACE

The extent of the adsorption process and the degree of competition at the surface are governed not only by the interfacial phenomena but also by interactions in the mobile phase. A thermodynamic treatment of the process is likely, therefore, to be complex and it is convenient to first establish an 'ideal' or 'perfect' reference system before considering deviations from ideality in real systems by introduction of activity coefficients.

Everett⁵⁷ has attempted to establish such a model for sorption at the solid-solution interface. This author pictures the solution as an array of plane lattices stacked together with their planes parallel to the sorbent surface. Adsorption in this pseudo-crystalline model is supposed to be monomolecular so that the average mole fractions of the components are constant in all lattice planes except that immediately adjacent to the solid surface, where variation is caused by selective adsorption of one or more of the solution components. This plane is the 'adsorbed phase' (hereafter designated by the superscript 's') and comprises N^s identical adsorption sites. A binary mixture is considered of components 1 and 2 of the same molecular size so that each molecule occupies one lattice point.

In the adsorbed phase there are N_1^s molecules of component 1 and N_2^s molecules of component 2, similarly in the liquid phase there are N_1^l and N_2^l molecules of 1 and 2 respectively. Then

$$N_1^s + N_2^s = N^s,$$

$$\text{and } N_1^{\ell} + N_2^{\ell} = N^{\ell}$$

where N^{ℓ} is the total number of lattice points in the liquid phase.

On this model the adsorbed phase could be referred to as 'a perfect adsorbed monolayer' and the concept has been used by other workers. 58, 59, 60, 61

If Ω^s and Ω^{ℓ} are the number of ways of arranging the molecules in the surface and in the solution respectively, the total number of arrangements Ω of the system is given by

$$\Omega = \Omega^s \cdot \Omega^{\ell} = \frac{N^s!}{N_1^s! N_2^s!} \cdot \frac{N^{\ell}!}{N_1^{\ell}! N_2^{\ell}!} \quad (35)$$

Since the configurational entropy of a system may be defined

$$S^{\text{config}} = k \ln \Omega, \text{ then}$$

$$S^{\text{config}} = k(\ln N^s! + \ln N^{\ell}! - \ln N_1^s! - \ln N_2^s! - \ln N_1^{\ell}! - \ln N_2^{\ell}!)$$

Applying Stirling's theorem ($\ln a! = a \ln a - a$):

$$S^{\text{config}} = k(N^s \ln N^s + N^{\ell} \ln N^{\ell} - N_1^s \ln N_1^s - N_2^s \ln N_2^s - N_1^{\ell} \ln N_1^{\ell} - N_2^{\ell} \ln N_2^{\ell})$$

If N_m represents Avogadro's number, then

$k \times N_m = R$, the universal gas constant and converting molecular numbers into molar quantities (n):

$$S^{\text{config}} = R (n^s \ln n^s - n_1^s \ln n_1^s - n_2^s \ln n_2^s + n^{\ell} \ln n^{\ell} - n_1^{\ell} \ln n_1^{\ell} - n_2^{\ell} \ln n_2^{\ell}) \quad (36)$$

The total entropy expression must include contributions from the vibrational and rotational entropy (i. e. the thermal entropy) of the molecules. The molar thermal entropies are denoted by S_1^{*s} , S_2^{*s} , S_1^{*l} , S_2^{*l} and are assumed to be independent of the composition of both surface and solution. The thermal entropy of the system (S^{therm}) is then given by

$$S^{\text{therm}} = n_1^s S_1^{*s} + n_2^s S_2^{*s} + n_1^l S_1^{*l} + n_2^l S_2^{*l} \quad (37)$$

Furthermore, since the solution is assumed to be perfect and all adsorption sites to have identical properties, the energy of the system (U) is given by

$$U = n_1^s u_1^s + n_2^s u_2^s + n_1^l u_1^l + n_2^l u_2^l \quad (38)$$

where u_1^s , u_2^s , u_1^l , u_2^l are the molar energies of molecules of the two kinds in the adsorbed and liquid phases respectively: these again are independent of composition.

The free energy, F , of the whole system is given by

$$F = U - T (S^{\text{config}} + S^{\text{therm}}).$$

The equilibrium state is that for which

$$\left(\frac{\partial F}{\partial n} \right)_{T, v} = 0$$

for a process in which, at constant temperature (T) and volume (v), dn moles of component 1 are transferred from the solution, i. e. the number of surface molecules (and hence the area of contact between solid and solution) remains constant. In effect the equilibrium constant for the phase-exchange reaction is required:



This leads to the condition

$$\ln\left(\frac{n_2^{\ell}}{n_1^{\ell}}\right) - \ln\left(\frac{n_2^s}{n_1^s}\right) = \frac{\Delta_a u_2 - \Delta_a u_1}{RT} - \frac{\Delta_a S_2^* - \Delta_a S_1^*}{R}$$

where $\Delta_a u_i$ and $\Delta_a S_i^*$ are the changes of energy and of the thermal part of the entropy on adsorption of component i :

$$\Delta_a u_i = u_i^s - u_i^{\ell} \quad \text{and} \quad \Delta_a S_i^* = S_i^{*s} - S_i^{*\ell}, \quad \text{where } i = 1, 2.$$

Thus

$$\frac{n_2^{\ell} \cdot n_1^s}{n_2^s \cdot n_1^{\ell}} = \exp \left[- \frac{\Delta_a u_1 - \Delta_a u_2}{RT} - \frac{\Delta_a S_1^* - \Delta_a S_2^*}{R} \right]$$

or, in terms of mole fraction, x , ($n_1^s = n^s x_1^s$ etc.):

$$\frac{x_1^s \cdot x_2^{\ell}}{x_2^s \cdot x_1^{\ell}} = K \tag{39}$$

Equation (39) is interesting on account of its close similarity to the familiar Langmuir isotherm, nonetheless it has been derived from first principles rather than by analogy from the gas-solid interface.

In order to determine the adsorption equilibrium constant, K , reliably from experimental data it is necessary to formulate a linear relationship from Equation (39) and by employing the relationships

$$x_1^s = n_1^s / n^s \quad \text{and} \quad n_2^s = n^s - n_1^s$$

it can be shown that

$$n_1^s = \frac{n^s K x_1^{\ell}}{1 + x_1^{\ell} (K-1)} \tag{40}$$

and

$$n_2^s = \frac{n^s (1 - x_1^{\ell})}{1 + x_1^{\ell} (K-1)} \tag{41}$$

If n° moles of mixture of components 1 and 2 are now brought into contact with m grams of solid sorbent, and if n_1^s and n_2^s are the moles sorbed by one gram of solid whilst n_1^l and n_2^l moles remain in the mobile phase at equilibrium, then

$$n^{\circ} = n_1^l + n_2^l + mn_1^s + mn_2^s$$

and the initial and equilibrium mole fractions of component 1 in the liquid phase (x_1° and x_1^l) are given by

$$x_1^{\circ} = \frac{n_1^l + mn_1^s}{n^{\circ}}, \quad (42)$$

$$x_1^l = \frac{n_1^l}{n_1^l + n_2^l}. \quad (43)$$

By simple manipulation of Equations (42) and (43) it can be shown that

$$\frac{n^{\circ} \Delta x_1^l}{m} = n_1^s (1 - x_1^l) - n_2^s x_1^l \quad (44)$$

Substituting Equations (40) and (41) into Equation (44):

$$\frac{n^{\circ} \Delta x_1^l}{m} = \frac{n^s x_1^l (1 - x_1^l)(K-1)}{1 + x_1^l (K-1)}$$

which can be presented in the linear form

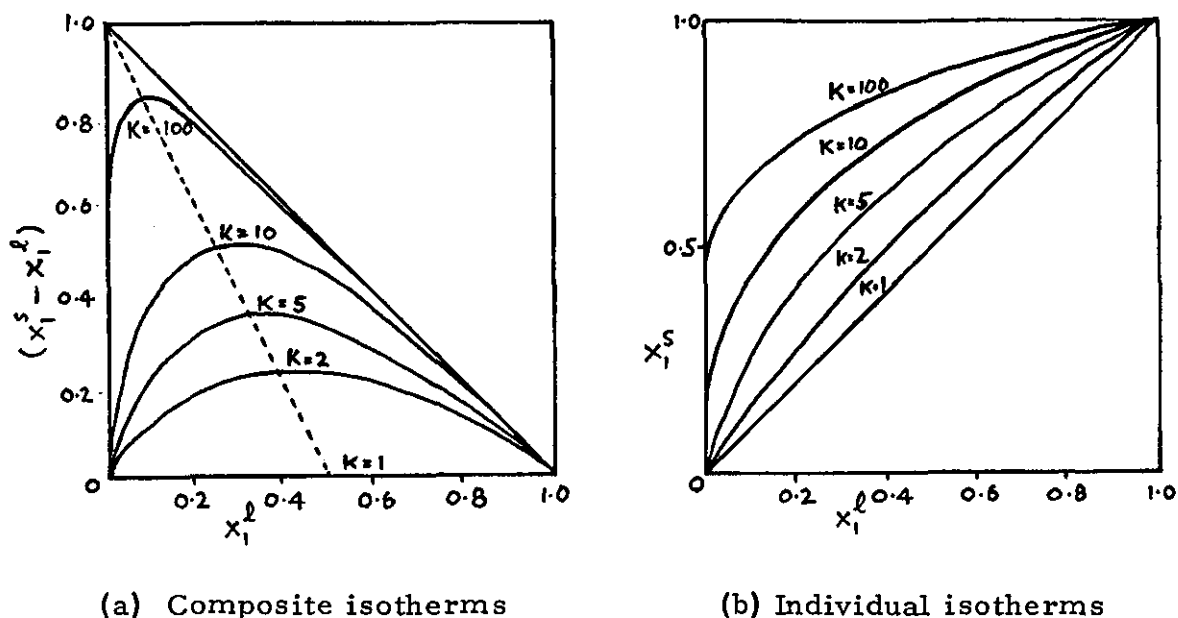
$$\frac{x_1^l (1 - x_1^l)}{n^{\circ} \Delta x_1^l / m} = \frac{1}{n^s} \left[x_1^l + \frac{1}{(K-1)} \right] \quad (45)$$

For a perfect system, therefore, the left-hand side of Equation (45) plotted against x_1^l will give a linear graph of slope $1/n^s$ and intercept when $x_1^l = 0$ of $1/n^s (K-1)$ enabling both n^s (the total number of moles which can be accommodated in the sorbed phase

per gram of solid) and K to be determined from experimental composite isotherm data. Provided the assumptions of the model are justified and that the areas occupied by the two kinds of molecule do not differ significantly, then by assuming an area per molecule the specific surface area of the solid can be calculated.

Theoretical composite and individual isotherms from the Everett equation for different values of K are shown in Fig. 1, the composite isotherms are seen to be U-shaped whilst the individual isotherms are of the Langmuir type.

Fig. 10 : Theoretical Isotherms



(a) Composite isotherms

(b) Individual isotherms

Wright⁶² has applied Everett's equation to adsorption from mixtures of benzene-ethylene dichloride and bromobenzene-chlorobenzene onto Graphon, a homogeneous surface, and Spheron 6, a heterogeneous surface. The composite isotherms appropriate to the benzene-ethylene dichloride system are shown in Fig. 11.

Preferential adsorption of benzene over the whole concentration range is seen to occur on Graphon whereas with Spheron 6 as adsorbent the negative section of the composite isotherm at high benzene concentrations reveals preferential adsorption of ethylene dichloride in that region.

Application of Equation (45) gives the plots shown in Figs. 12 and 13. Whereas the plot for Graphon is found to be linear, that for Spheron 6 is seen to be only linear at low concentrations. By determining the area requirements of each adsorbate from vapour phase adsorption, Wright calculated the surface area of Graphon from the slope of the Everett plot as $119.4 \text{ m}^2 \text{ g}^{-1}$ in reasonable agreement with that determined by low temperature nitrogen

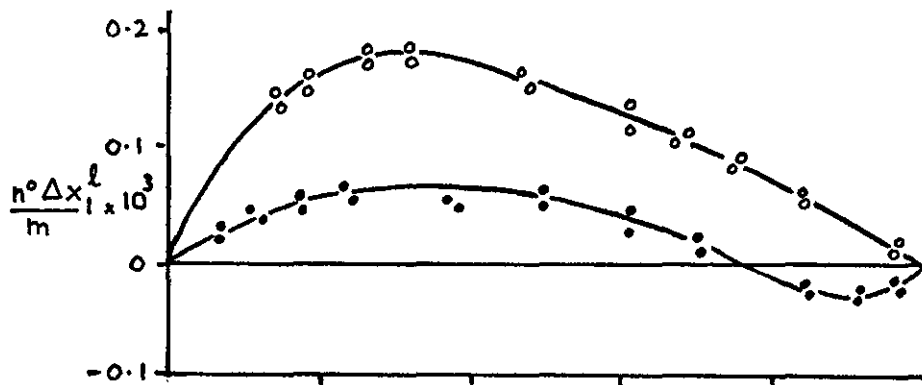


Fig. 11

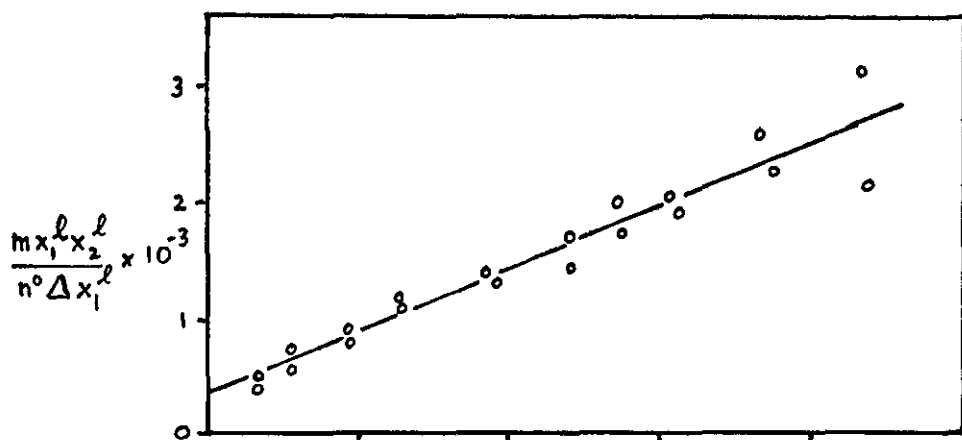


Fig. 12

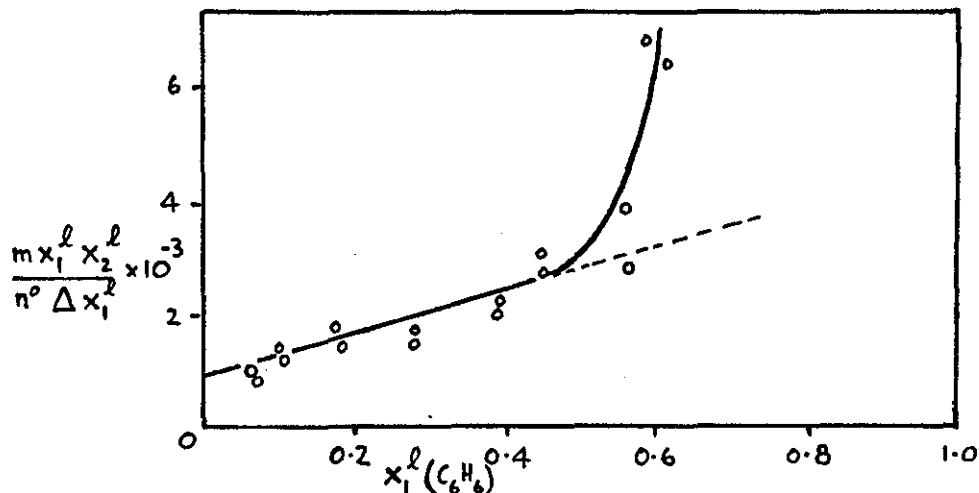


Fig. 13

Adsorption from Benzene and Ethylene Dichloride Solutions

at 30°C. ◊ Graphon. • Spheron 6.

adsorption, $89.4 \text{ m}^2 \text{ g}^{-1}$. Wright considered that the results obtained on Spheron 6 have no significance owing to lack of linearity of the Everett plot and concluded that the deviations observed with Spheron 6 were due to the nature of the adsorbent surface and the absence of any significant preferential adsorption of any one component over the whole concentration range.

More recently, Kagiya et al⁶³ have applied Equation (45) to the adsorption from binary solutions of cyclohexane-aromatic compounds on to silica gel. Good linear plots were obtained and the values of $\log K$ (referred to as the separation factor, α , by the authors) were found to correlate well with the electron donating properties of these compounds as measured by their ionisation potentials or, in the case of substituted aromatics, their Hammett sigma substituent values. The authors were able to conclude that the adsorption of the aromatic compounds was mainly due to the π - electrons of the benzene nuclei, except for anisole whose deviation from the observed correlations suggested adsorption via its oxygen atom.

In reality, most systems must fall short of Everett's thermodynamic ideals discussed earlier in this section. Accordingly, Everett⁶⁴ has developed a rigorous thermodynamic treatment for adsorption from real systems by considering how non-ideality of the surface and bulk phases causes deviations from his 'perfect system' model.

Thus Equation (39) can be rewritten

$$\frac{x_1^{s f_1 s} \cdot x_2^{l f_2 l}}{x_1^{l f_1 l} \cdot x_2^{s f_2 s}} = K \quad (47)$$

where $f_1^s, f_2^s, f_1^l, f_2^l$ are the activity coefficients for components 1 and 2 in the adsorbed and mobile phases respectively.

If p_1 and p_2 are the partial vapour pressures of components 1 and 2 over the bulk solution at the equilibrium composition and p_1^o and p_2^o are the vapour pressures of the pure components at the same temperature, then

$$p_1 = p_1^o x_1^l f_1^l \quad \text{and} \quad p_2 = p_2^o x_2^l f_2^l$$

so that Equation (47) now becomes

$$\frac{f_2^s}{f_1^s} \cdot K = \frac{x_1^s \cdot x_2^l f_2^l}{x_2^s \cdot x_1^l f_1^l} = \frac{p_2 \cdot p_1^o}{p_1 \cdot p_2^o} \left[\frac{x_1^l + (n^o/n^s) x_1^l}{x_2^l - (n^o/n^s) x_1^l} \right] \quad (48)$$

The value of n^s can be found from a knowledge of the surface area of the solid, and the individual values of K, f_1^s and f_2^s by the application of the Gibbs adsorption equation which Everett showed leads to :

$$\int_0^1 \ln \left[\frac{x_1^s \cdot x_2^l f_2^l}{x_2^s \cdot x_1^l f_1^l} \right] dx_1^s = \ln K \quad (49)$$

and

$$\ln f_2^s = x_1^s \cdot \ln \left[\frac{x_1^s \cdot x_2^l f_2^l}{x_2^s \cdot x_1^l f_1^l} \right] - \int_0^{x_1^s} \ln \left[\frac{x_1^s \cdot x_2^l f_2^l}{x_2^s \cdot x_1^l f_1^l} \right] dx_1^s \quad (50)$$

Thus the equilibrium constant, K , can be evaluated for an imperfect system without knowledge of the surface activity coefficients. Calculation of the surface activity coefficients from adsorption experiments using Equation (50) enables a comparison to be made with those predicted by theoretical models of imperfect surface phases assuming that accurate data on the vapour pressures of the bulk solution are known.

For a theoretical model of the 'imperfect system', Everett considered adsorption from regular solutions, the properties of which can be discussed in terms of the quantity

$$\alpha = Nz \left[\epsilon_{12} - \frac{1}{2} (\epsilon_{11} + \epsilon_{22}) \right]$$

where ϵ_{ij} ($i, j = 1, 2$) is the energy of interaction between a pair of molecules i, j on adjacent Lattice sites, N is Avogadro's number, and

z is the number of nearest neighbours to a given Lattice site.

For adsorption at a solid surface, Everett used the model defined previously for perfect systems⁶⁴ and assumed that of the nearest neighbours, a fraction ℓ were in the same Lattice plane as the molecule considered and fractions m in each of the adjacent planes such that $\ell + 2m = 1$. By using the same procedure as Guggenheim⁶⁵ for the discussion of the liquid-vapour interface but including interactions between surface molecules and the adsorbing solid, Everett derived the following equation for the adsorption equilibrium :

$$\ln \left[\frac{x_1^s x_2^\ell}{x_1^\ell x_2^s} \right] = \ln K + \frac{(\ell + 2m)\alpha}{RT} (x_2^{-x_1}) + \frac{\ell\alpha}{RT} (x_1^s - x_2^s) \quad (51)$$

Equation (51) can be solved graphically or by an iterative procedure to obtain x_1^s as a function of x_1^ℓ corresponding to chosen values of K and α . For a close packed cubic Lattice arrangement ($\ell = \frac{1}{2}$, $m = \frac{1}{4}$), Everett obtained S-shaped curves (Figs. 14 and 15).

In order to test the conformity of a system to regular surface behaviour Everett proposed the use of Equation (48) to calculate $f_2^s \cdot K / f_1^s$ which is related to the bulk and surface concentrations by the expression:

$$\ln (f_2^s \cdot K / f_1^s) = \ln K + (\alpha / RT) \times \quad (52)$$

$$\left[(1 - 2x_2^s) + m(1 - 2x_2^l) \right]$$

A plot of this equation enables values for K and α to be calculated for comparison with the K obtained from Equation (49) experimentally and α derived from properties of the bulk solution.

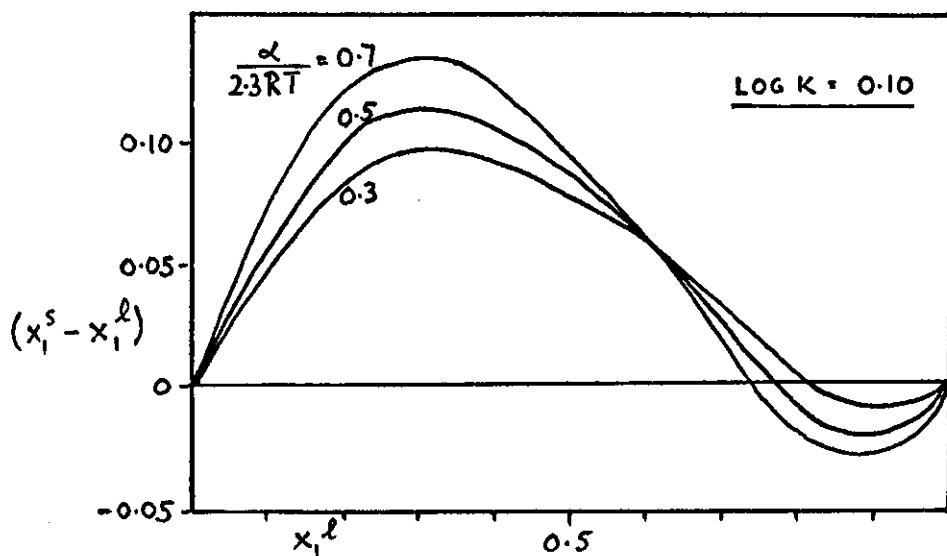


Fig. 14

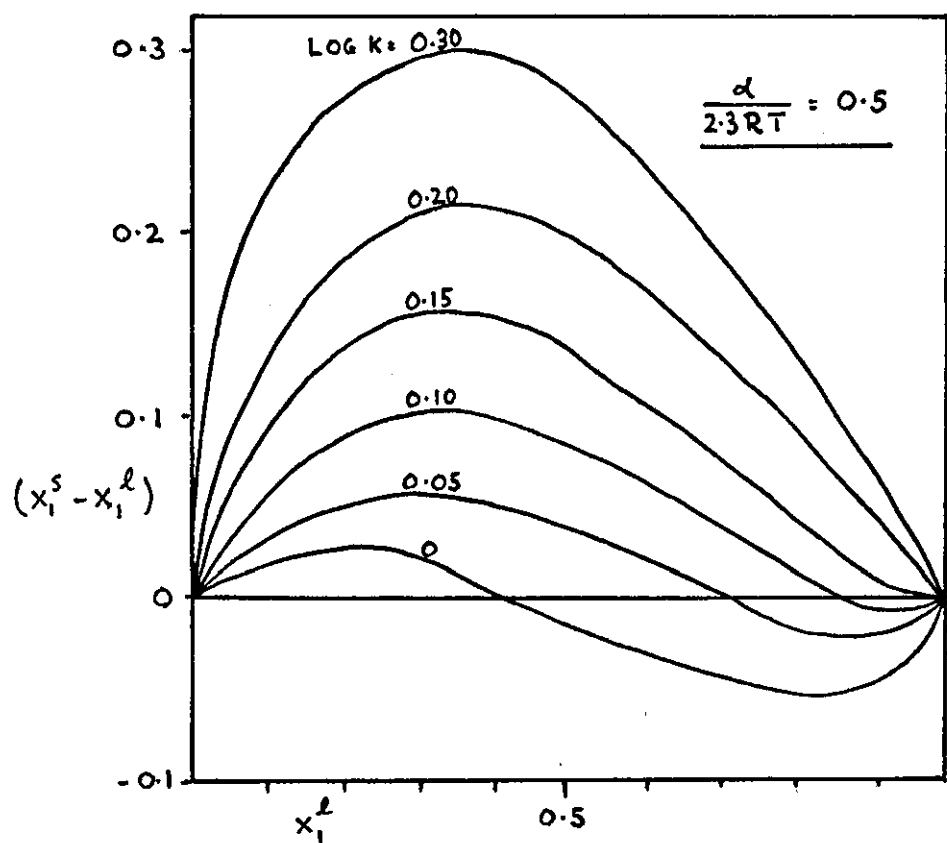


Fig. 15

Day, Eltekov, Parfitt and Thompson⁶⁶ have studied adsorption from binary liquid mixtures of p-xylene and n-heptane at 25°C onto characterised rutile surfaces containing various amounts of molecular water and hydroxyl groups. The composite isotherms obtained are shown in Fig. 16. Surface S1 was outgassed at 450°C and contained no molecular water on the surface, S4 had a water coverage approximating to one monolayer and S5 contained two to three monolayers of adsorbed water.

Values of the surface activity coefficients were calculated using the theory of Everett and are plotted against the surface mole fractions in Fig. 17. For the S1 surface, the surface activity coefficients for both components deviate markedly from unity and the authors attributed the non-ideality of the adsorbed phase to the presence on the surface of isolated hydroxyl groups and vacancy defects associated with the strong dehydroxylation which provide adsorption centres capable of strong interaction with the p-xylene. For the surfaces S4 and S5 which contain increasing amounts of adsorbed water the surface activity coefficients are seen to approach unity indicating that removal of the specific influence of the hydroxyl groups with adsorbed water leads to a surface phase which is approximately ideal over the whole range of composition. The authors concluded that the adsorbed layers formed on the surfaces S4 and S5 were sufficiently ideal for a thermodynamic analysis using the theory of Everett.

Fig. 16

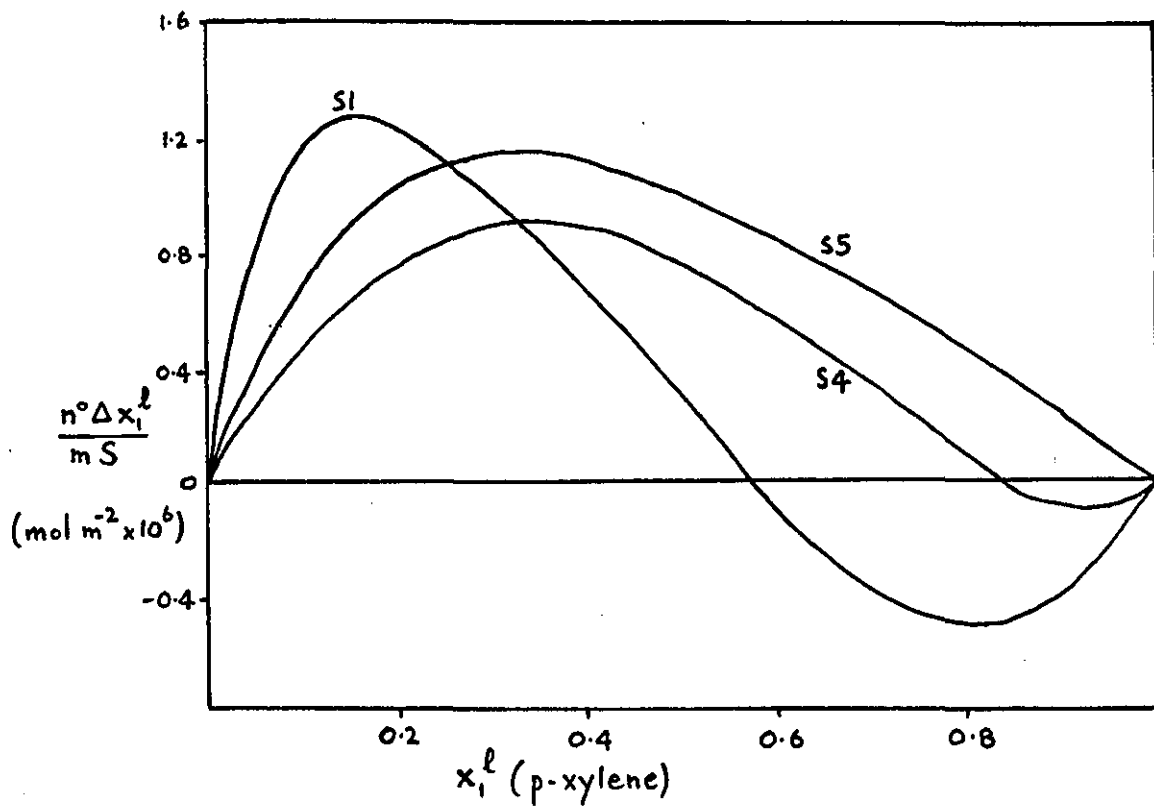
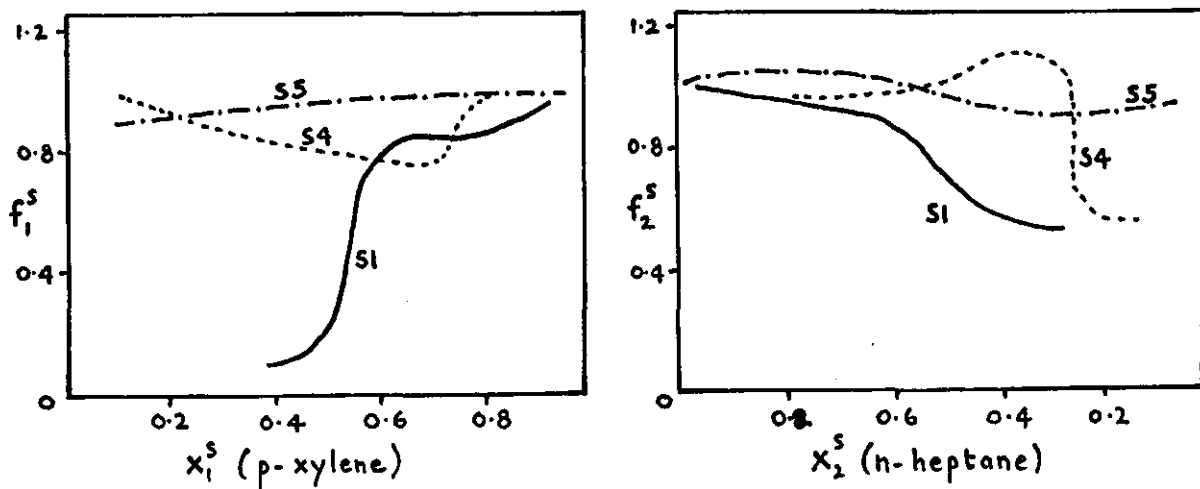


Fig. 17



Adsorption of p-Xylene from n-Heptane onto Rutile

(E) THE PRESENT INVESTIGATION

The benzene aromatic system has sustained a detailed physical and chemical exploration and has, to an extent, deprived other deserving systems of attention. It was with this premise in mind that the present investigation was conceived: it was hoped to supplement the author's earlier work on 4-substituted phenols with a similar study of a polynuclear series. So that new variables, which always seem to proliferate so freely with increasing molecular complexity, should not obscure the congruity intended between the two series, a parallel sequence of 4-substituted-1-naphthols was selected for study.

This investigation comprises two main parts: firstly, a consideration of association in the liquid phase, and secondly, adsorption at an activated alumina-solution interface from a binary liquid phase. For solute-solvent interactions in solution, quantitative measures are provided by the change in the naphtholic OH stretching frequency in the infrared and by the association constant, the temperature dependence of which enables estimates of the strength of bonding in the complexes formed to be made and estimates of other thermodynamic functions, such as entropy and free energy changes. For adsorption at the solid-solution interface, the adsorption affinity of the molecules for the surface is considered on a quantitative basis by means of Everett's thermodynamic theory of adsorption. In both sections changes in behaviour thought to be due to the influence of the 4-substituent are correlated with appropriate Hammett constants derived from data for naphthalene systems as outlined in Section (A) of this Introduction.

EXPERIMENTAL

(A) ASSOCIATION IN SOLUTION

1. Group Stretching Frequency in the Infrared

The frequencies of absorption maxima in the near infrared region of the spectrum have been measured in both cyclohexane and dioxan solutions for a series of 4-substituted-1-naphthols and the changes in frequency upon hydrogen bond formation with dioxan calculated.

(a) Materials and Apparatus

The preparation of the naphthols and the purification of solutes and solvents are described in the Appendix.

Spectroscopic measurements in the near infrared were made using a Unicam SP 700 recording spectrophotometer. The instrument was fitted with an absorbance unit (Unicam) and aluminium cell housings which permit the control of cell temperature by pumped circulation of water at $25 \pm 0.02^\circ\text{C}$ from a thermostatically controlled water bath.

In the region of interest, $4000 - 3000 \text{ cm}^{-1}$, the radiation from a tungsten filament lamp is dispersed by a grating (Merton - N.P.L. replica, 7500 lines/in., blazed at 3333 cm^{-1}) disposed at an angle to the incident beam. The monochromatic radiation from the exit slit is divided into two parts and passed alternatively through the sample and reference cells. The two beams are then focussed onto a lead sulphide detector and the signal from the latter passes to a recorder which displays the transmittance or absorbance of the sample cell with respect to the reference cell. The slit width is controlled automatically such that the energy detected in the reference beam is constant at a level determined by the resolution setting.

The spectrum is presented on the chart of a Honeywell recorder as a linear graph of percentage transmittance or absorbance against wavenumber (cm^{-1}), every 20 cm^{-1} being marked automatically by two pens at the edges of the chart.

The instrument has 5 scanning speeds and 4 chart speeds which allows optimum conditions to be selected for frequency measurement. A series of multipots are provided at 100 cm^{-1} intervals, to adjust the 100% transmittance line as a function of wavenumber and so compensate for differences in the transmission of the sample and reference cells or for differences in the optics of the two beams.

(b) Procedure

Solutions were prepared containing initial concentrations of naphthol and dioxan molecules such that the complex formed in solution gave approximately 50% transmittance. At these concentrations, solute-solute interactions were found to be negligible. Flasks containing the solutions were stored in a thermostatically controlled water bath ($25 \pm 0.02^\circ\text{C}$) and water from the latter was pumped through the cell housings for about two hours before any measurements were made. The two cells were rinsed and filled with carbon tetrachloride and then mounted in the cell compartments. The multipots were adjusted at 100 cm^{-1} intervals over the range required and a solvent-solvent base line recorded. The sample cell was then refilled with the solution under investigation and the spectrum recorded after the cell had attained thermal equilibrium. After a series of measurements had been made the solvent-solvent base line was rechecked.

The stretching frequencies of the 'free' and 'bonded' OH group in the naphthols were measured and the shift occurring on association calculated. Calibration of the instrument in the 3700 - 3500 cm^{-1} range was achieved by recording the absorption bands of water vapour in the atmosphere at the end of each series of measurements. The peak frequencies were located with a vernier scale to the nearest 0.5 cm^{-1} and compared with the precise literature values⁶⁷. The indene peak⁶⁷ at $3297.0 \pm 1.5 \text{ cm}^{-1}$ was used for frequency calibration in the vicinity of 3300 cm^{-1} .

(c) Experimental Results

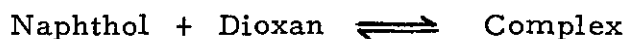
The experimental results are recorded in Table 6.

TABLE 6: IR FREQUENCY SHIFTS

Solute	Frequency of max. adsorption (cm^{-1})		Frequency Shift $\Delta\nu$ (cm^{-1})
	<u>Cyclohexane</u>	<u>Dioxan</u>	
4-t-butyl-1-naphthol	3622	3336	286
4-methyl-1-naphthol	3621	3332	289
1-naphthol	3616	3313	303
4-chloro-1-naphthol	3611	3288	323
4-bromo-1-naphthol	3609	3281	328
4-cyano-1-naphthol	3595	3222	373
4-nitro-1-naphthol	3598	3221	377

2. Association Constants

Hydrogen bonding association constants for the process



have been determined from absorbance measurements at a pre-determined wavelength in the ultraviolet for a series of solutions of the naphthol in cyclohexane-dioxan mixtures of varying composition.

(a) Apparatus

A Unicam SP 500 Photo-electric Quartz Spectrophotometer fitted with an accurately thermostatted cell compartment was used to measure absorbances. The instrument can be used to investigate the absorption characteristics of compounds in solution throughout the visible and ultraviolet regions (200 - 1000nm) of the spectrum. A deuterium discharge lamp, supplied with stabilised current of 300 mA is used for the ultraviolet region (200 - 320 nm), and a tungsten lamp for the visible region (320 - 1000 nm). The monochromator assembly consists of a quartz prism and collimating mirror with a slit aperture calibrated from 0.01 to 2.00 nm. Two photocells are employed, a red sensitive cell for use above 625 nm and an ultraviolet sensitive cell for use below 625 nm. A Labgear Power Supply Unit 115D provides a supply of 6V at 6A DC for the filament light source, and also 6V and 2V at 100 mA DC for valve heating. The photocell current is fed to a two stage amplifier and passes to an indicating meter which is adjusted to zero current by a potentiometer calibrated in both absorbance and percentage transmission scales.

(b) Preparation of Solutions

An approximately 10^{-4} molar solution of naphthol (of accurately known strength) in cyclohexane was prepared at 25°C (Solution A). In the event of very low solubility (4-cyano- and 4-nitro-1-naphthols) it proved impossible to prepare such a standard solution and so a saturated solution in cyclohexane was employed (probably 10^{-6} - 10^{-5} molar).

A solution of dioxan also in cyclohexane of known weight fraction was prepared by weighing (Solution B).

Solutions for absorbance measurements were prepared by weighing suitable volumes of solution B (e.g. 0, 0.5, 0.7, 1.1, 1.6, 2.5, 5.0 and 10.0 cm^3), adding 20 cm^3 of Solution A and diluting to 50 cm^3 with cyclohexane at 25°C . As reference solutions, solvent mixtures of composition identical to the solutions under examination were used.

(c) Determination of Optimum Wavelength for Absorbance Measurements

As a preliminary to the main experiment, ultraviolet spectra were recorded (using a Unicam SP 800 chart recording spectrophotometer) of approximately 10^{-4} molar solutions of the naphthol in cyclohexane and dioxan respectively. Upon superimposing and inspecting, a wavelength was chosen at which the difference between the absorbances of the two solutions was a maximum. An optimum wavelength for each of the substituted naphthols studied was determined in this manner.

(d) Measurement

Each sample solution was placed in the cell compartment together with the corresponding reference solution. After allowing sufficient time (at least 10 mins.) for thermal equilibrium to be established at 25°C, the absorbance of the Solution A was measured and in a similar manner the absorbance A° of the solution containing no dioxan was measured with the cyclohexane solvent as reference. The measurements were repeated at 35°C and to compensate for changes in density of the liquids a correcting factor was calculated from the ratio of the solution densities, giving

$$({}^C D)_{35^{\circ}C} = ({}^C D)_{25^{\circ}C} \times 0.98792$$

(e) Experimental Results

The results for the 1-naphthol-dioxan system are reported in full (Table 7) as a typical example: ultraviolet spectra are recorded in cyclohexane and dioxan solutions in Fig. 18, and Fig. 19 shows the Nagakura plot of $1/(A-A^{\circ})$ against $1/C_D$ from Equation (27) in the Introduction. The equilibrium constant values (negative intercepts on the $1/C_D$ axis) are reported from a 'least squares' assessment of the straight lines.

For the 4-substituted-1-naphthols results are reported more briefly in Tables 8 to 13 and the Nagakura plots are shown in Figs. 20 to 25 on pages 72, 73 and 74 .

TABLE 7 : 1-NAPHTHOL

- (i) Stock soln. : 0.0112g of 1-naphthol in 250cm³ cyclohexane soln.
 i. e. Molarity = 3.107×10^{-4} (20 cm³ in each 50 cm³ sample flask).
- (ii) Stock Soln. : 21.8514g of dioxan in 82.7468g of cyclohexane soln.
 i. e. 0.26856g of dioxan per 1g of solution.
- (iii) Optimum wavelength : 310 m μ when $A_{25^{\circ}\text{C}}^{\circ} = 0.304$,
 $A_{35^{\circ}\text{C}}^{\circ} = 0.298$.

(iv) Concentrations C_D expressed in mol dm⁻³.

<u>Dioxan soln. (g)</u>	<u>∴ Dioxan (g)</u>	<u>C_D</u>	<u>$1/C_D(25^{\circ}\text{C})$</u>	<u>$1/C_D(35^{\circ}\text{C})$</u>
0.4022	0.10801	0.02452	40.7830	41.2818
0.4869	0.13076	0.02968	33.6893	34.1013
0.5666	0.15216	0.03454	28.9503	29.3044
0.7277	0.19543	0.04436	22.5413	22.8170
0.8876	0.23837	0.05411	18.4805	18.7065
1.3082	0.35133	0.07975	12.5389	12.6923
2.2025	0.59150	0.13427	7.4476	7.5387
8.1768	2.19594	0.49849	2.0061	2.0306

<u>25°C:</u>	<u>A</u>	<u>A-A^o</u>	<u>1/(A-A^o)</u>	<u>35°C:</u>	<u>A</u>	<u>A-A^o</u>	<u>1/(A-A^o)</u>
	0.356	0.052	19.231		0.334	0.036	27.778
	0.363	0.059	16.949		0.340	0.042	23.810
	0.368	0.064	15.625		0.344	0.046	21.739
	0.378	0.074	13.514		0.353	0.055	18.182
	0.384	0.080	12.500		0.362	0.064	15.625
	0.403	0.099	10.101		0.372	0.077	12.987
	0.423	0.119	8.403		0.393	0.095	10.526
	0.453	0.149	6.711		0.427	0.129	7.752

$K_c = 18.45$

$K_c = 12.95$

Fig. 18

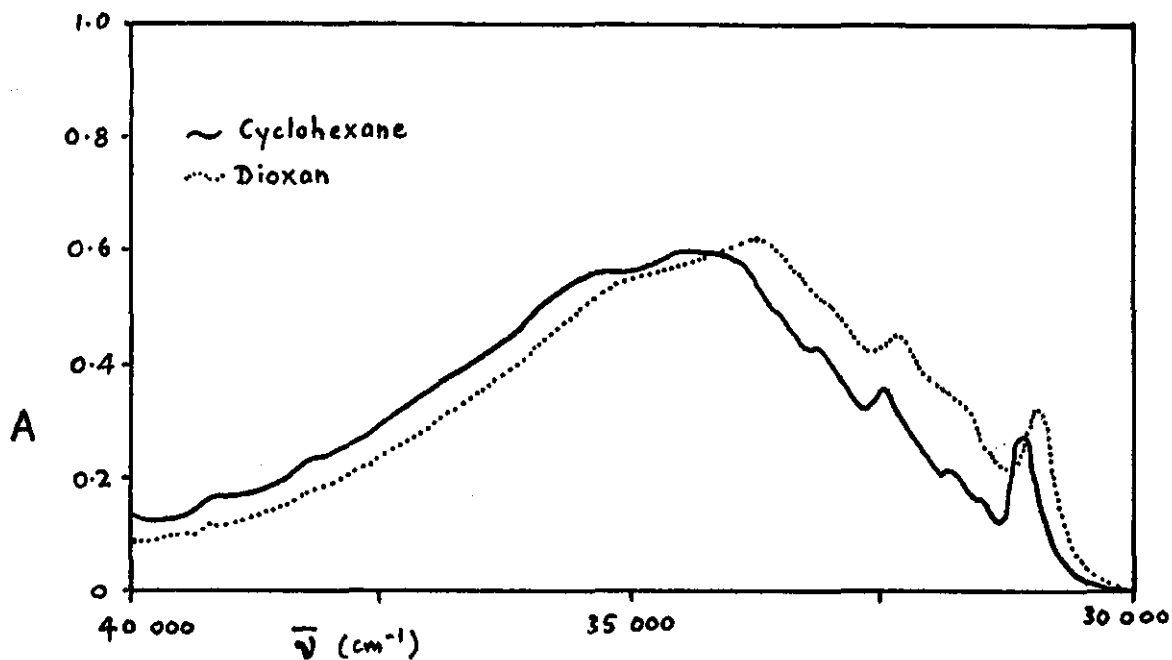


Fig. 19

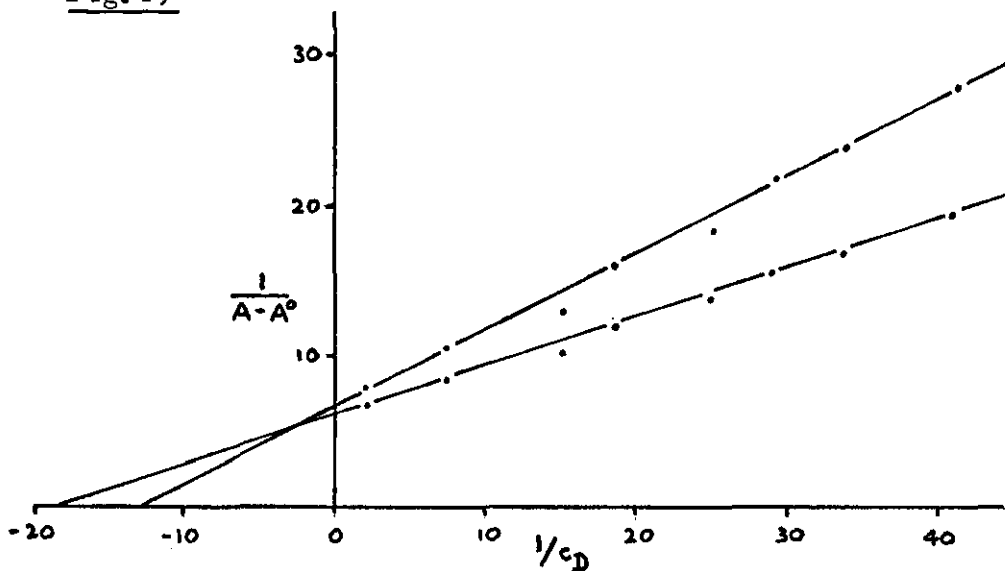


TABLE 8 : 4-t-BUTYL-1-NAPHTHOL

25°C

$$C_A = 0.8585 \times 10^{-4} \text{M}, A^0 = 0.068$$

<u>C_D</u>	<u>1/C_D</u>	<u>A</u>	<u>1/(A-A⁰)</u>
0.02554	39.152	0.103	28.571
0.03004	33.288	0.108	25.000
0.03602	27.759	0.113	22.222
0.04629	21.603	0.121	18.868
0.06939	14.411	0.135	14.925
0.08723	11.464	0.145	12.987
0.15911	6.285	0.166	10.204
0.42194	2.370	0.192	8.065

$$K_c = 12.14 \text{ dm}^3 \text{ mol}^{-1}$$

35°C

$$C_A = 0.8481 \times 10^{-4} \text{M}, A^0 = 0.065$$

<u>C_D</u>	<u>1/C_D</u>	<u>A</u>	<u>1/(A-A⁰)</u>
0.02523	39.631	0.091	38.462
0.02968	33.695	0.096	32.258
0.03559	28.098	0.100	28.571
0.04573	21.867	0.106	24.390
0.06855	14.587	0.119	18.519
0.08618	11.604	0.128	15.873
0.15718	6.362	0.148	12.048
0.41684	2.399	0.176	9.009

$$K_c = 9.17 \text{ dm}^3 \text{ mol}^{-1}$$

TABLE 9 : 4-METHYL-1-NAPHTHOL

25°C

$$C_A = 0.6759 \times 10^{-4} \text{ M}, \quad A^\circ = 0.079$$

<u>C_D</u>	<u>1/C_D</u>	<u>A</u>	<u>1/(A-A^o)</u>
0.02446	40.885	0.111	31.250
0.02950	33.894	0.114	28.571
0.03414	29.293	0.118	25.641
0.04349	22.992	0.124	22.222
0.05374	18.607	0.130	19.608
0.07855	12.730	0.141	16.261
0.13229	7.559	0.156	12.992
0.49173	2.034	0.183	9.662

$$K_c = 13.75 \text{ dm}^3 \text{ mol}^{-1}$$

35°C

$$C_A = 0.6677 \times 10^{-4} \text{ M}, \quad A^\circ = 0.072$$

<u>C_D</u>	<u>1/C_D</u>	<u>A</u>	<u>1/(A-A^o)</u>
0.02416	41.385	0.098	39.216
0.02915	34.308	0.100	35.712
0.03373	29.651X	0.104	31.250
0.04297	23.273	0.108	27.778
0.05309	18.835	0.116	22.994
0.07760	12.886	0.128	18.018
0.13069	7.652	0.148	14.605
0.48579	2.059	0.174	9.804

$$K_c = 10.23 \text{ dm}^3 \text{ mol}^{-1}$$

TABLE 10 : 4-CHLORO-1-NAPHTHOL

25°C

$$C_A = 0.8062 \times 10^{-4} \text{ M}, A^\circ = 0.071$$

<u>C_D</u>	<u>1/C_D</u>	<u>A</u>	<u>1/(A-A^o)</u>
0.02302	43.440	0.117	21.739
0.02801	35.700	0.114	23.263
0.03264	30.641	0.119	20.833
0.04175	23.950	0.126	18.182
0.05085	19.664	0.136	15.385
0.07462	13.401	0.139	14.706
0.12621	7.923	0.150	12.658
0.46773	2.138	0.166	10.526

$$K_c = 26.50 \text{ dm}^3 \text{ mol}^{-1}$$

35°C

$$C_A = 0.7964 \times 10^{-4} \text{ M}, A^\circ = 0.070$$

<u>C_D</u>	<u>1/C_D</u>	<u>A</u>	<u>1/(A-A^o)</u>
0.02274	43.971	0.101	33.333
0.02767	36.137	0.102	32.261
0.03224	31.016	0.105	28.571
0.04125	24.243	0.110	25.000
0.05024	19.904	0.120	20.000
0.07372	13.565	0.122	18.231
0.12469	8.020	0.134	15.625
0.46211	2.164	0.151	12.346

$$K_c = 20.15 \text{ dm}^3 \text{ mol}^{-1}$$

TABLE 11 : 4-BROMO-1-NAPHTHOL

25°C

$$C_A = 0.8444 \times 10^{-4} \text{ M}, A^{\circ} = 0.125$$

<u>C_D</u>	<u>1/C_D</u>	<u>A</u>	<u>1/(A-A^o)</u>
0.02234	44.757	0.168	23.256
0.02717	36.807	0.173	20.833
0.03172	31.529	0.176	18.868
0.04056	24.657	0.184	16.949
0.04974	20.104	0.190	15.385
0.07256	13.781	0.199	13.514
0.12274	8.147	0.211	11.628
0.45663	2.190	0.227	9.804

$$K_c = 29.32 \text{ dm}^3 \text{ mol}^{-1}$$

35°C

$$C_A = 0.8342 \times 10^{-4} \text{ M}, A^{\circ} = 0.122$$

<u>C_D</u>	<u>1/C_D</u>	<u>A</u>	<u>1/(A-A^o)</u>
0.02207	45.305	0.155	30.303
0.02684	37.257	0.160	26.316
0.03133	31.914	0.164	23.810
0.04007	24.959	0.170	20.833
0.04914	20.350	0.175	18.868
0.07168	13.950	0.185	15.873
0.12126	8.247	0.197	13.333
0.45106	2.217	0.216	10.638

$$K_c = 21.21 \text{ dm}^3 \text{ mol}^{-1}$$

TABLE 12 : 4-CYANO-1-NAPHTHOL

25°C

$$A^{\circ} = 0.105$$

<u>C_D</u>	<u>1/C_D</u>	<u>A</u>	<u>1/(A-A[°])</u>
0.01316	75.975	0.246	7.092
0.01447	69.105	0.256	6.623
0.01853	53.979	0.271	6.024
0.02213	45.188	0.284	5.587
0.03229	30.970	0.305	5.000
0.05822	17.176	0.336	4.329
0.11558	8.652	0.360	3.922
0.23821	4.198	0.374	3.717

$$K_c = 75.91 \text{ dm}^3 \text{ mol}^{-1}$$

35°C

$$A^{\circ} = 0.099$$

<u>C_D</u>	<u>1/C_D</u>	<u>A</u>	<u>1/(A-A[°])</u>
0.01300	76.923	0.204	9.524
0.01429	69.979	0.212	8.850
0.01831	54.615	0.225	7.937
0.02186	45.746	0.239	7.143
0.03190	31.348	0.262	6.135
0.05752	17.385	0.296	5.076
0.11418	8.758	0.322	4.484
0.23533	4.249	0.340	4.149

$$K_c = 51.42 \text{ dm}^3 \text{ mol}^{-1}$$

TABLE 13 : 4-NITRO-1-NAPHTHOL

25°C

$$A^{\circ} = 0.102$$

<u>C_D</u>	<u>1/C_D</u>	<u>A</u>	<u>1/(A-A^o)</u>
0.01093	91.528	0.155	6.452
0.01479	67.610	0.178	5.618
0.01923	52.006	0.198	5.051
0.02616	38.233	0.218	4.587
0.03731	26.799	0.239	4.184
0.05827	17.161	0.265	3.774
0.09223	10.842	0.283	3.534
0.27693	3.611	0.305	3.279

$$K_c = 83.49 \text{ dm}^3 \text{ mol}^{-1}$$

35°C

$$A^{\circ} = 0.094$$

<u>C_D</u>	<u>1/C_D</u>	<u>A</u>	<u>1/(A-A^o)</u>
0.01080	92.647	0.222	7.813
0.01461	68.437	0.242	6.757
0.01900	52.642	0.264	5.882
0.02584	38.701	0.285	5.236
0.03686	27.127	0.311	4.608
0.05756	17.371	0.339	4.082
0.09111	10.975	0.362	3.731
0.27358	3.655	0.393	3.344

$$K_c = 59.81 \text{ dm}^3 \text{ mol}^{-1}$$

Fig. 20 4-t-Butyl-1-naphthol

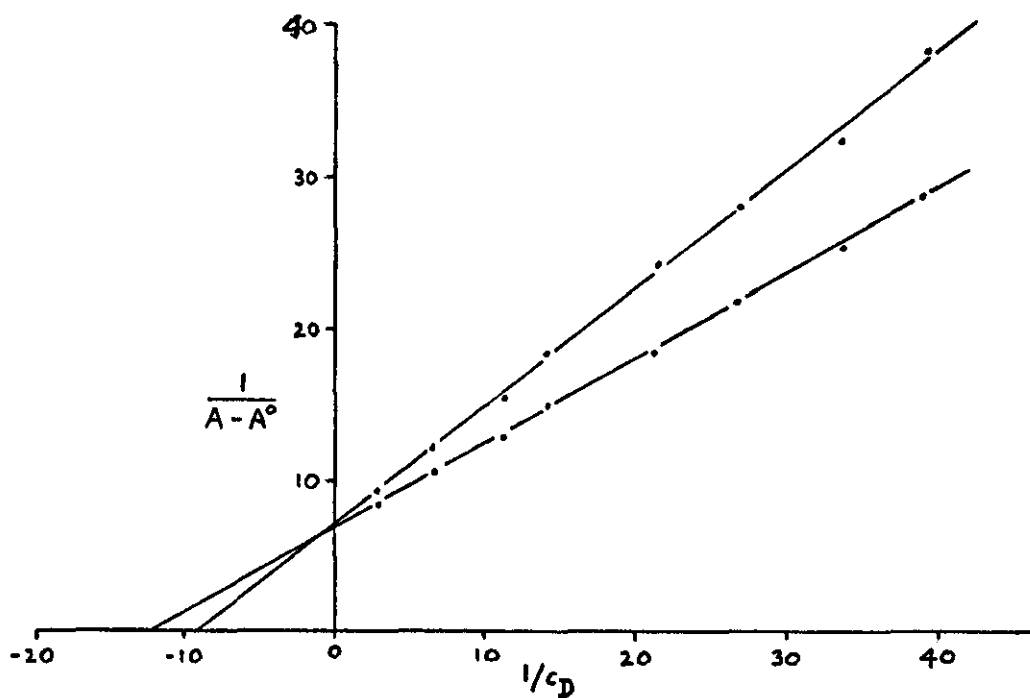


Fig. 21 4-Methyl-1-naphthol

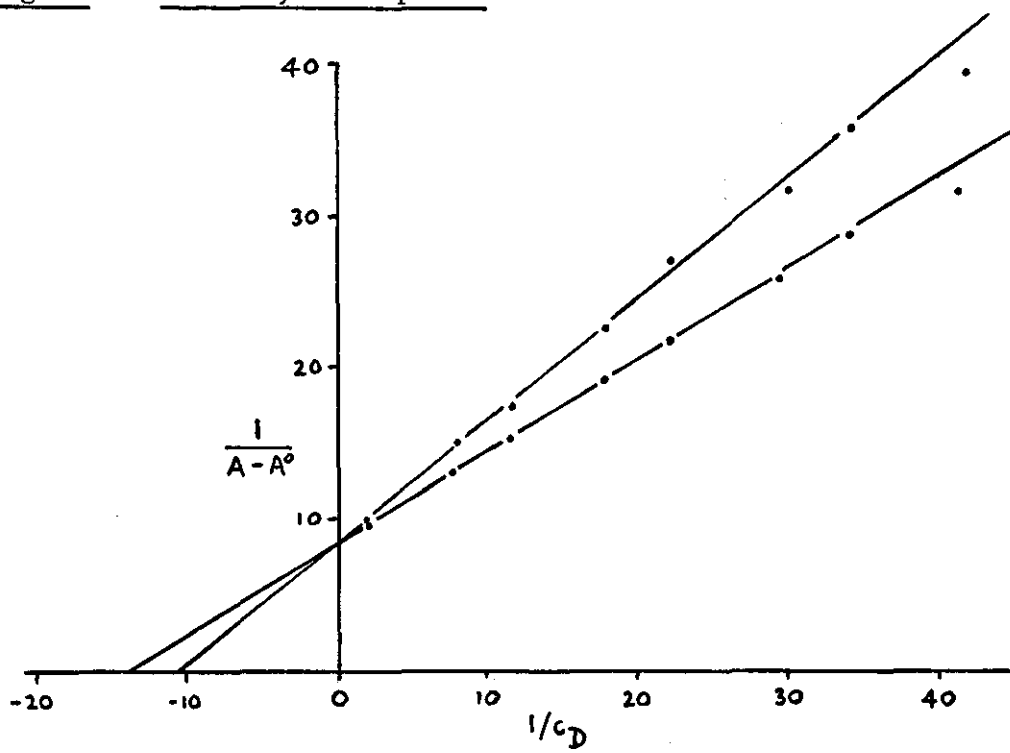


Fig. 22 4-Chloro-1-naphthol

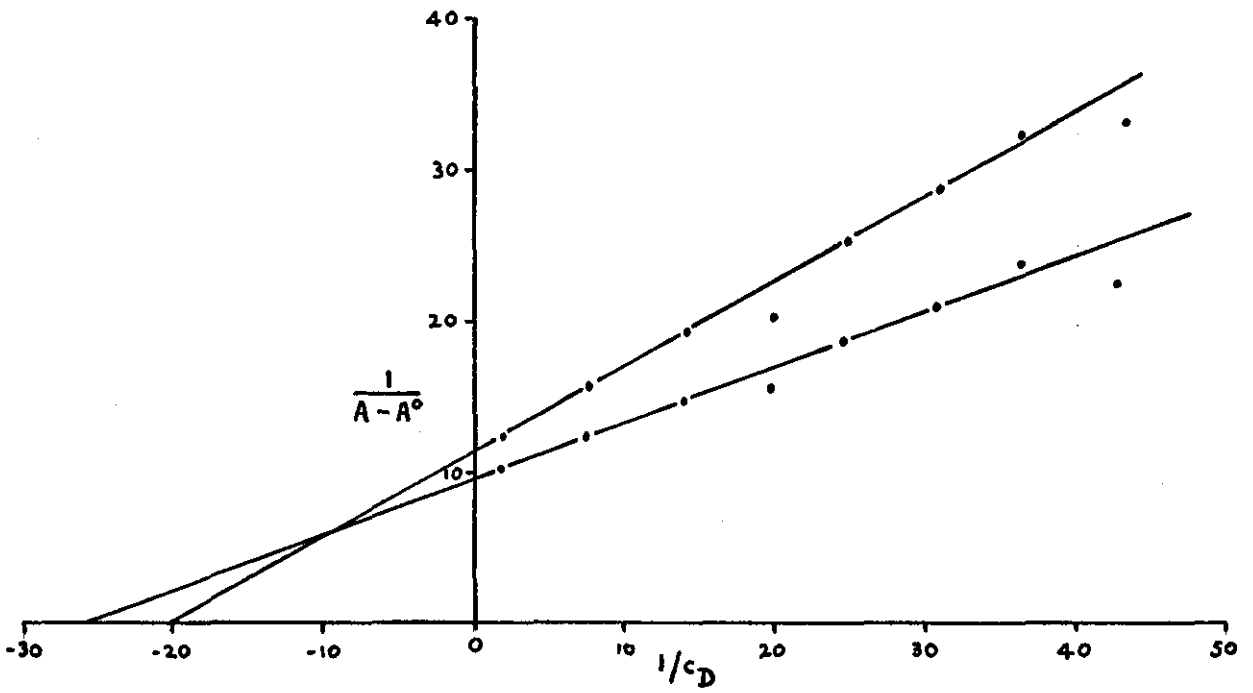


Fig. 23 4-Bromo-1-naphthol

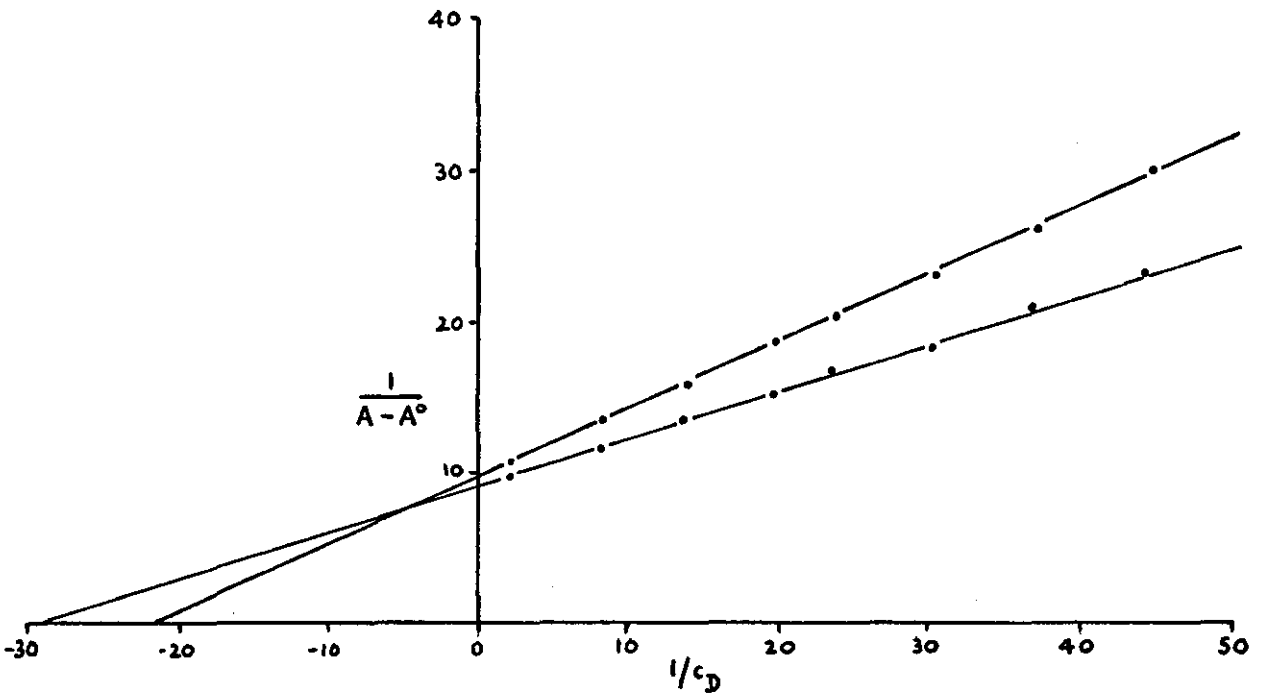


Fig. 24 4-Cyano-1-naphthol

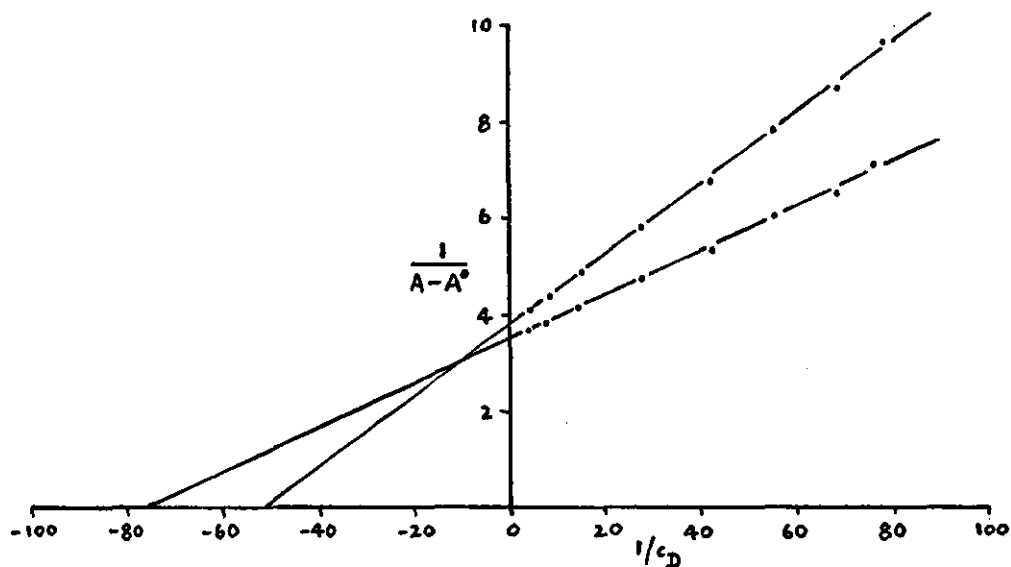
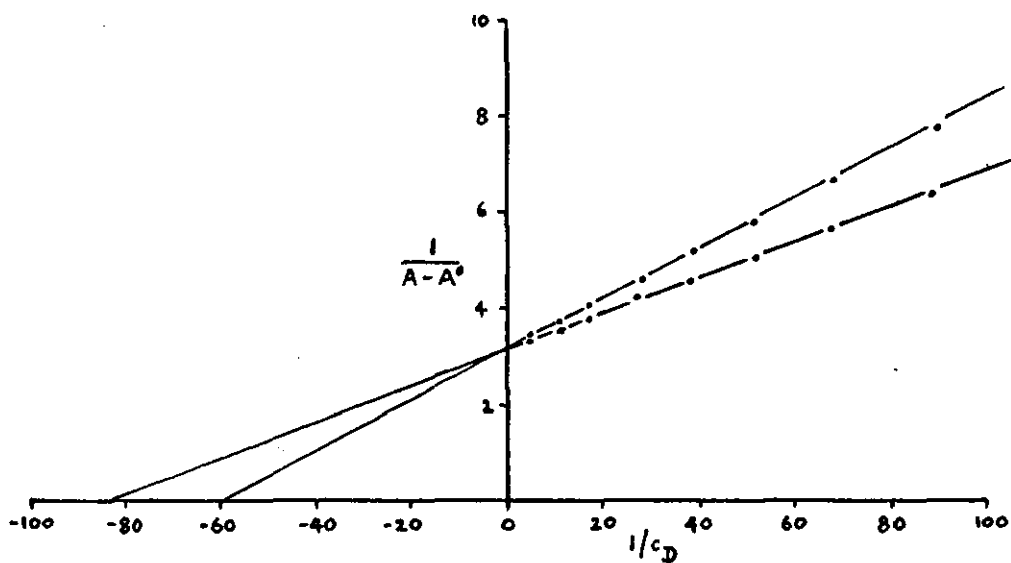


Fig. 25 4-Nitro-1-naphthol



Association constants were also calculated by the more rigorous procedure of Rose and Drago²⁹ based on Equation (26). An approximate value of K_c was first calculated from Equation (27) and used to calculate a series of values for ${}_e c_c$ (equilibrium concentration of complex) and ${}_e c_A$ (equilibrium concentration of acceptor) from the experimentally determined values of C_D and C_A by application of Equations (21) and (23). Substituting these values in Equation (22) enables the extinction coefficient of the complex ϵ_c to be evaluated at each donor concentration. An average extinction coefficient was calculated and values taken either side of the mean. Insertion of these values in Equation (26) gives further K_c values and a plot of K_c^{-1} against ϵ_c can be constructed for each donor concentration. As the true value of K_c is constant, the straight lines corresponding to different values of donor concentration should intersect at one point. In practice, the majority of the intersections occur in a small area (Fig. 26) indicating good experimental precision and strong support for the assumption that a 1:1 complex is formed in solution. Association constants for the complexes were determined for all intersections and an average K_c and standard deviation calculated. By eliminating those K_c values outside twice the standard deviation, until the latter changed by less than 20%, association constants were obtained with standard deviations of the order of 5%.

An IBM 1130 computer was programmed to carry out the calculations and the author is grateful to J. Deuchar for processing the results reported earlier. The method of calculation is illustrated below and in Table 14 for the association of 1-naphthol to

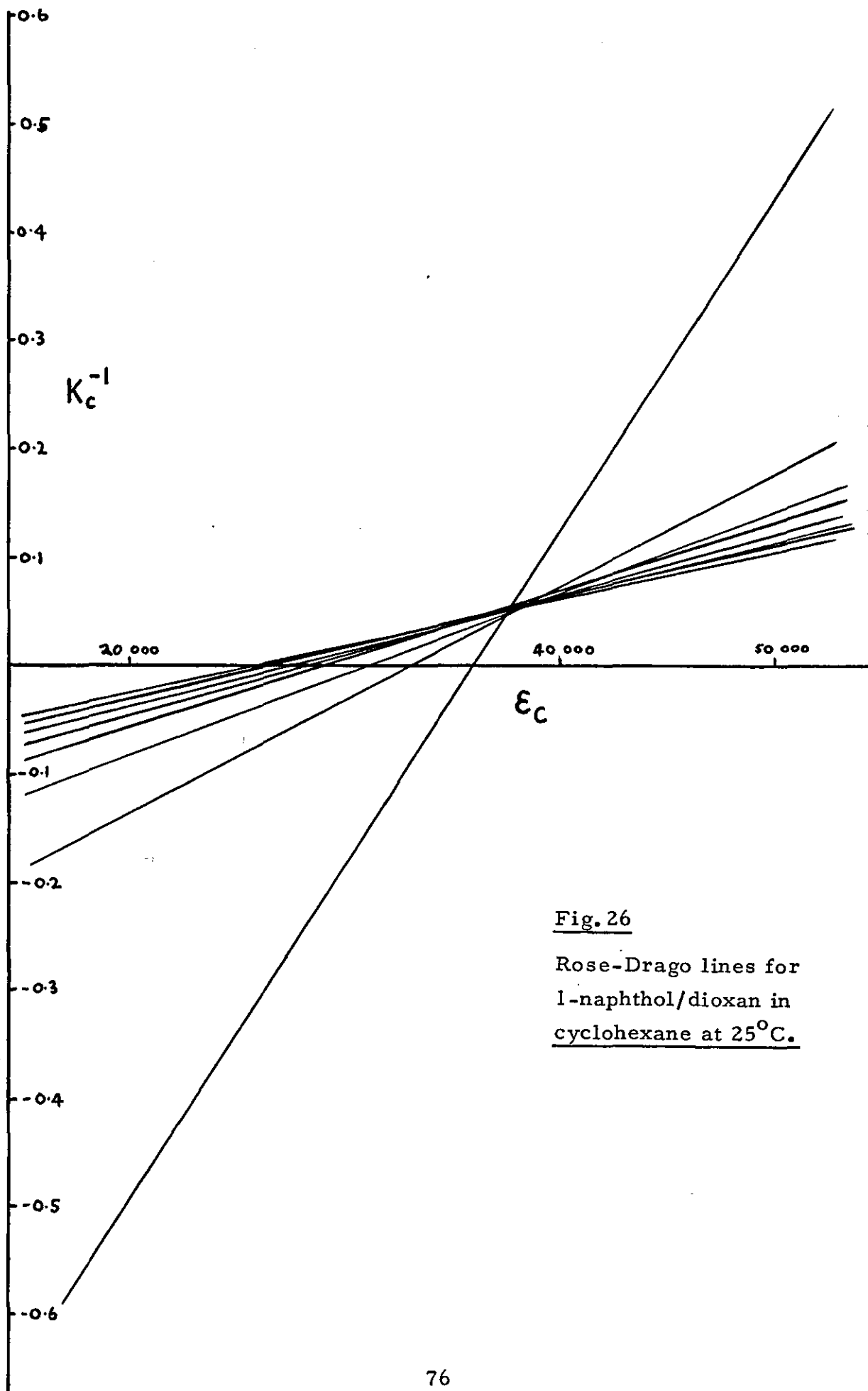


Fig. 26

Rose-Drago lines for
1-naphthol/dioxan in
cyclohexane at 25°C.

dioxan in cyclohexane solution at 25°C. (It should be noted that the Rose-Drago treatment could not be accurately applied to data for 4-cyano- and 4-nitro-1-naphthols owing to their very low, and therefore indeterminate, solubility in cyclohexane.)

The experimental data are given in Table 7 from which the mean extinction coefficient of the complex is calculated to be $37,620 \text{ dm}^2 \text{ mol}^{-1}$ for a path length of 0.1 dm. Using values $37,620 \pm 1000$ for the extinction coefficient, ϵ_c , two values of K_c are found from Equation (26) and a series of plots for each donor concentration of K_c^{-1} against ϵ_c constructed (Fig. 26). The points of intersection of each line with each other, representing values of K_c , are given in Table 14. Values marked * are rejected as outside twice the standard deviation and the process repeated until a standard deviation is obtained which is a change of less than 20% on the previous value.

Finally, the results of calculations on association in solution measurements are summarised in Table 15.

TABLE 14

<u>K_c</u> /(dm ³ mol ⁻¹)	<u>Deviation</u>	<u>K_c</u> /(dm ³ mol ⁻¹)	<u>Deviation</u>
19.038	- 0.635	23.471	+ 3.799
22.391	+ 2.719	17.512	- 2.160
20.633	+ 0.960	17.611	- 2.062
23.009	+ 3.336	18.312	- 1.361
18.757	- 0.916	31.716	+12.043*
18.466	- 1.207	17.108	- 2.565
18.816	- 0.857	17.408	- 2.265
27.087	+ 7.414	18.284	- 1.389
21.377	+ 1.705	12.500	- 7.173
24.332	+ 4.659	15.210	- 4.463
18.708	- 0.965	17.118	- 2.555
18.399	- 1.273	17.783	- 1.890
18.799	- 0.874	18.871	- 0.801
18.525	- 1.148	19.596	- 0.076

Mean K_c value = 19.672

Standard deviation = 3.717

Further refinement and rejection reduces the number of intersections from 28 to 19 and the standard deviation down to 1.079 giving a final mean K_c value of 18.556.

TABLE 15: A Summary of Hydrogen Bonding Association Constants

<u>4-Substituent</u>	<u>Nagakura & Baba²⁴</u>	<u>Rose & Drago²⁹</u>	<u>Preferred Values[*]</u>
C(CH ₃) ₃ : 25°C	12.17	12.22	12.14
35°C	8.42	8.42	9.17
CH ₃ : 25°C	15.41	13.84	13.75
35°C	10.32	9.57	10.23
H : 25°C	18.82	18.56	18.45
35°C	12.99	12.94	12.95
Cl 25°C	29.08	27.23	26.50
35°C	21.71	20.13	20.15
Br 25°C	28.26	28.49	29.32
35°C	20.91	21.17	21.21
CN 25°C	74.71	-	75.91
35°C	52.90	-	51.42
NO ₂ 25°C	83.62	-	83.49
35°C	58.95	-	59.81

* Results with appreciable (obvious) experimental error excluded from the outset.

(B) SORPTION STUDIES

For an understanding of the adsorption process at the solid-solution interface a knowledge of the character of the adsorbent surface is essential, and information on the following is required :-

- (a) the nature and distribution of surface adsorption sites on the polar adsorbent used,
- (b) the 'external' and 'internal' surface areas of the adsorbent, i. e. the extent of porosity of the surface obtained from a pore size distribution analysis assuming a predominant pore shape for the adsorbent, and
in the light of the above information, the determination of the specific surface area available to the adsorptive molecules.

Since considerable work has already been carried out on the alumina used in this study by the author and others^{32, 34, 68} these data will be summarised during the course of this section.

1. Adsorption at the Gas-solid Interface: Characterisation of the Alumina

(a) Structure

(i) The Bulk Composition

Activated alumina such as the type used in this study is produced by the controlled heating of the hydrate which exists in four different modifications, i. e. hydrargillite, bayerite, diaspore and boehmite. X-ray diffraction examination^{69, 70, 71} has shown the existence of seven nearly anhydrous forms of alumina intermediate between the hydrate and the final decomposition product, α alumina, obtained at 1000°C. The alumina used in this investigation was heated to 800°C during manufacture and the suppliers (Camag) classify the material as ' γ -alumina'. A sample of the alumina was submitted to a detailed X-ray diffraction examination at the laboratories of the B.P. Research Centre at Sunbury-on-Thames, who report that the sample consists mainly of γ -alumina admixed with approximately 10% boehmite (the γ -monohydrate). Electron micrographs of the alumina revealed the presence of slit and wedge-shaped pores.³⁴

De Boer et al⁷² report that the bulk structure of all aluminas formed between the decomposition temperature of the hydrates and 1000°C approximate closely in arrangement to a close packed cubic oxygen sub-lattice similar to that of the spinels. Accordingly, the bulk structure can be taken as a pseudo-spinel type but with a cation deficiency, i. e. the thirty two oxygen ions are arranged as in cubic close packing with the appropriate number of aluminium ions (namely, $21\frac{1}{2}$) in both tetrahedrally and octahedrally co-ordinated

interstices but distributed at random over the twenty four sites normally occupied by the cations. On average, therefore, there are $2\frac{2}{3}$ vacant cation sites per unit cell which is the γ -alumina structure⁷³ with lattice parameter 0.795nm.⁶⁹

(ii) Nature of the Surface

In his investigations on alumina Peri⁷⁴ has proposed a theoretical model for the surface which agrees well with experimental results from infrared and gravimetric studies of surface hydration of γ -alumina. After drying at 100°C a monolayer of hydroxyl ions was thought to occupy the surface which was then progressively denuded by elimination of water molecules as the temperature was raised. The very high frequencies observed for the O-H stretching vibrations of hydroxyl groups on alumina prompted Peri to regard these as ions rather than groups covalently bound to surface aluminium ions although some degree of covalent character is probably present.

Peri considered an array of 10,000 sites and programmed a computer to remove at random the maximum number of adjacent hydroxyl pairs without producing surface defects. He found that only 67% of the original hydroxide layer could be removed giving an ordered lattice with no immediately adjacent aluminium ions and no immediately adjacent oxygen ions (Fig. 27). Further removal of hydroxyl pairs results in defects and when 90.4% have been removed the remainder (9.6%) are in isolated positions necessitating surface migration of ions for further elimination of water molecules. The remaining 9.6% of the surface hydroxyls find themselves distributed between five possible types of environment having 0, 1, 2, 3 or 4 nearest oxide neighbours respectively as shown in Fig. 28.

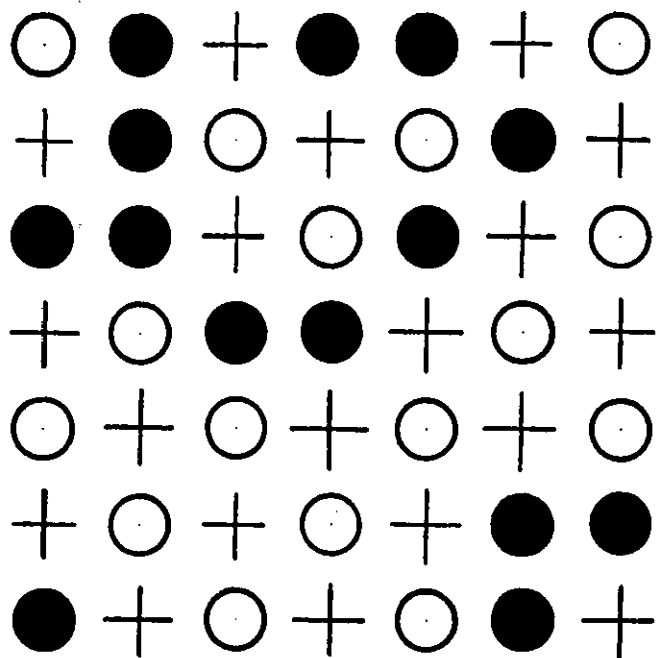


Fig. 27

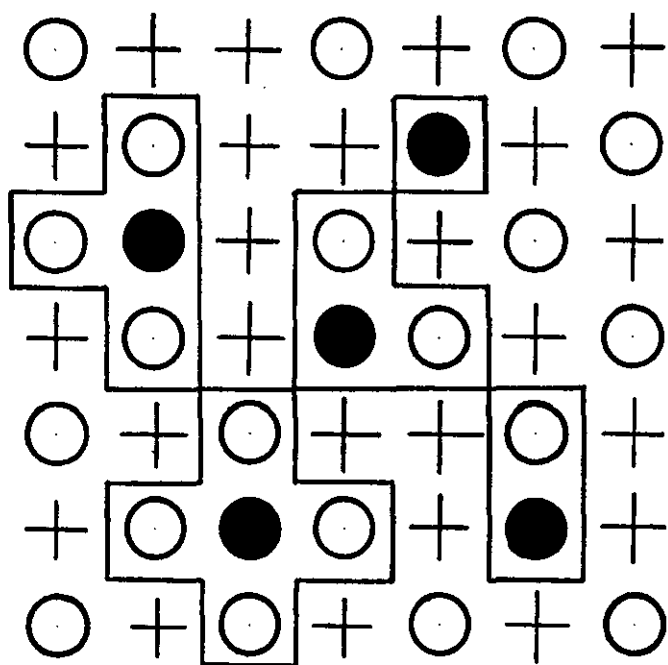
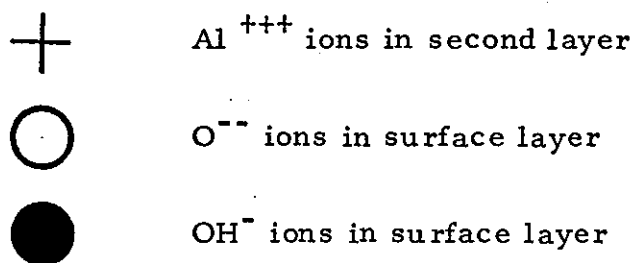


Fig. 28

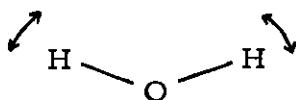
Peri found in practice that evacuation of alumina at 650°C left approximately 10% of the surface covered by hydroxyl groups and that a sample in this state gave rise to five hydroxyl bands in the infrared spectrum. Returning to the model, he assumed that surface migration tended to minimise the number of defects; that mobility of ions increased in the order : oxide ion, hydroxyl ion, proton; and that the band intensity for any of the five types of isolated groups should be proportional to the number of hydroxyl groups appearing on the model. Further dehydration under these conditions demonstrated that the various types of isolated groups were removed at different rates so enabling Peri to assign an absorption band to a particular type :-

Absorption band frequency (cm ⁻¹)	No. of nearest oxide neighbours
3800	4
3744	2
3700	0
3780	3
3733	1

Peri's speculative model for the surface of γ -alumina gives a plausible explanation of dehydroxylation experiments in terms of defects persisting in boundaries between odd and even surface oxide domains, rather than strained oxide linkages⁷⁵. Further, that experimental findings complement results predicted from the model so well, supports Peri's original hypothesis that the 100, 010 and 001 faces are exposed rather than the 111 faces of the oxygen sub-lattice upon cleavage of the alumina matrix.

Infrared spectroscopy is of the greatest value in observing perturbation of the surface groups which occurs during adsorption. Hydrogen bonding displaces the frequency of the OH stretching vibration to lower values and considerably broadens and intensifies the absorption band. This is a general finding and occurs for OH groups in solution^{76, 18} and also for structural OH groups on surfaces⁷⁷.

It is possible to distinguish between OH groups and water molecules adsorbed on the oxide surface by examination of the infrared spectrum in the regions $3800-3300\text{ cm}^{-1}$ and $1650-1600\text{ cm}^{-1}$. Molecular water exhibits an infrared active deformation vibration with movement of the hydrogen atoms in the plane of the molecule:



which produces an absorption band in the region of 1630 cm^{-1} for liquid water. The OH stretching vibrations of liquid water occur at about 3450 cm^{-1} and show marked evidence for hydrogen bonding.

γ -Alumina upon drying exhibits some interesting spectral changes⁷⁸ suggesting that calcination at 600°C and subsequent exposure to moist air results in molecular water and OH groups on the surface. Reheating causes desorption of some water molecules and forms OH groups from the rest, although at higher temperatures this is reversed and OH groups combine to form water which is removed. Ultimately three types of OH group remain which represent isolated groups on different types of surface site.

Broad absorption bands corresponding to stretching and bending frequencies found in the spectrum of liquid water are shown near 3300 and 1650 cm^{-1} by undried alumina but after evacuation at 650-700°C well defined absorption maxima at 3698, 3737 and 3795 cm^{-1} were displayed. These were due to OH stretching vibrations confirmed by deuterium exchange which produced new bands at 2733, 2759 and 2803 cm^{-1} . Quantitative measurements of surface coverage by hydroxyl groups were made by deuterium exchange and showed a 40% coverage after drying at 400°C, a 2% coverage at 800°C and less than 1% above 900°C, nonetheless the three OH bands were still evident on such very dry alumina.

Groups of a single type could not readily be converted into other types indicating that hydroxyl groups occupied specific sites, precluding random motion, and the high band frequencies suggest that attachment to the surface is largely ionic in character, as is γ -alumina itself.⁷⁹

Peri⁸⁰ heated γ -aluminas at 800°C and then resorbed water onto the surface (which even after this treatment would still hold 1-2% of water as hydroxyl groups^{78, 81}). He found at the B-point (monolayer coverage) that 6.25 molecules of water per nm^2 were rapidly and irreversibly adsorbed, i.e. each molecule required 0.16 nm^2 of surface, and that when exposed to water vapour at saturation pressure (about 200 nm) at room temperature for sixteen hours followed by two hours at 100°C at the same pressure the total adsorption was 12.5 molecules per nm^2 or 0.08 nm^2 of surface per molecule. Kipling and Peakall⁸² quote 13 molecules per nm^2 after evacuation at 25°C for 100 hours.

Fig. 29

Thermogravimetric analysis (T.G.A.)

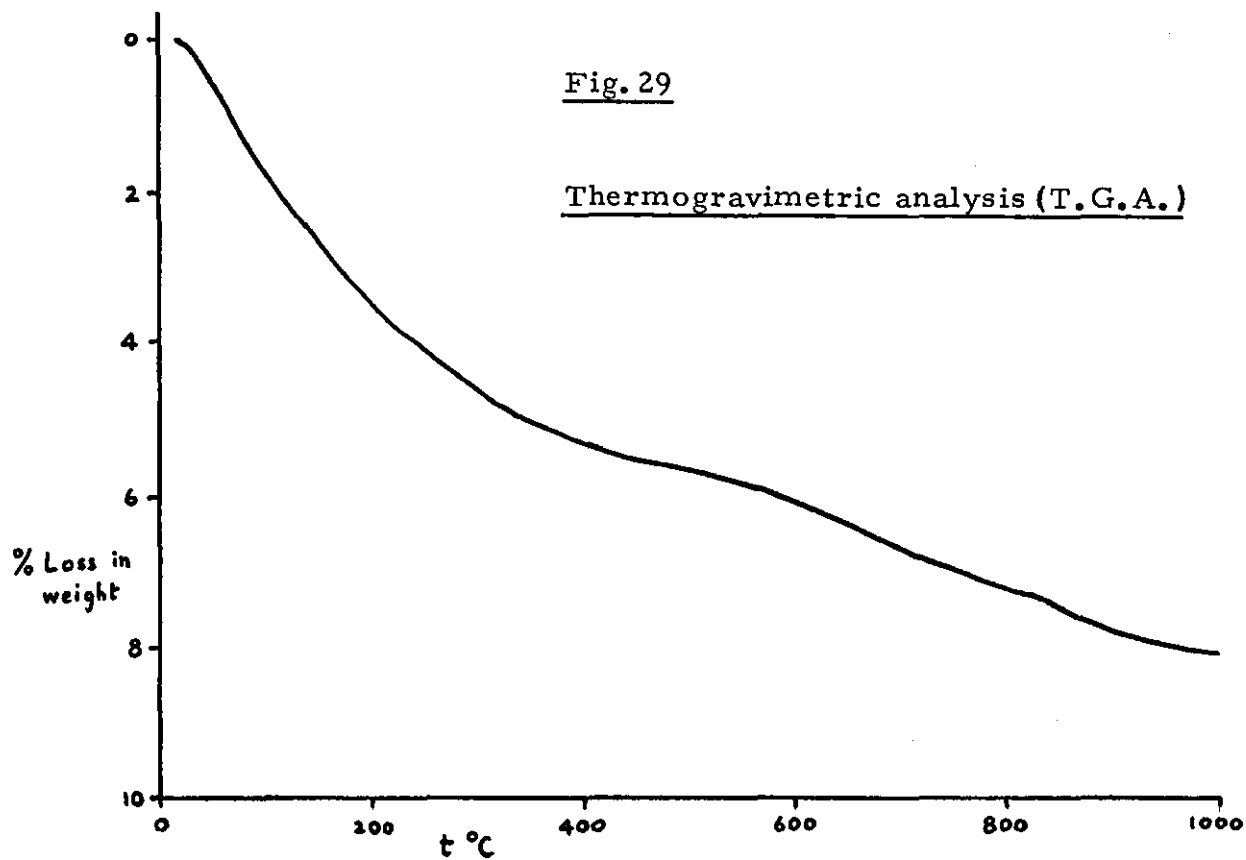


Fig. 30

DIFFERENTIAL PLOT OF THE THERMOGRAVIMETRIC CURVE

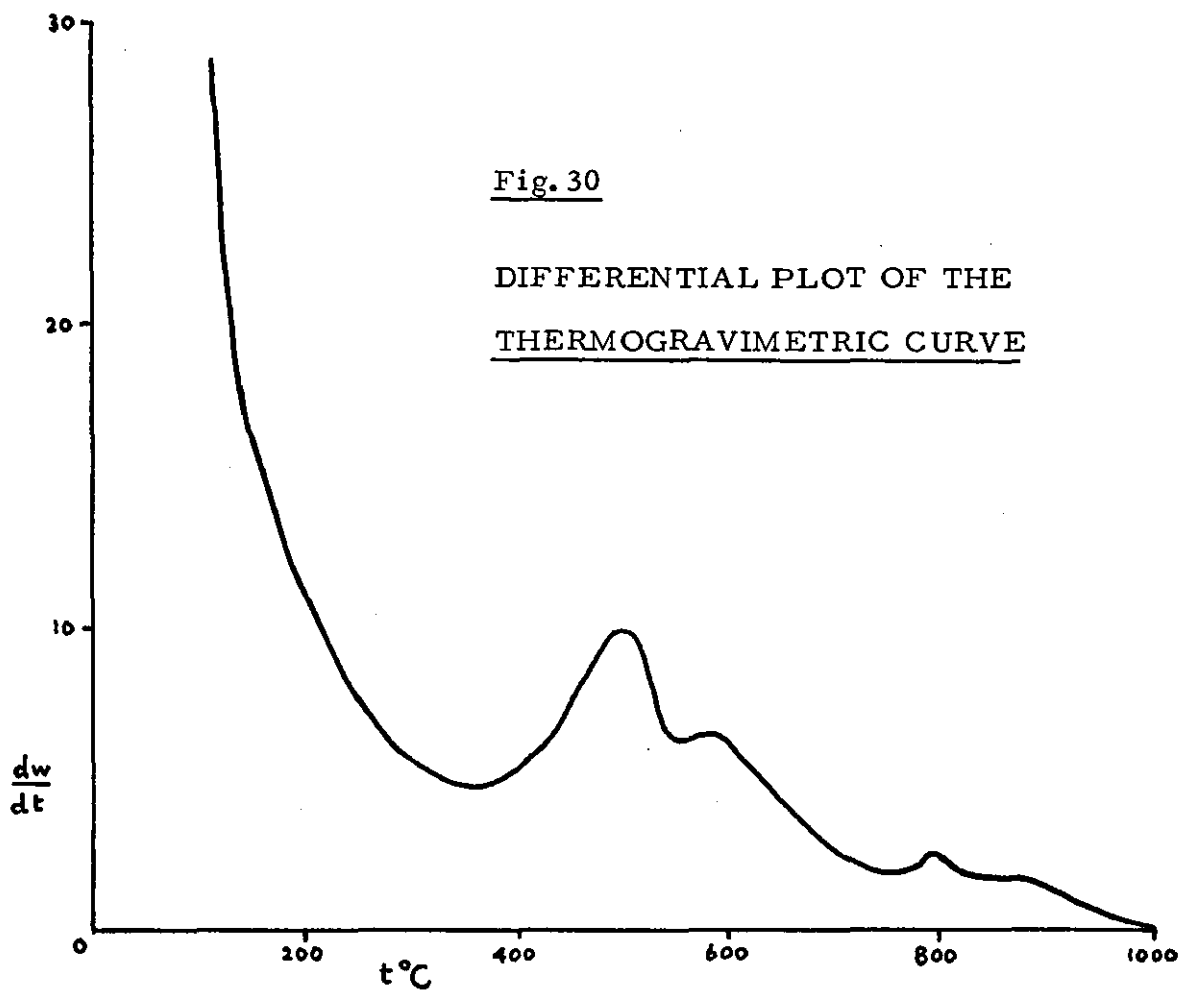


Fig. 31 Differential thermal analysis (D.T.A.)

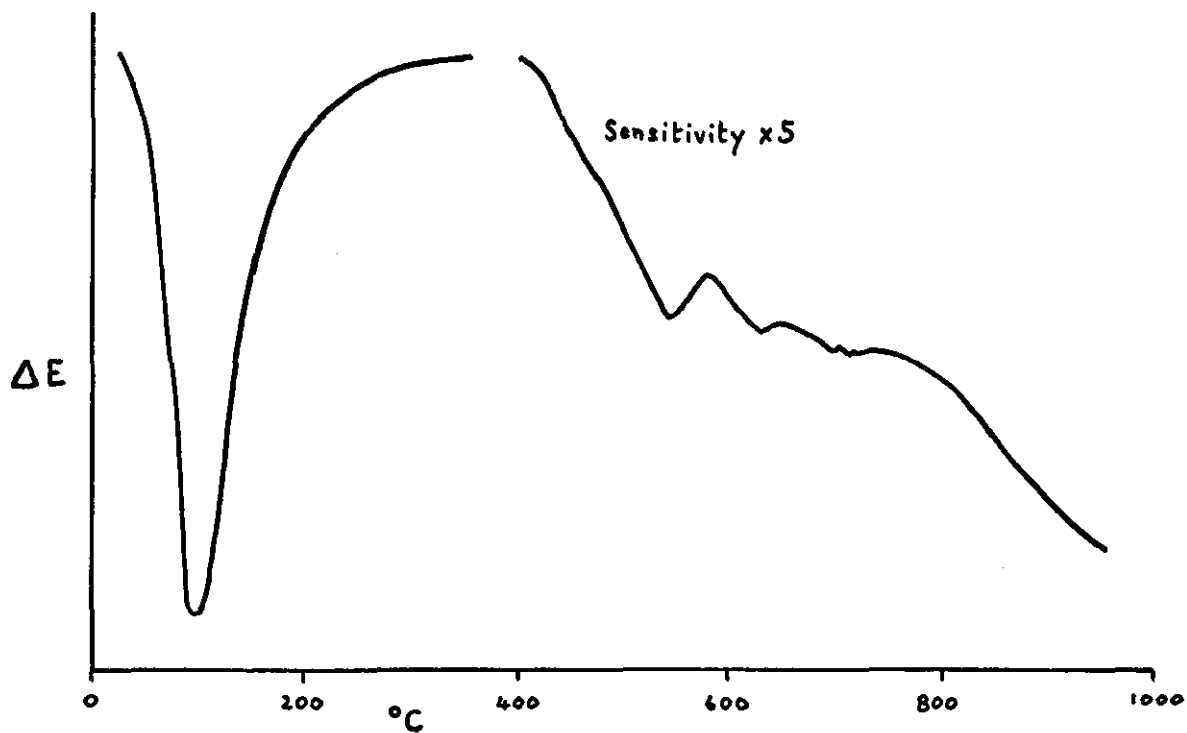
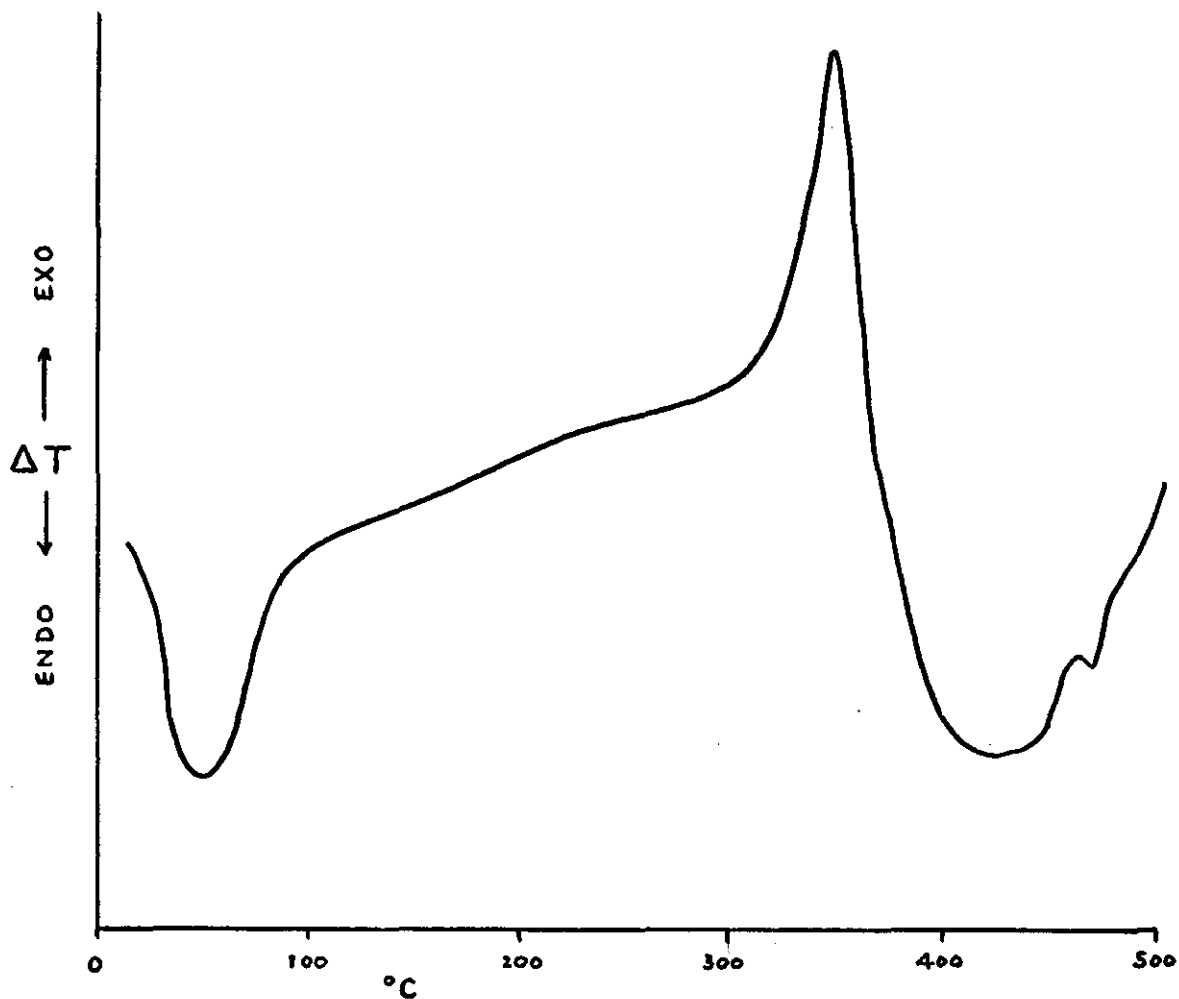


Fig. 32 Differential scanning calorimetry (D.S.C.)



As water molecules reach the surface they are vigorously held: the enthalpy of adsorption of water increases with the temperature at which the alumina is predried and may exceed 400 kJ mol^{-1} for very low surface coverages on alumina predried above 500°C ⁷⁵. After resorption of 6.25 molecules of water per nm^2 the surface is covered by a monolayer of hydroxyl ions: the water has been chemisorbed. Adsorption of the remaining 6.25 molecules per nm^2 to a point of surface saturation implies that one water molecule is physically adsorbed onto a site having the same area as two surface ions.

Evacuation for two hours at 100°C resulted in 8.3 molecules of water per nm^2 (de Boer et al quoted 8.25 molecules per nm^2 after drying at 120°C) which correspond to an hydroxyl monolayer (chemisorbed water) with additional water molecules physically adsorbed on this layer (approximately one molecule per six ion sites).

In the light of the preceding discussion attempts have been made to carry out thermogravimetric investigations on the alumina used in this work (by courtesy of the British Railways Research Centre in Derby). The results are displayed in Figs. 29 to 32.

Fig. 29 represents changes in weight which occur upon steadily raising the temperature (10°C per minute) of an alumina sample: this continuous recording technique is referred to as 'T.G.A.' - thermogravimetric analysis. In order to emphasize the main features a differential plot has been constructed and is shown in Fig. 30 (i. e. dW/dT against T).

Differential thermal analysis (D.T.A.) is a technique which permits the monitoring of energy absorption by the alumina sample during its heating as compared to a non-active reference material and the resulting trace is shown in Fig. 31.

Finally, in differential scanning calorimetry (D.S.C.) the temperature of reference and sample is steadily raised by external heating and electric current is passed through internal heating coils, thus continuously compensating for abnormal rates in temperature change in the sample (caused by endothermic or exothermic changes taking place) and the recorder registers this compensating current. The result is shown in Fig. 32. The discernible features in these diagrams are summarised in Table 16.

Assuming that reductions in weight are solely due to elimination of water molecules it is possible to account for some of the features observed qualitatively and to place an approximate quantitative interpretation upon the data. However, caution is necessary since the large amounts of water involved may tend to mask or distort small features and, more seriously the recommended reference material (where required) is itself alumina. Moreover, when this recommended alumina was used as reference the results were confusing and so a sample of the alumina under investigation was first taken through the heating cycle and then used as a reference with fresh alumina as the sample. Interpretation was further complicated by the instruments' sensitivity to external spurious switching surges.

TABLE 16: THERMOGRAVIMETRIC ANALYSIS
OF THE ALUMINA

<u>Temperature</u> <u>°C</u>	<u>T.G.A.</u> <u>(Loss in weight)</u>	<u>D.T.A.</u>	<u>D.S.C.</u>
100	3.0%	Large energy absorption peak	peak of large endotherm
120	3.4%		
200	4.6%*	small absorption peak	small endotherm
355			exotherm peak
500	6.5%		
535		energy absorption peak**	
600	7.2%	small absorption peak	
800	7.9%		
1000	8.1%***		

* Loss of physically adsorbed water substantially complete.

** Decomposition of remaining bochmite.

*** Loss of chemisorbed water (i. e. OH groups) substantially complete.

Brown et al⁷⁰ report that gibbsite (hydrargillite, $\text{Al}(\text{OH})_3$) begins to decompose between 200 and 300°C when boehmite (γ -aluminium oxide monohydrate) is slowly formed. It is unlikely that any gibbsite remains in the alumina studied, it having been heated to 800°C, and so the peaks at 200°C and 350°C remain unassigned. At 530°C Brown reports that boehmite decomposes sharply to γ -alumina and this would account for the peaks on the D.T.A. and differential T.G.A. plots, remembering that the X-ray diffraction results diagnosed the presence of approximately 10% boehmite. No further assignable changes occur below 800°C.

At 1000°C γ -alumina assumes the bulk structure of α -alumina, the stable modification, with a total loss of 8.1% in weight. This reduction is the consequence of three distinct processes: loss of physically adsorbed water molecules, removal of chemisorbed water (i. e. OH groups) and decomposition of the boehmite admixed with the γ -alumina. From the symmetry of the D.T.A. and D.S.C. peaks around 100°C it can be estimated that the desorption of physically adsorbed water molecules may be complete by 200°C and so a nominal 4.6% loss in weight may be assigned for this water. The decomposition of approximately 10% boehmite (represented stoichiometrically as $\text{Al} 0.0\text{H}$) in the original sample would account for a 1.5% loss which would make the loss of chemisorbed water responsible for a 2.0% reduction in weight.

It is enlightening to pursue the implications of these speculative divisions, but this necessitates the adoption of a definitive value for the specific surface area of the alumina and so analysis is continued in the 'Discussion of Results'.

(b) Surface Area

The low temperature adsorption of nitrogen has proved the most widely applicable and reliable method available for the determination of the surface areas of solid adsorbents, although not the simplest from manipulative considerations. Further, if the nitrogen is progressively desorbed a desorption isotherm may be constructed; the appearance of a hysteresis loop between adsorption and desorption isotherms points to porosity of the sorbent and enables a pore size distribution to be calculated. Thus a porous sorbent may be considered to have an 'external' surface area and an 'internal' area (the lining of the pores): pore size distribution and cumulative surface area plots quickly show the presence of very small cavities (micro pores) which may be accessible to nitrogen molecules but not to larger molecules of other adsorbates.

It is useful to briefly survey an analysis of the alumina carried out by an earlier worker³⁴ since some of these standard calculation techniques are applied to the noble gas and vapour sorptions carried out in the course of this study.

Calculation of Specific Surface Area.

Brunauer, Emmett and Teller^{83, 84} derived the following equation for multimolecular adsorption of a gas on a non-porous surface :-

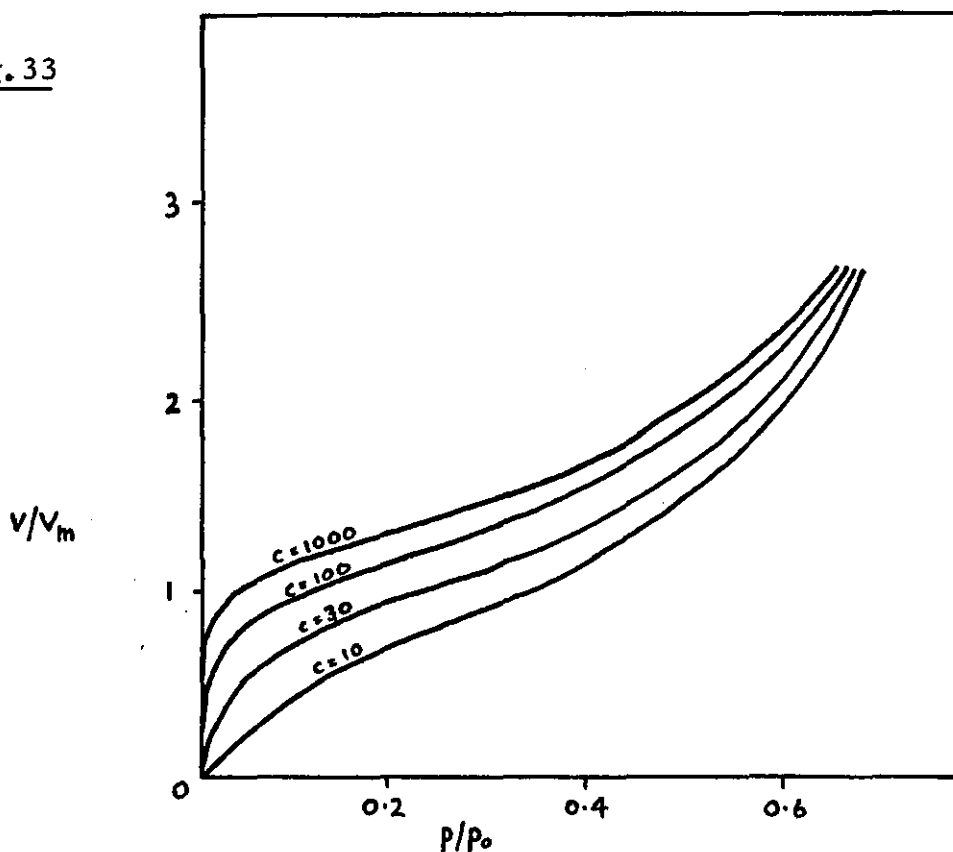
$$\frac{p}{v(p_0 - p)} = \frac{1}{v_m c} + \frac{c-1}{v_m c} \cdot \frac{p}{p_0} \quad (53)$$

where v is the volume of gas adsorbed (cm^3 at S.T.P.) on the surface at equilibrium pressure p
 v_m is the volume of gas adsorbed (cm^3 at S.T.P.) corresponding to monolayer coverage of the surface
 p_0 is the saturation pressure of the gas
 c is the a constant related to the heat of adsorption in the first layer.

It is assumed that the forces responsible for adsorption are the same as those involved in the process of liquefaction. The theory retains the concept of fixed, energetically uniform, adsorption sites as proposed by Langmuir, but allows for the formation of an adsorbed layer more than one molecule in thickness. The lateral interactions between molecules in the adsorbed phase are neglected and the molecules in all layers after the first are assumed to be subject to forces of similar magnitude.

The shape of the isotherm obtained by plotting v/v_m against p/p_0 varies according to the magnitude of ' c ' as shown in Fig. 33.

Fig. 33



Isotherms of these shapes are widely realised on the plotting of experimental data. Equation (53) can be used to calculate the monolayer capacity v_m by plotting $p/v(p_0-p)$ against p/p_0 when values for the intercept and slope of the linear plot are given by $1/v_m c$ and $(c-1)/v_m c$ respectively.

In practice, reliable v_m values are only obtained when the isotherm has a well defined 'knee' or plateau, implying a high value for the constant ' c ' and a reasonably strong interaction between adsorbate and adsorbent surface. In such a case, the isotherm is

found to have a linear section and Brunauer and Emmett⁸⁵ concluded that the beginning of this section (designated 'point B') corresponds to coverage of the adsorbent surface by a complete monolayer of adsorbed gas. Isotherms of this shape have been designated 'Type 11'.

Having obtained the value of v_m from the experimental data, the surface area of the adsorbent can be determined using a knowledge of the area occupied by each molecule of the gas on the surface, although the most appropriate value can sometimes be a matter for speculation. The average cross-sectional area of the adsorbed molecules is usually assumed to be the same as that obtained from the normal packing of the molecules in the liquefied gas⁸⁶, giving :-

$$A_m = f \left(\frac{M}{dN} \right)^{2/3} \times 10^{14} \text{ nm}^2 \quad (54)$$

where A_m is the cross sectional area of the molecule (nm^2) in the adsorbed phase

M is the molecular mass of the adsorbate

N is Avogadro's number

d is the density of the liquefied gas (g cm^{-3})

f is a packing factor for the gas molecules on the surface of the adsorbent

For nitrogen, the packing of the molecules on the surface is assumed to be hexagonal with each molecule having twelve nearest neighbours, giving a value of 1.091 for the factor 'f'. The specific surface area, S , of the adsorbent is then calculated from Equation (55).

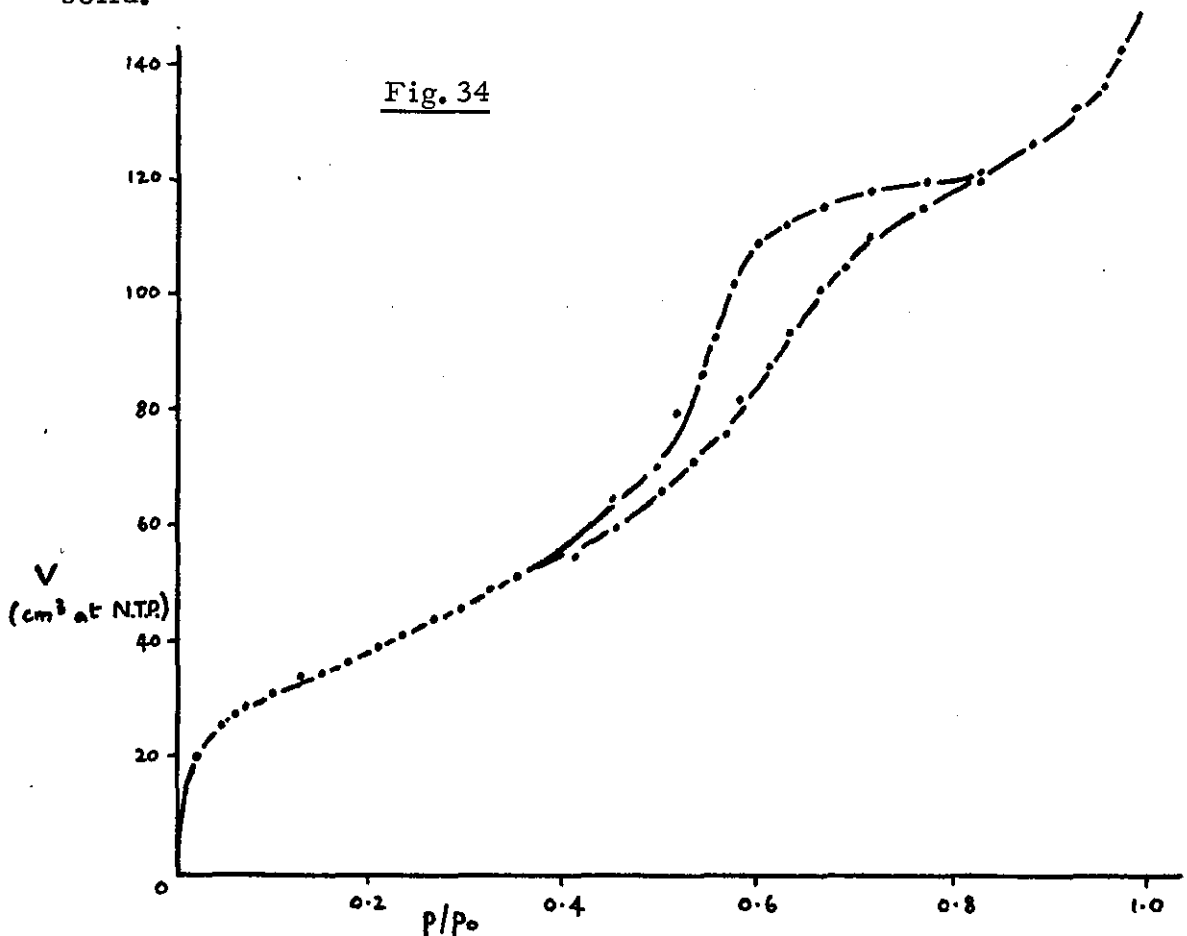
$$S = \frac{v_m}{22,400} \cdot N \cdot A_m \times 10^{-18} \text{ m}^2 \text{ g}^{-1} \quad (55)$$

The adsorption and desorption isotherms for nitrogen on the alumina at 77.4K are shown in Fig. 34 and the B.E.T. plot in Fig. 35. The specific surface area was calculated as $131.9 \text{ m}^2 \text{ g}^{-1}$.

Assessment of Surface Porosity

(i) The 't' Curve.

Lippens and de Boer⁸⁶ have developed a graphical procedure which enables interpretation to be made of nitrogen adsorption isotherms in terms of porosity of the solid adsorbent. The method involves plotting the volume of nitrogen adsorbed on the adsorbent under investigation against the corresponding statistical thickness 't' of the adsorbed layer of nitrogen on a non-porous reference solid.



Adsorption and desorption of nitrogen on alumina at 77.4K

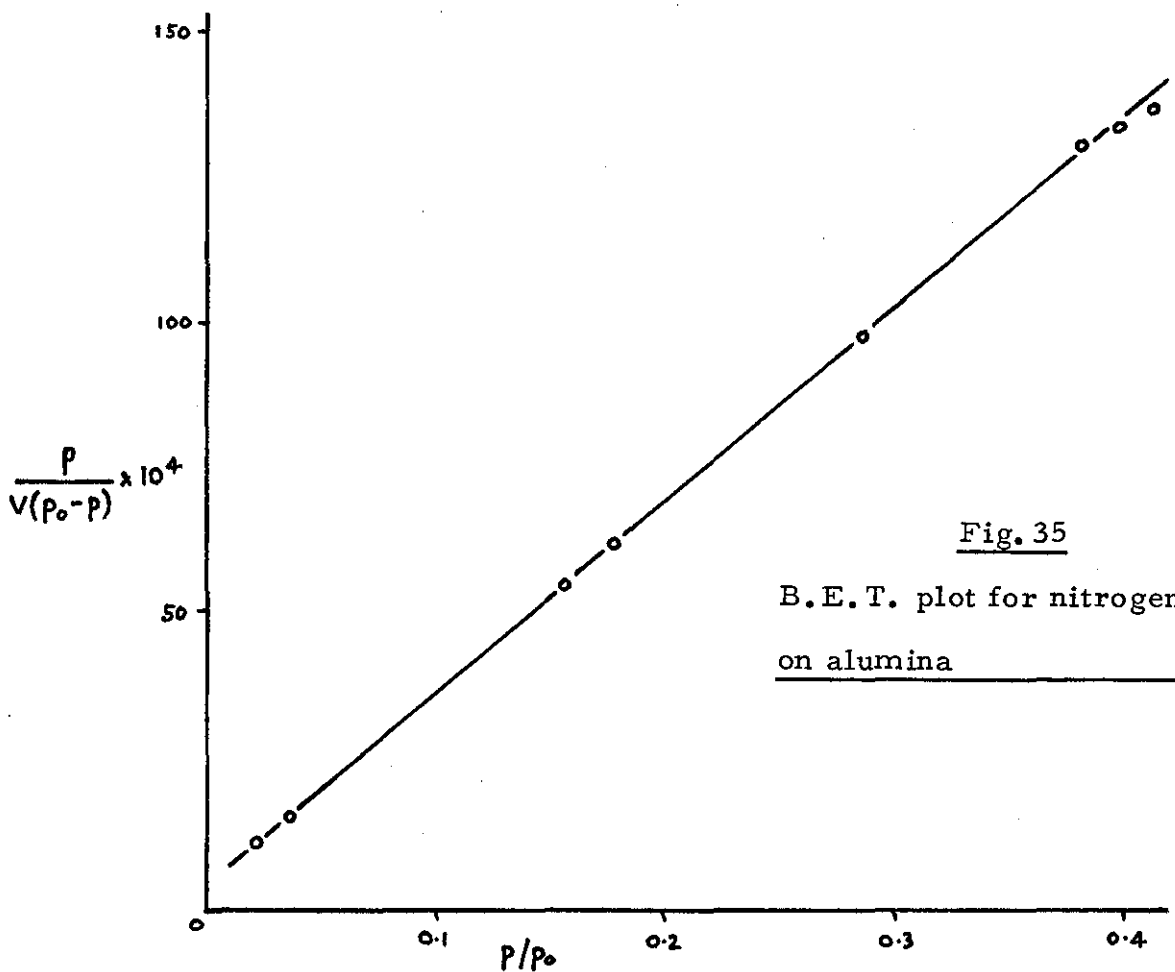


Fig. 35
B.E.T. plot for nitrogen
on alumina

The statistical thickness 't' of the adsorbed layer is given by

$$t = (v/v_m)_{\ell} \times 0.354 \equiv (v/v_m)_g \times 0.354 \quad (56)$$

where v is the volume adsorbed corresponding to a thickness 't', v_m is the volume adsorbed corresponding to a monolayer, subscripts ' ℓ ' and ' g ' refer to volumes of liquid and gas respectively (cm^3 at S. T. P.).

The factor 0.354 represents a monolayer thickness in nm and is equal to the volume of nitrogen which occupies 1nm^2 of surface. This volume is calculated simply from the density of liquid nitrogen (0.81 g cm^{-3}), the area requirement of a nitrogen molecule (0.162 nm^2) and the molecular mass of nitrogen, 28.

Several workers^{87, 88, 89} have noted that nitrogen adsorption isotherms for many non-porous substances are almost superimposable when plotted in a reduced form (v/v_m against p/p_0) and that deviations from this standard isotherm may be analysed in terms of micropore filling and capillary condensation. De Boer, Linsen and Osinga⁹⁰ suggested that the adsorption data of Lippens, Linsen and de Boer⁹¹ obtained by using several well selected samples of non-porous aluminas and aluminium hydroxides was suitable for the construction of an 'experimental master curve' up to a relative pressure of 0.98. The thickness of the adsorbed layer 't' was calculated from Equation (56) and tabulated as a function of relative equilibrium pressure, p/p_0 .

The thickness of the adsorbed layer 't' can be related to the surface area of the adsorbent as follows :-

$$t = \frac{v_l}{S} \times 10^{-6} \times 10^9 \text{ nm} \quad (57)$$

where v_l is the volume of liquid nitrogen adsorbed (cm^3)

S is the specific surface area of adsorbent ($\text{m}^2 \text{g}^{-1}$)

Volume of nitrogen gas adsorbed at S.T.P. (v)

$$= \frac{v_l \cdot 22400}{v_{sp} \cdot M} \text{ cm}^3 \quad (58)$$

where v_{sp} is the specific volume of liquid nitrogen ($\text{cm}^3 \text{g}^{-1}$)

M is the molecular mass of nitrogen

Substituting (58) in (57) gives

$$t = \frac{v \cdot M \cdot v_{sp}}{22400 S} \times 10^3 \text{ nm}$$

$$\text{i.e. } t = 1.55 (v/S) \text{ nm} \quad (59)$$

Rearranging Equation (59) gives

$$v = \frac{S}{1.55} \cdot t \quad (60)$$

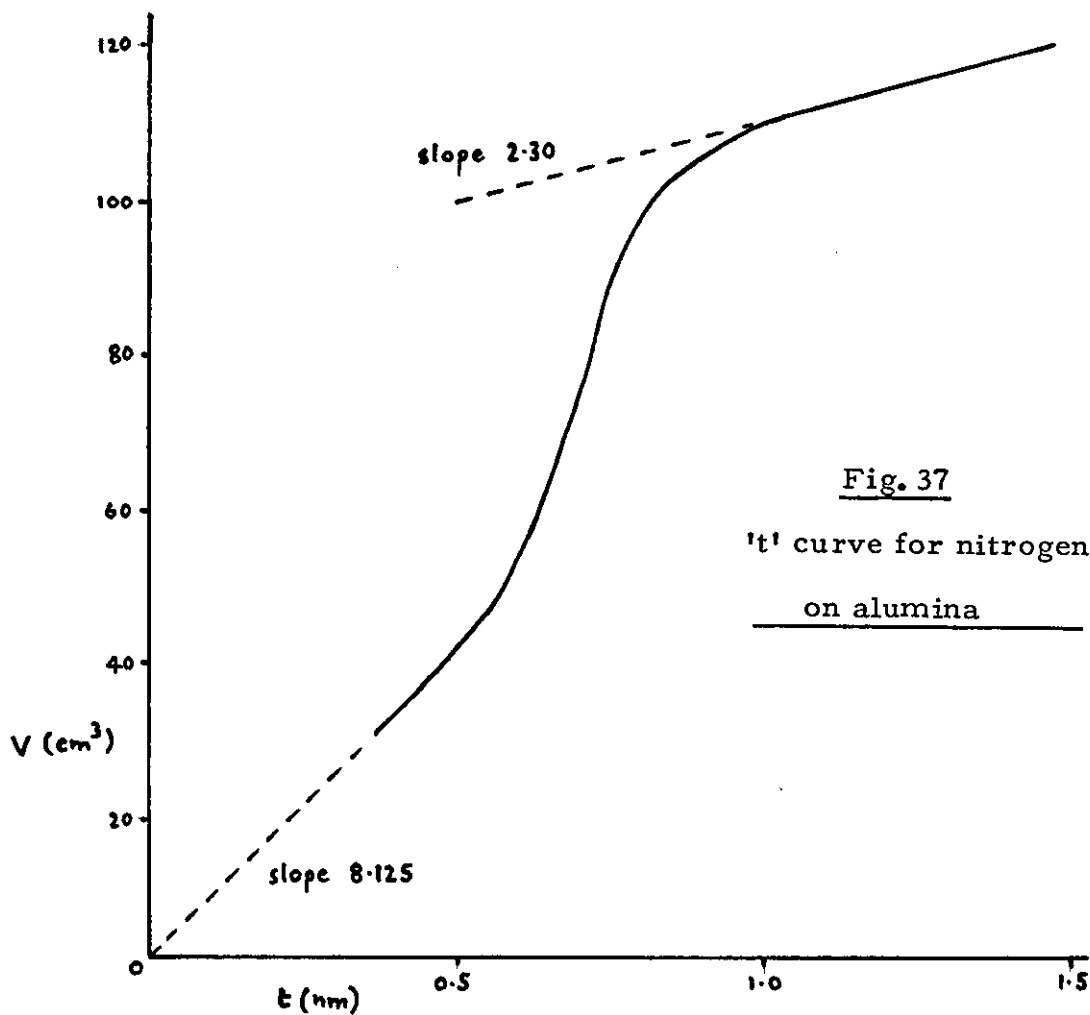
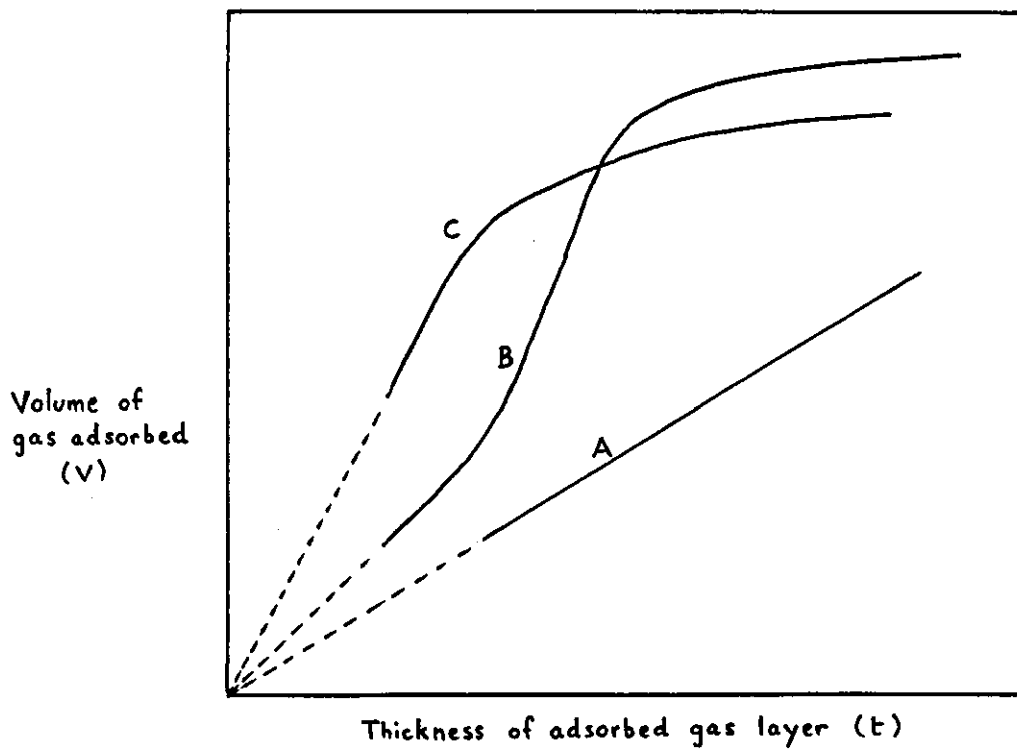
Thus a plot of v against t for non-porous solids should be linear, should pass through the origin and have a slope related to the surface area of the solid (Fig. 36, curve A). No deviation from this linear plot should be observed unless the adsorbent considered is porous when capillary condensation or closing of pores may occur. If at some value of ' t ' a positive deviation is observed then more nitrogen is being taken up than corresponds to multimolecular adsorption and the onset of capillary condensation is suggested (Fig. 36, curve B). When the pores are full, the plot should become linear and almost parallel to the ' t ' axis, the slope indicating the 'external' surface area. Thus curve C in Fig. 36 shows capillary condensation occurring in very narrow pores and the initial slope is indicative of the surface area of these pores.

The ' t ' curve plot for the alumina used in this study is shown in Fig. 37, and is seen to be of type B. From the initial slope and Equation (60) the surface area was found to be $125.7 \text{ m}^2 \text{ g}^{-1}$, the second linear section corresponds to an area of $35.6 \text{ m}^2 \text{ g}^{-1}$ and represents the 'external' surface of the alumina.

(ii) The ' v_s ' curve

Recently, Sing⁹² has developed a method similar to that of Lippens and de Boer⁸⁶ but which is independent of the B.E.T. analysis of the adsorption isotherm. The method consists of plotting the amount of nitrogen adsorbed on the adsorbent under

Fig. 36 't' curves



investigation v against v_s (instead of t), where v_s is the ratio of the amount of nitrogen adsorbed on a non-porous reference solid at the given relative pressure p/p_0 to that adsorbed at a selected relative pressure $(p/p_0)_x$. The value of $(p/p_0)_x$ is chosen as 0.4 since monolayer coverage and micropore filling usually occur at $(p/p_0) < 0.4$ whereas capillary condensation in association with hysteresis takes place at $(p/p_0) > 0.4$. Deviation of the v_s curve from linearity at $(p/p_0) \lesssim 0.4$ suggests micropore filling whilst at $(p/p_0) > 0.4$ capillary condensation may accompany multilayer formation. When micropore filling is absent, the surface area of the adsorbent under investigation can be calculated from the initial slope of the v_s curve by using a normalising factor, obtained from the standard isotherm on a non-porous reference solid of known surface area.

For alumina,

$$S = 2.87 \times (\text{initial slope of } v_s \text{ curve}) \text{ m}^2 \text{ g}^{-1} \quad (61)$$

The factor 2.87 is obtained by calibration against the surface area of Degussa Aluminiumoxid C, the standard reference solid, determined by electron microscopy.

(iii) Pore Size Distribution Analysis

The method of pore size analysis based on nitrogen isotherms was introduced by Wheeler⁹³ in 1945 although numerous modifications have been made since then. The analysis is performed on the desorption or adsorption branch of the hysteresis loop and it is assumed that all pores in the adsorbent are either cylindrical or slit-shaped. The Kelvin equation is used to calculate the radius at

each relative pressure considered and the pore radius ' r ' calculated from this parameter by allowing for the thickness of the adsorbed layer ' t '. Values of the latter are obtained from a suitable ' t ' curve and a variety of these are available in the literature. The ' t ' curves of different investigators^{87, 88, 89} differ from each other, depending on the group of adsorbents used for their determination and a ' t ' curve is selected which corresponds to the type of adsorbent under investigation. However, the choice of ' t ' curve is not critical, partly because such curves do not differ greatly from each other, and partly because the t -values constitute only a part of the pore radius. The cumulative pore volume and surface area are then determined by summing the pore volumes and surfaces of groups of pores that have radii between $(r + \Delta r)$ and $(r - \Delta r)$ over the range of the hysteresis loop.

An earlier worker³⁴ has carried out a stepwise analysis of the desorption branch of the nitrogen isotherm for the alumina used in this study and the plots of cumulative surface area against pore width and pore surface area distribution against pore width are reproduced in Figs. 38 and 39.

From these diagrams it can be verified that approximately 90% of the alumina surface area is accounted for by (slit-shaped) pores having a width greater than 2 nm and the largest fraction of the specific surface area arises from pores having a diameter between 2.7 and 3.2 nm.

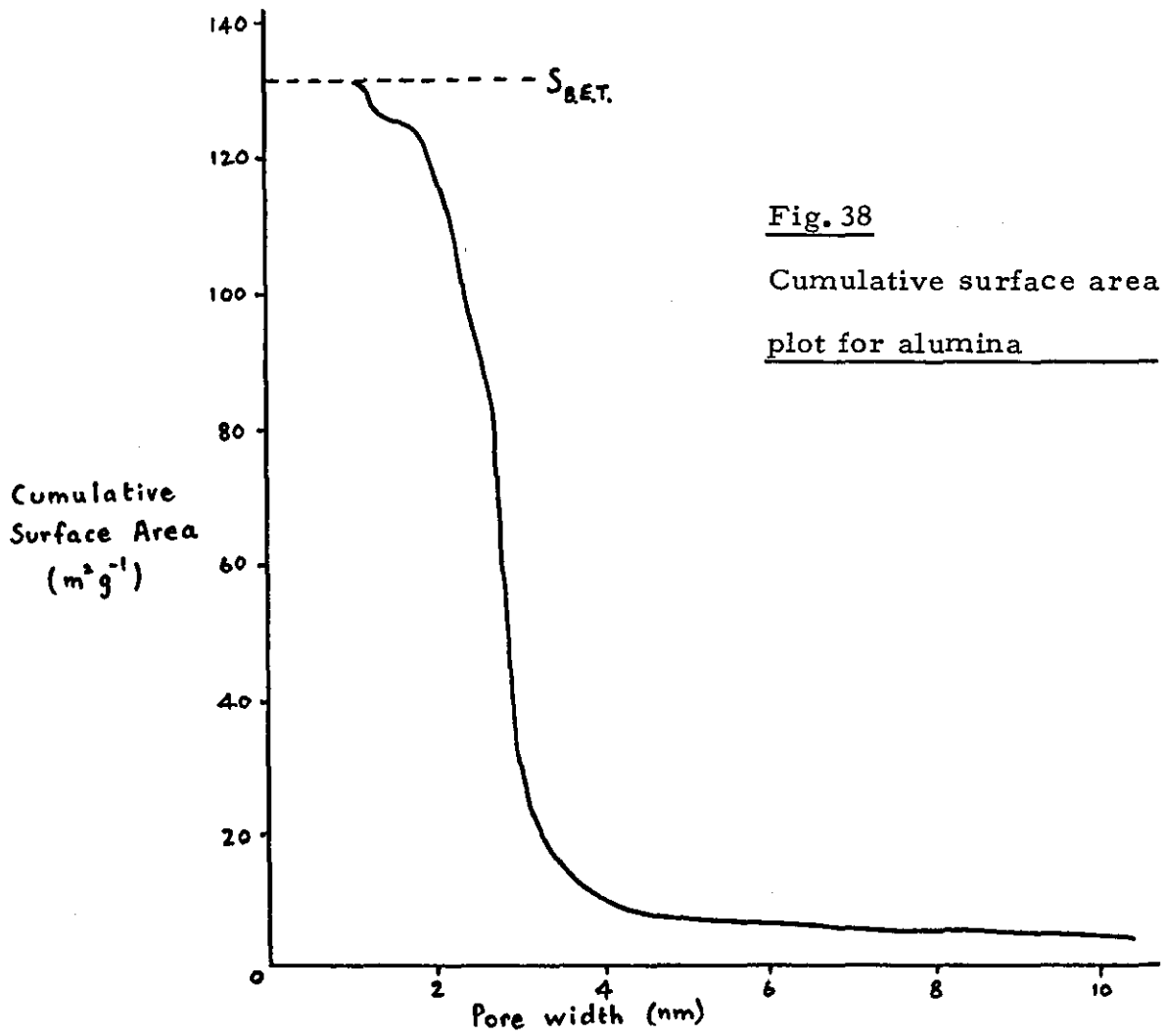


Fig. 38
Cumulative surface area plot for alumina

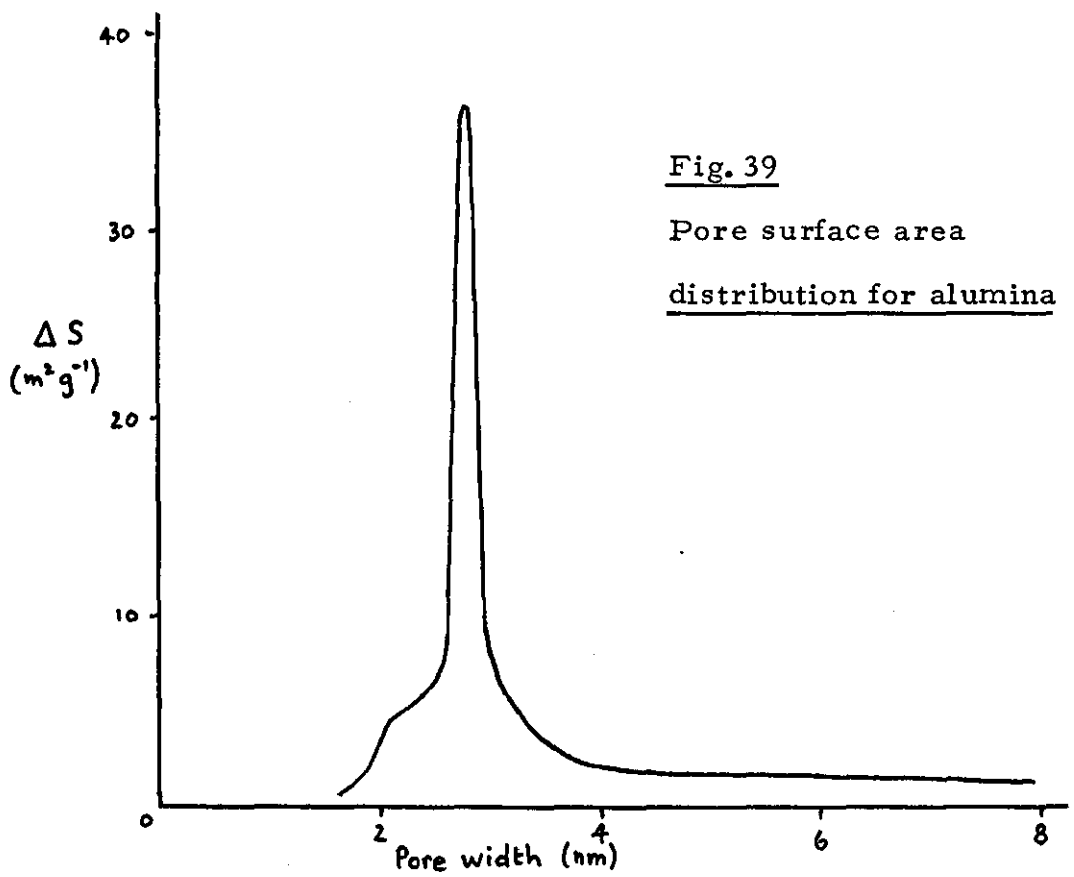


Fig. 39
Pore surface area distribution for alumina

(c) The Present Investigation

Adsorption from the gaseous phase of molecules of known physical dimensions other than nitrogen can provide information on the available surface area of an absorbent and can be most useful in interpreting adsorption from solution. The noble gases are an obvious choice, argon, for example, complements nitrogen and for some purposes has even been recommended in preference⁹⁴, whereas krypton with its much lower vapour pressure is useful for determining low surface areas.

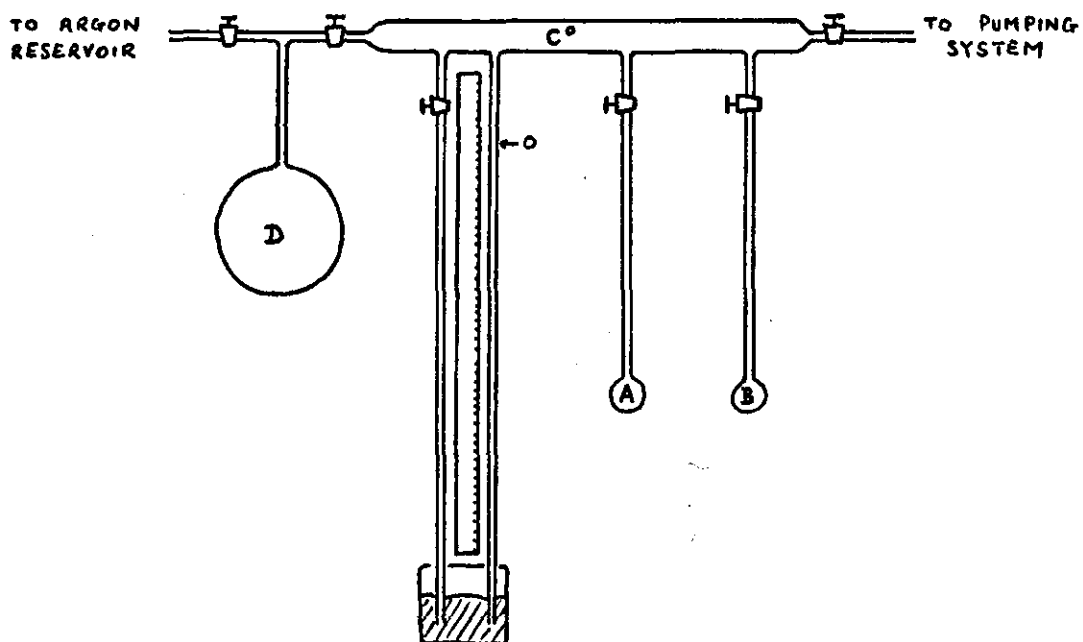
Accordingly, a low temperature sorption of argon has been carried out and ambient temperature vapour sorptions of the two main solvents employed in this study, dioxan and cyclohexane.

(i) Adsorption of Argon

The gas adsorption experiments were carried out using a conventional arrangement shown diagrammatically in Fig. 40. A careful calibration from p-v relationships at room temperature using argon was first carried out so that the volumes of the various sections, bores of tubing etc., were accurately known. The argon for adsorption (from a cylinder) was dried by passage through a column of molecular sieves and stored in the reservoir. The density of the solid alumina was measured so that the volume the sample occupied in the apparatus could be deducted. The alumina was pre-treated by drying in an oven at 120°C for 48 hours and outgassed (together with the rest of the apparatus) at room temperature for several hours prior to the sorption experiment. Evacuation was achieved by means of a Tower mercury diffusion pump backed up with a Speedivac oil vacuum pump and a McLeod

Fig. 40.

Gas Sorption Apparatus



Vol. of D = 1198.3 cm³

Vol. of C° = 149.6 cm³

Vol. of A = 14.1 cm³

Vol. of B = 15.0 cm³

Vol. of 1 g of Alumina = 0.3 cm³

Radius of manometer tubing = 0.256 cm.

gauge incorporated in the system checked the 'hardness' of the vacuum obtained. When it was quite certain leaks were absent, the adsorption bulb was immersed in liquid nitrogen (maintained at a constant level) and at equilibrium the volumes of argon adsorbed by a sample of the alumina (1 g 'wet' weight) were measured for a series of different equilibrium pressures. Adsorption and desorption measurements were carried out over a continuous period of 36 hours. Finally, the saturated vapour pressure of argon (p_0) was measured at the liquid nitrogen temperature which revealed the fact that the sorption temperature was not exactly the boiling point of liquid nitrogen under 101325 Nm^{-2} pressure (77.4K) but slightly higher (78.7K).

To report all readings and calculations would be tedious and superfluous and so Table 18 lists only a summary of the more important quantities. Figs. 41 and 42 show the adsorption and desorption branches of the argon isotherm and the B. E. T. plot of $p/v(p_0 - p)$ against p/p_0 .

A computerised assessment of the experimental data has made possible the calculation of a series of values of v_m (the volume of argon in cm^3 at S. T. P. adsorbed at monolayer coverage) and c by limiting the range of p/p_0 values. The results are shown in Table 17.

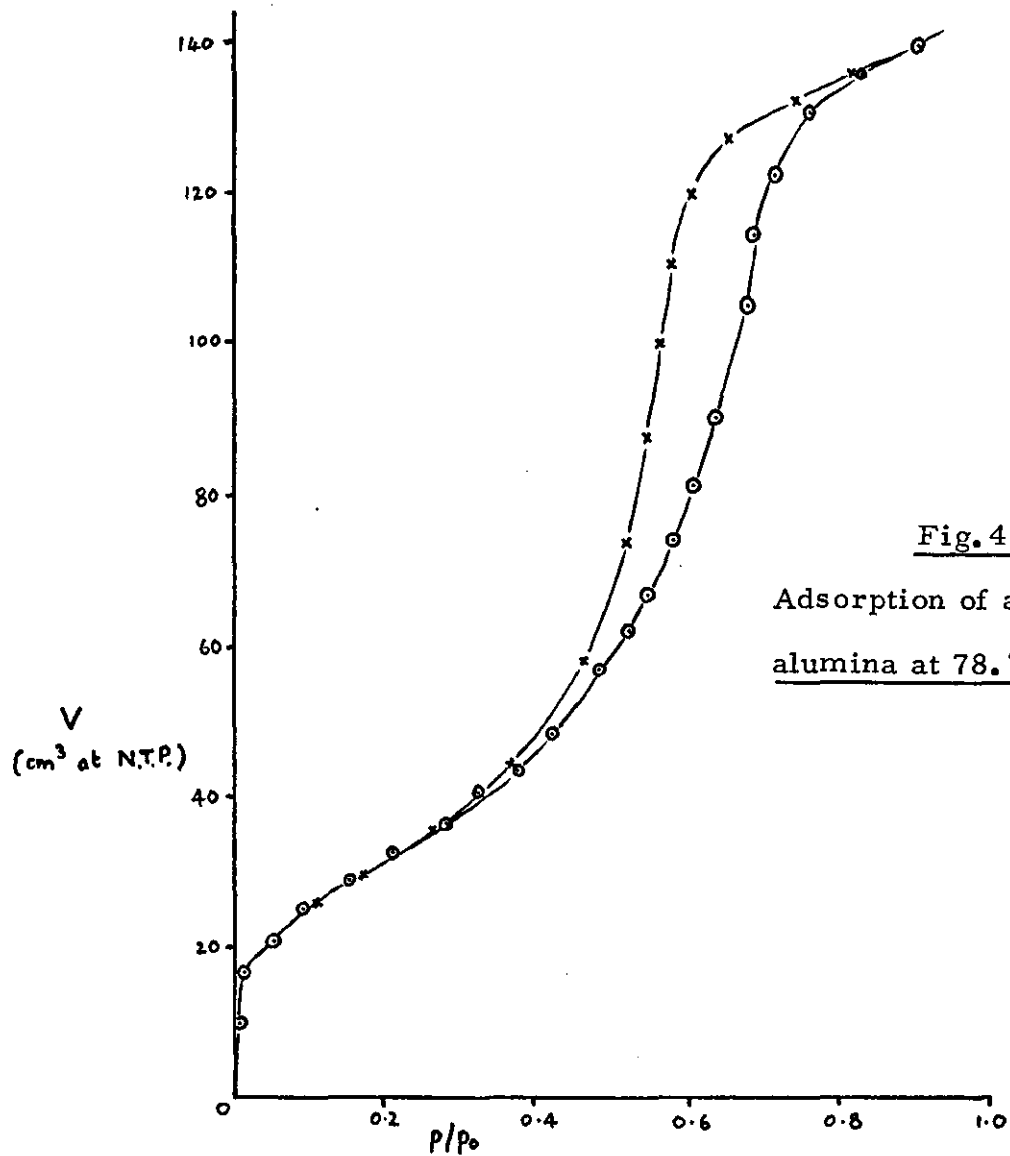


Fig. 41
Adsorption of argon onto alumina at 78.7K

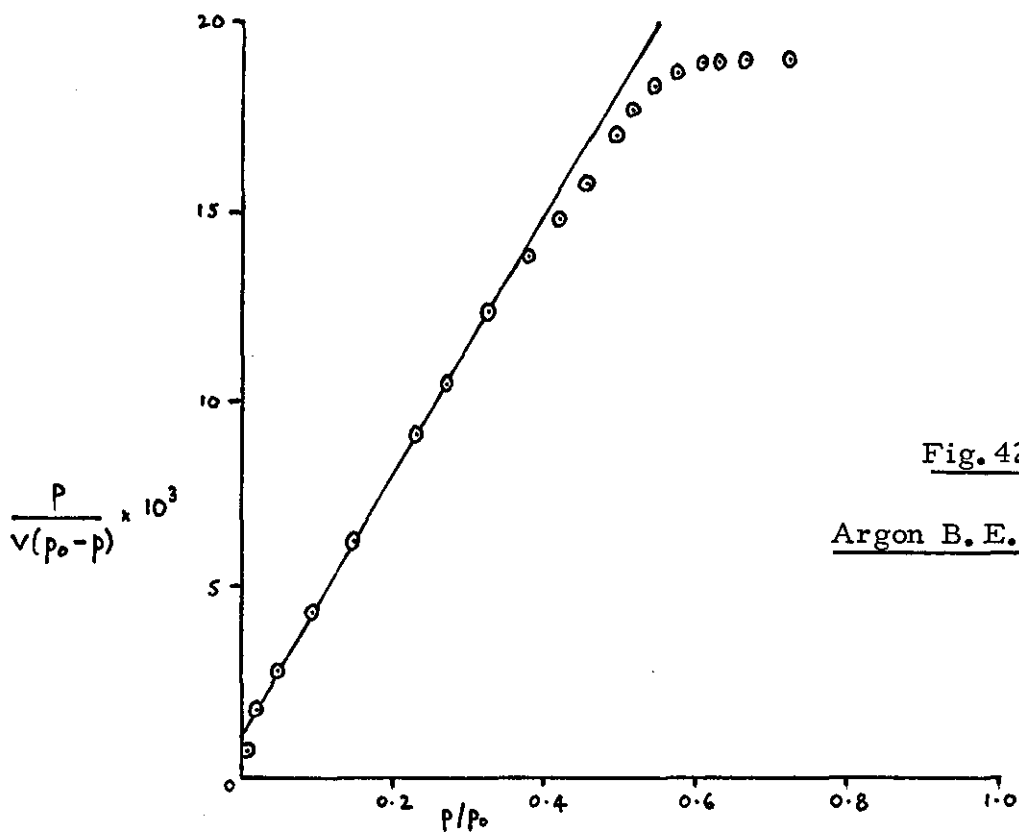


Fig. 42
Argon B. E. T. plot

TABLE 17 :

v_m and c values from the argon isotherm

<u>Maximum p/p_o</u>	<u>c</u>	<u>v_m (cm³)</u>
0.250	42.33	27.597
0.275	41.56	27.677
0.300	39.49	27.904
0.325	39.49	27.904
0.350	37.13	28.154
0.375	32.12	28.762
0.400	31.66	28.825

Estimates of the specific surface area of the alumina from these data are considered in the Discussion of Results.

Item	Quantity	Unit Price	Total Price
1	1	100	100
2	2	200	400
3	3	300	900
4	4	400	1600
5	5	500	2500
6	6	600	3600
7	7	700	4900
8	8	800	6400
9	9	900	8100
10	10	1000	10000
11	11	1100	12100
12	12	1200	14400
13	13	1300	16900
14	14	1400	19600
15	15	1500	22500
16	16	1600	25600
17	17	1700	28900
18	18	1800	32400
19	19	1900	36100
20	20	2000	40000
21	21	2100	44100
22	22	2200	48400
23	23	2300	52900
24	24	2400	57600
25	25	2500	62500
26	26	2600	67600
27	27	2700	72900
28	28	2800	78400
29	29	2900	84100
30	30	3000	90000
31	31	3100	96100
32	32	3200	102400
33	33	3300	108900
34	34	3400	115600
35	35	3500	122500
36	36	3600	129600
37	37	3700	136900
38	38	3800	144400
39	39	3900	152100
40	40	4000	160000
41	41	4100	168100
42	42	4200	176400
43	43	4300	184900
44	44	4400	193600
45	45	4500	202500
46	46	4600	211600
47	47	4700	220900
48	48	4800	230400
49	49	4900	240100
50	50	5000	250000
51	51	5100	260100
52	52	5200	270400
53	53	5300	280900
54	54	5400	291600
55	55	5500	302500
56	56	5600	313600
57	57	5700	324900
58	58	5800	336400
59	59	5900	348100
60	60	6000	360000
61	61	6100	372100
62	62	6200	384400
63	63	6300	396900
64	64	6400	409600
65	65	6500	422500
66	66	6600	435600
67	67	6700	448900
68	68	6800	462400
69	69	6900	476100
70	70	7000	490000
71	71	7100	504100
72	72	7200	518400
73	73	7300	532900
74	74	7400	547600
75	75	7500	562500
76	76	7600	577600
77	77	7700	592900
78	78	7800	608400
79	79	7900	624100
80	80	8000	640000
81	81	8100	656100
82	82	8200	672400
83	83	8300	688900
84	84	8400	705600
85	85	8500	722500
86	86	8600	739600
87	87	8700	756900
88	88	8800	774400
89	89	8900	792100
90	90	9000	810000
91	91	9100	828100
92	92	9200	846400
93	93	9300	864900
94	94	9400	883600
95	95	9500	902500
96	96	9600	921600
97	97	9700	940900
98	98	9800	960400
99	99	9900	980100
100	100	10000	1000000

ADSORPTION

Relative Pressure (p/p_0)	Total volume adsorbed (v) ₃ at S.T.P. (cm^3)	$\frac{p}{v(p_0-p)} \times 10^3$ (cm^{-3})
0	2.6374	0
0.00687	9.9207	0.6969
0.02557	16.1936	1.6203
0.05540	21.0332	2.7886
0.09612	25.1318	4.2312
0.15459	28.9559	6.3151
0.22017	33.0585	8.5403
0.27675	36.5967	10.4559
0.33215	40.5307	12.2707
0.37737	44.2790	13.6878
0.41785	48.3786	14.8365
0.45833	52.6820	16.0615
0.48935	56.8160	16.8663
0.52178	61.8785	17.6327
0.54924	67.0631	18.1692
0.57860	73.7658	18.6133
0.60440	80.8257	18.9027
0.63116	90.1423	18.9827
0.66643	104.8628	19.0522
0.71709	122.2486	20.7342
0.90459	139.0172	68.2031

1	2	3	4	5
1	2	3	4	5
2	3	4	5	6
3	4	5	6	7
4	5	6	7	8
5	6	7	8	9
6	7	8	9	10
7	8	9	10	11
8	9	10	11	12
9	10	11	12	13
10	11	12	13	14
11	12	13	14	15
12	13	14	15	16
13	14	15	16	17
14	15	16	17	18
15	16	17	18	19
16	17	18	19	20
17	18	19	20	21
18	19	20	21	22
19	20	21	22	23
20	21	22	23	24
21	22	23	24	25
22	23	24	25	26
23	24	25	26	27
24	25	26	27	28
25	26	27	28	29
26	27	28	29	30
27	28	29	30	31
28	29	30	31	32
29	30	31	32	33
30	31	32	33	34
31	32	33	34	35
32	33	34	35	36
33	34	35	36	37
34	35	36	37	38
35	36	37	38	39
36	37	38	39	40
37	38	39	40	41
38	39	40	41	42
39	40	41	42	43
40	41	42	43	44
41	42	43	44	45
42	43	44	45	46
43	44	45	46	47
44	45	46	47	48
45	46	47	48	49
46	47	48	49	50
47	48	49	50	51
48	49	50	51	52
49	50	51	52	53
50	51	52	53	54
51	52	53	54	55
52	53	54	55	56
53	54	55	56	57
54	55	56	57	58
55	56	57	58	59
56	57	58	59	60
57	58	59	60	61
58	59	60	61	62
59	60	61	62	63
60	61	62	63	64
61	62	63	64	65
62	63	64	65	66
63	64	65	66	67
64	65	66	67	68
65	66	67	68	69
66	67	68	69	70
67	68	69	70	71
68	69	70	71	72
69	70	71	72	73
70	71	72	73	74
71	72	73	74	75
72	73	74	75	76
73	74	75	76	77
74	75	76	77	78
75	76	77	78	79
76	77	78	79	80
77	78	79	80	81
78	79	80	81	82
79	80	81	82	83
80	81	82	83	84
81	82	83	84	85
82	83	84	85	86
83	84	85	86	87
84	85	86	87	88
85	86	87	88	89
86	87	88	89	90
87	88	89	90	91
88	89	90	91	92
89	90	91	92	93
90	91	92	93	94
91	92	93	94	95
92	93	94	95	96
93	94	95	96	97
94	95	96	97	98
95	96	97	98	99
96	97	98	99	100

DESORPTION

Relative Pressure p/p_0	Total volume adsorbed at S.T.P. $v/(\text{cm}^3)$	
0.82599	135.6101	
0.73982	131.6987	Temp. of adsorption :
0.65033	127.0254	78.7K
0.60535	119.6936	p_0 for argon at 78.7K :
0.58215	110.4891	211.2 mm Hg
0.56392	99.5405	
0.54309	87.2514	
0.51941	72.8054	
0.46638	57.9230	
0.36671	44.5897	
0.26752	35.7964	
0.17282	29.7892	
0.10630	25.9341	

(ii) Adsorption of Dioxan Vapour

The apparatus used has been described in the previous section. The alumina was pre-treated as before and purified dioxan was out-gassed by repeated freezing and melting under vacuum prior to the adsorption, which was carried out at ambient temperature. Initially, difficulties were encountered with the absorption of organic vapours by the Edwards Hi-Vac Silicone grease used for the glass taps and equilibrium could not be obtained; more polar lubricants, prepared by dissolving cellulose triacetate in polyethylene glycol or phthalic anhydride in glycerol, overcame the problem.

The results are reported, once again in a condensed form, in Table 19 and the isotherm and B.E.T. plot in Figs. 43 and 44. Analysis of the B.E.T. plot gave

$$v_m = 8.996 \text{ cm}^3 \text{ of dioxan vapour at S.T.P.,}$$

$$\text{i. e. } 0.402 \times 10^{-3} \text{ mol, and } C = 20.57$$

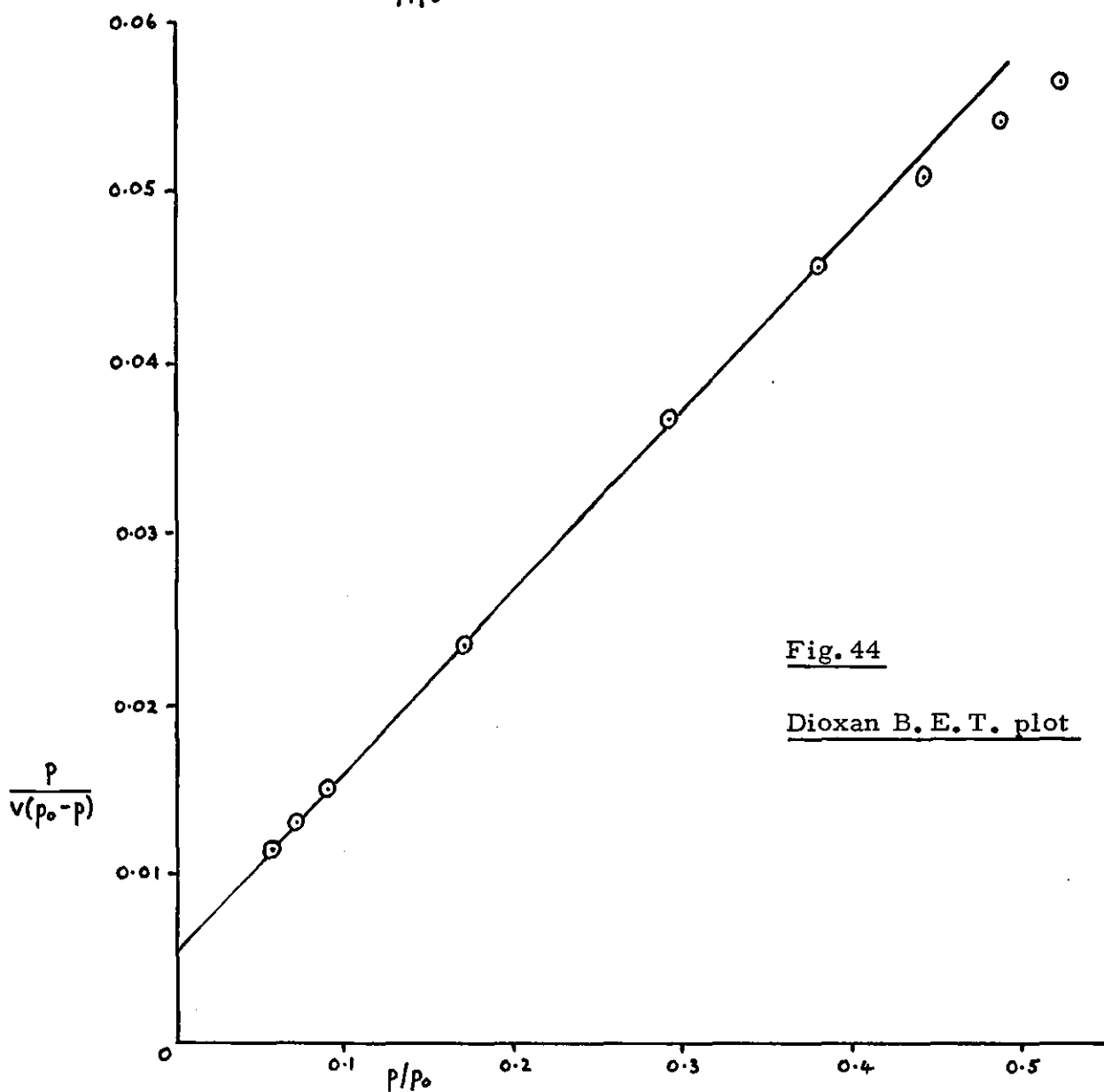
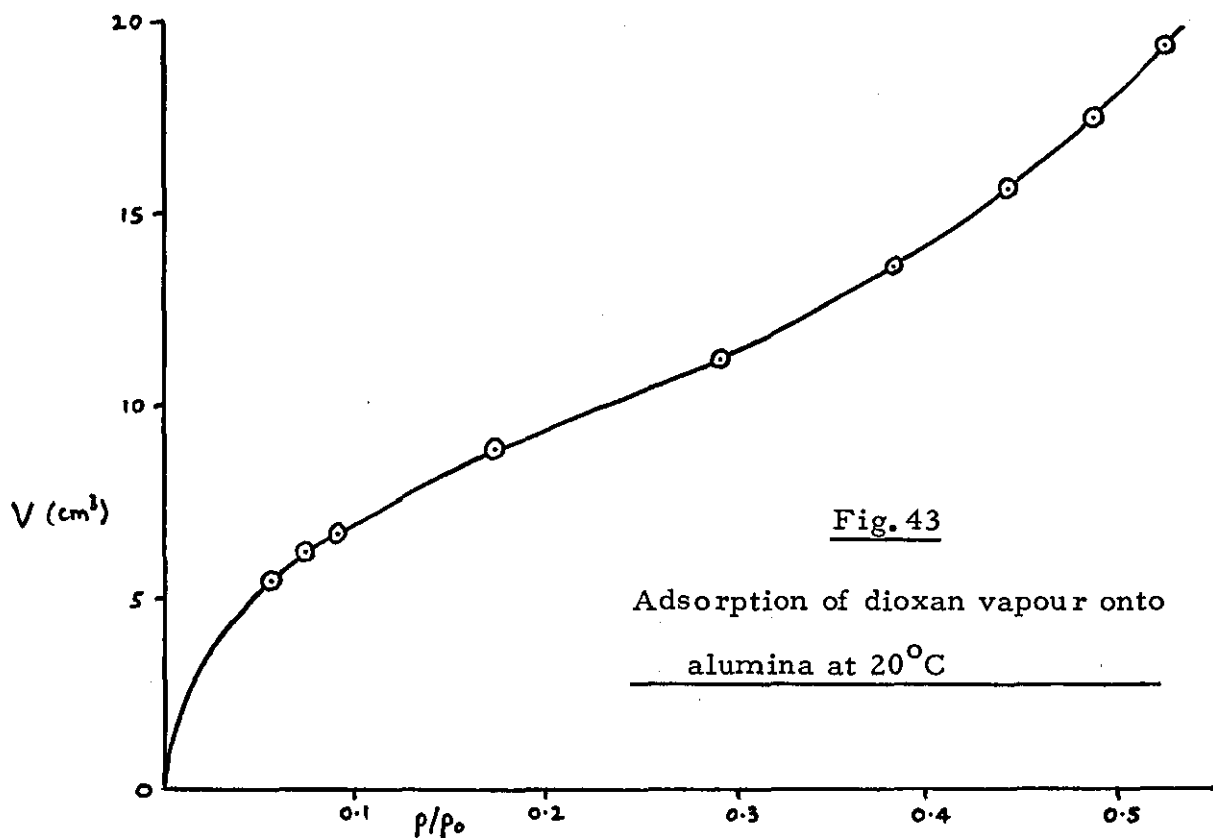
The comparatively high 'C' value indicates strong interaction between the dioxan molecules and the surface hydroxyl groups and reflects the sharpness of the isotherm 'knee'.

TABLE 19

Doser Temperature (K)	Doser Pressure (mm Hg)	Equilibrium Temperature (K)	Equilibrium Pressure p/(mm Hg)
295.8	12.1	295.9	1.6
295.9	13.4	295.8	2.0
295.8	16.0	295.6	2.5
295.6	17.5	295.6	4.8
295.6	20.6	295.4	8.1
295.4	23.4	295.7	10.6
295.7	23.7	295.2	12.3
295.2	23.5	295.5	13.5
295.5	24.6	295.3	14.5

Relative Pressure p/p ₀	Total volume adsorbed at S. T. P. v/(cm ³)	$\frac{p}{v(p_0 - p)} \times 10^3$ (cm ⁻³)
0.05776	5.3530	11.4515
0.07220	6.0228	12.9206
0.09025	6.5808	15.0746
0.17329	8.9213	23.4959
0.29242	11.2055	36.8808
0.38267	13.5687	45.6845
0.44404	15.6740	50.9564
0.48736	17.5361	54.2131
0.52347	19.4176	56.5723

$p_0 = 27.7 \text{ mm Hg}$



(iii) Adsorption of Cyclohexane Vapour

The procedure was identical to that for the dioxan vapour sorption.

The results are reported in Table 20 and the isotherm and B.E.T. plot in Figs. 45 and 46. It is immediately obvious that the isotherm is of a different type ('Type 111') to the argon and dioxan ones. Type 111 isotherms (i. e. those with no distinct 'knee') result when the value of 'c' is very low (almost unity in this case) and imply very weak forces of interaction between adsorbate molecules and the adsorbent surface. It is easy to imagine there would be little affinity between non-polar cyclohexane molecules and the highly polar alumina surface and these results confirm this suggestion. Reliable estimates for the volume of vapour adsorbed at monolayer coverage (and hence possible estimates of the specific surface area) cannot be made from Type 111 isotherms.⁹⁴

TABLE 20

Doser Temperature (K)	Doser Pressure (mm Hg)	Equilibrium Temperature (K)	Equilibrium Pressure p/(mm Hg)
295.8	1.68	296.0	0.44
296.1	2.39	295.9	1.06
296.0	3.78	296.1	1.65
296.1	4.87	295.6	2.27
295.5	5.75	295.0	2.85
294.8	7.71	293.8	3.42
294.1	8.07	295.7	4.02

Relative Pressure p/p ₀	Total volume adsorbed at S. T. P. v/(cm ³)	$\frac{p}{v(p_0 - p)} \times 10^3$ (cm ⁻³)
0.050	2.252	23.38
0.120	5.635	24.20
0.188	9.528	24.30
0.258	14.297	24.32
0.324	19.659	24.38
0.389	25.745	24.73
0.457	33.800	24.90

p₀ = 88 mm Hg

Fig. 45

Adsorption of cyclohexane vapour onto alumina at 20°C

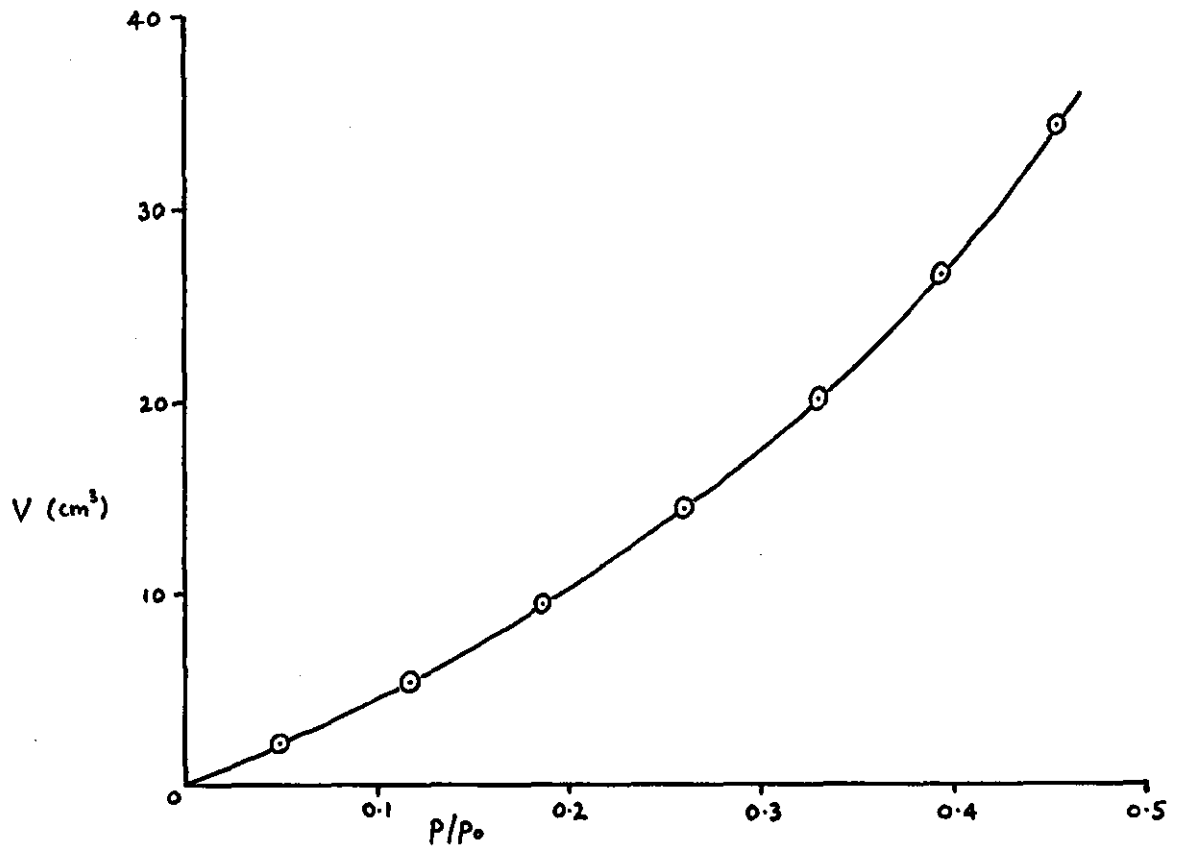
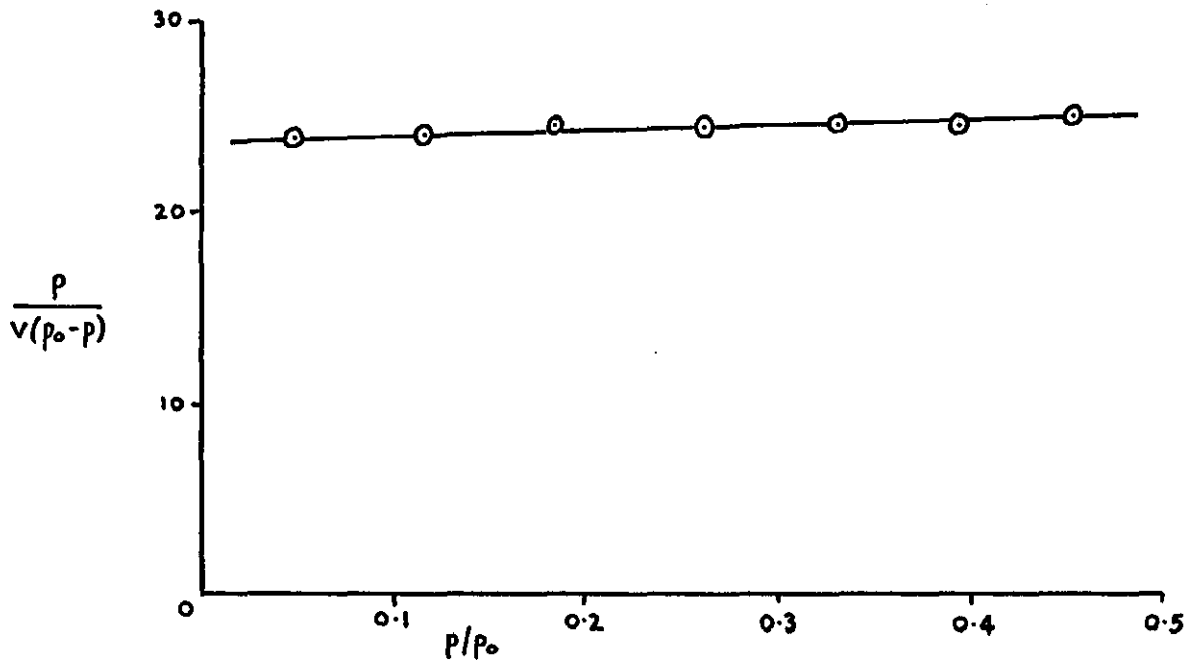


Fig. 46

Cyclohexane B.E. T. plot



2. Adsorption at the Solution-solid Interface.

This section of the experimental work is in two parts: firstly, the sorption of the parent 1-naphthol from a series of solvents which are not able to form hydrogen bonds with either the sorptive or the sorbent surface, and secondly, the sorption of a series of 4-substituted-1-naphthols from dioxan which is able to form hydrogen bonds with both sorptive and sorbent surface.

In selecting solvents for the first group of sorptions regard was given to a stipulation of Everett's ideal theory of adsorption, namely that the solute and solvent molecules should have the same cross-sectional area requirement. Accordingly, where possible, solvents closely related to the parent 1-naphthol were used, viz. cyclohexane, decalin (decahydronaphthalene), tetralin (1, 2, 3, 4-tetrahydronaphthalene) and 1-methylnaphthalene. It is interesting, too, that this series exhibits an increasing degree of aromaticity and an increasing interaction with a polar surface might therefore be expected.

In the second group of sorptions, the solvent dioxan is clearly able to compete effectively for hydroxylic adsorption sites with the naphthols and the effect of the 4-substituent in the naphthol upon the reaction centre (i.e. the naphtholic OH group) should be revealed.

(a) Adsorption of 1-Naphthol

The purification of solute and solvents is described in the Appendix. The alumina was prepared by heating 0.5g aliquots at 120°C for 48 hours prior to sorption.

A stock solution of 1-naphthol in the appropriate solvent was prepared at 25°C. Suitable volumes of this solution were measured

into a series of drawn out test-tubes and made up to 12.0 cm³ by addition of an appropriate volume of solvent. Solutions of each concentration were dispensed in triplicate. Commercial nitrogen from a gas cylinder was then bubbled firstly through a trap containing the appropriate solvent and then through each of the prepared solutions. The preliminary passage through solvent precluded concentration changes due to evaporation of the prepared solutions, and flushing with nitrogen in this manner not only created an inert atmosphere, necessary for hermetically sealing the tubes safely, but also removed dissolved oxygen which would otherwise cause oxidation and consequent discoloration of the adsorbed naphthol on the alumina surface.

To two of each set of three solutions was then added 0.5g of the pretreated alumina ensuring that contact with the air was kept to an absolute minimum (less than five seconds) and all three tubes were then immediately sealed. All of the tubes were thermostatted in a water bath at $35.0 \pm 0.1^{\circ}\text{C}$ and gently agitated from time to time. Preliminary experiments had shown that equilibrium was established after a period of three days under these conditions.

After four days a Unicam SP 500 Spectrophotometer (described fully in the 'Association' section) was adjusted to read absorbances over the concentration range employed by careful selection of wavelength and silica cell thickness, the absorbances of the solutions without alumina were measured first, giving a calibration line, and then each sorption tube was opened, the solution decanted into the cell and absorbances once again measured. Mean equilibrium concentrations of 1-naphthol in the liquid phase

were determined from the calibration graph and the amounts of naphthol adsorbed per gram of alumina calculated.

Saturated solutions of 1-naphthol in the solvents were simultaneously prepared at 35°C. A weighed quantity of the solution was transferred to a volumetric flask and diluted with a known weight of the solvent. The absorbance of the resulting solution was noted and from the calibration graph the concentration of the naphthol in the diluted solution was found, enabling the saturation mole fraction of the naphthol in the organic solvent at 35°C to be calculated.

As a typical example the results obtained for the sorption of 1-naphthol in cyclohexane onto alumina are reported in full in Table 21 and the calibration graph and adsorption isotherm in Figs. 47 and 48. Other results are recorded more briefly in Tables 22 to 24 and corresponding isotherms, constructed by plotting the moles of naphthol adsorbed ($n^{\circ} \Delta x_1^{\ell} / m$) against the equilibrium mole fraction of naphthol in the liquid phase, are shown collectively in Fig. 49.

Experimental Results

In the tables of results which follow, the symbols used have the following significance :-

n^0	total number of moles in 12 cm ³ of solution before adsorption
x_1^0	mole fraction of the naphthol in the liquid phase before adsorption
n^l	total number of moles in 12 cm ³ of solution after adsorption
x_1^l	mole fraction of the naphthol in the liquid phase after adsorption
Δx_1^l	change in mole fraction of the naphthol during adsorption = $x_1^0 - x_1^l$
x_2^l	mole fraction of solvent after adsorption = $1 - x_1^l$
$(x_1^l)_s$	mole fraction of the naphthol in a saturated solution at 35°C

TABLE 21: SORPTION OF 1-NAPHTHOL FROM CYCLOHEXANE

Before Sorption

<u>Initial conc. x 10² /mol dm⁻³</u>	<u>Absorbance</u>	<u>Moles of naph. in 12 cm³ x 10⁴ /mol</u>	<u>n^o</u>	<u>x₁^o x 10³</u>
0	0.002	0	0.1111	0
0.458	0.053	0.5492	0.1112	0.49389
0.899	0.109	1.0788	0.1112	0.97014
1.426	0.171	1.7117	0.1113	1.53791
1.982	0.240	2.3787	0.1113	2.13721
2.528	0.294	3.0330	0.1114	2.72266
3.080	0.367	3.6961	0.1114	3.31785
3.594	0.423	4.3128	0.1115	3.86798
3.958	0.477	4.7501	0.1115	4.26016
4.493	0.535	5.3916	0.1116	4.83118
4.942	0.585	5.9304	0.1117	5.30922
5.391	0.638	6.4692	0.1117	5.79159

TABLE 21 (continued)

After Sorption

Absorbance	Equilibrium Conc. $\times 10^2$ / mol dm ³	Moles of naph. in 12 cm ³ $\times 10^4$ /mol	n^{ℓ} / mol	$x_1^{\ell} \times 10^3$
0.002	0	0	0.1111	0
0.007	0.026	0.0315	0.1111	0.02839
0.012	0.074	0.0888	0.1111	0.07993
0.018	0.122	0.1460	0.1111	0.13143
0.033	0.255	0.3057	0.1111	0.27516
0.079	0.563	0.6759	0.1112	0.60784
0.120	1.003	1.2038	0.1112	1.08251
0.171	1.436	1.7232	0.1113	1.54825
0.213	1.781	2.1371	0.1113	1.92011
0.264	2.221	2.6652	0.1114	2.39246
0.322	2.715	3.2580	0.1114	2.92460
0.373	3.146	3.7752	0.1115	3.38583

TABLE 21 (continued)

$\Delta x_1^l \times 10^3$	$\frac{n^\circ \Delta x_1^l \times 10^4}{m}$	x_2^l	$\frac{m x_1^l x_2^l}{n^\circ \Delta x_1^l}$
0	0	1.000	-
0.46550	1.03526	1.000	0.2743
0.89622	1.97984	1.000	0.4037
1.40648	3.13082	1.000	0.4198
1.86205	4.14493	1.000	0.6638
2.11482	4.71183	0.999	1.2900
2.23534	4.98033	0.999	2.1736
2.31973	5.17301	0.998	2.9884
2.34005	5.21831	0.998	3.6722
2.43872	5.44323	0.998	4.3848
2.38463	5.32725	0.997	5.4740
2.40576	5.37446	0.997	6.2784

Fig. 47 Calibration graph for 1-naphthol in cyclohexane

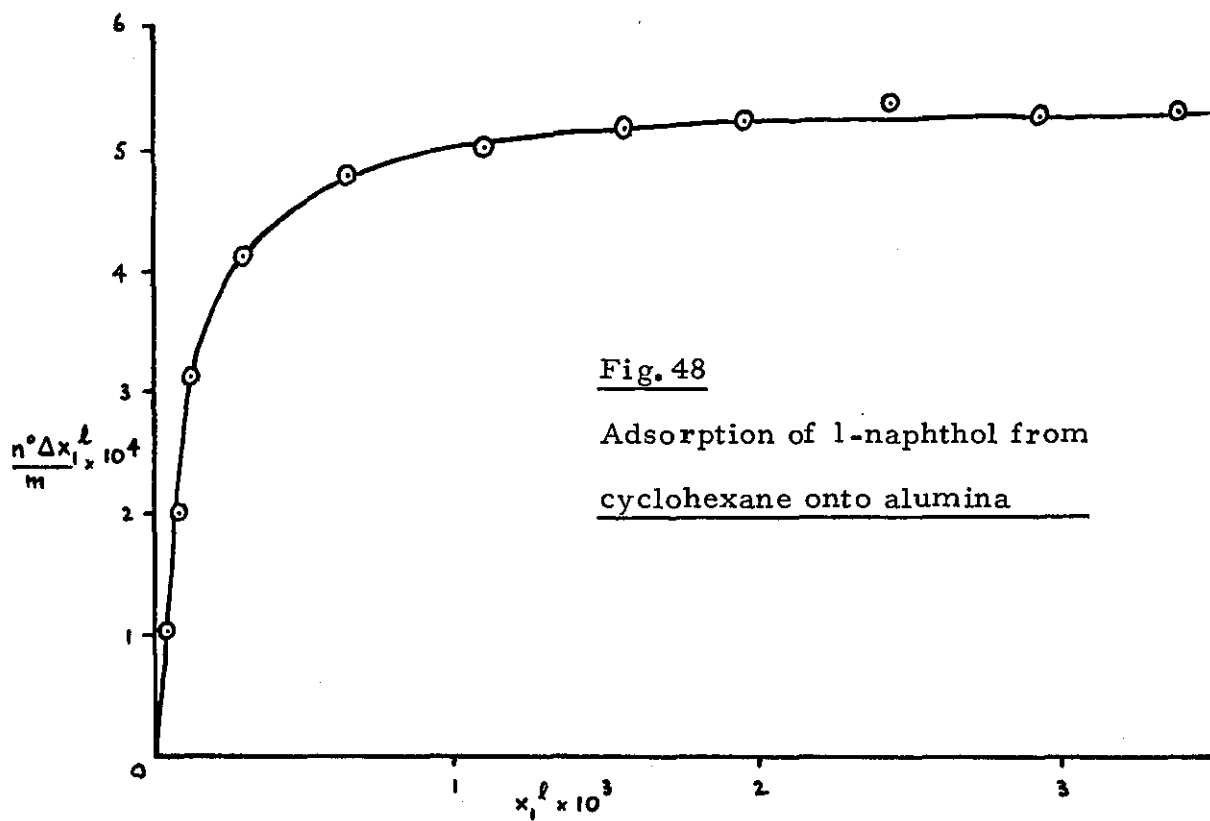
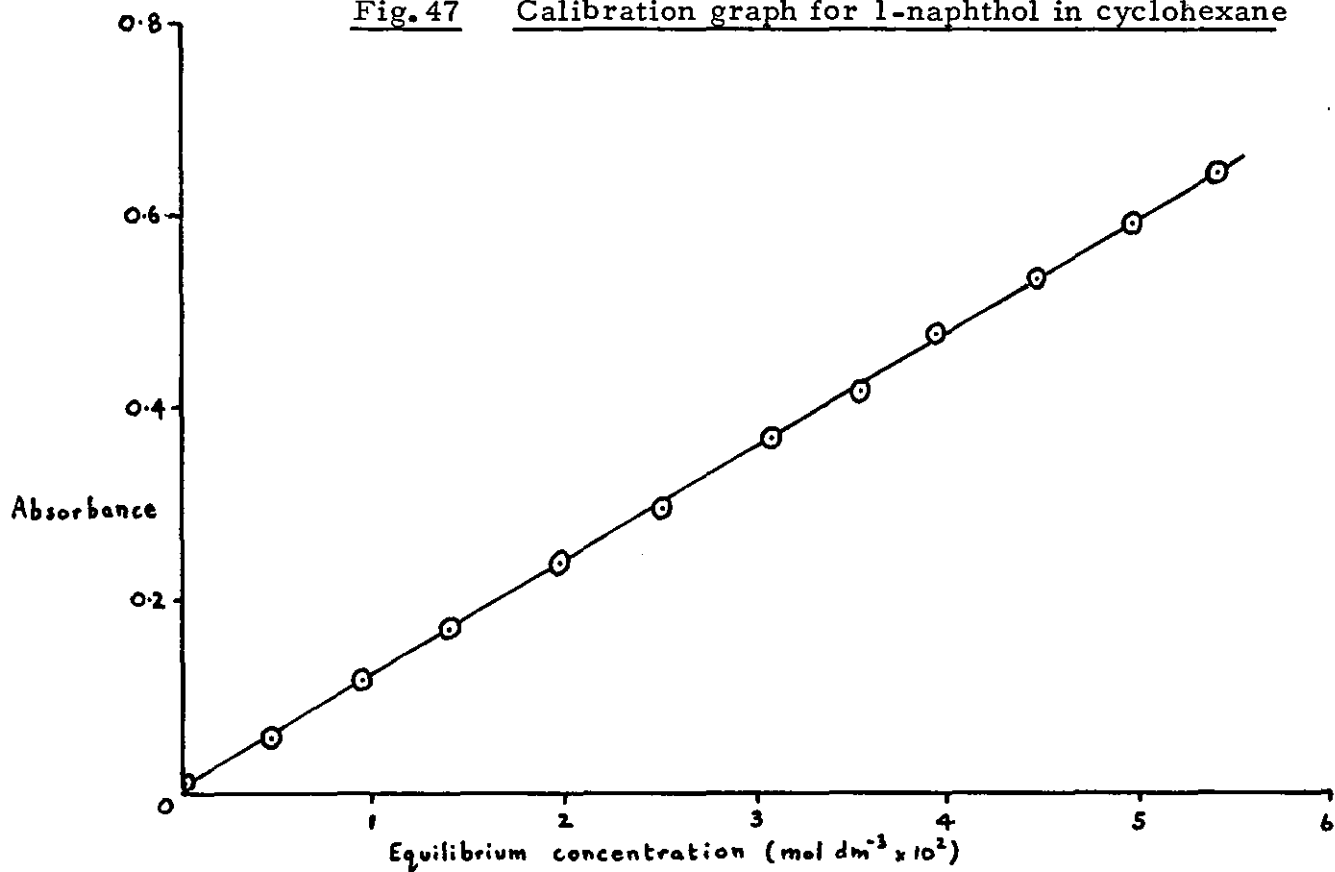


Fig. 48

Adsorption of 1-naphthol from
cyclohexane onto alumina

TABLE 22: SORPTION OF 1-NAPHTHOL FROM DECALIN

n^o	$x_1^o \times 10^3$	$x_1^l \times 10^3$	$\Delta x_1^l \times 10^3$
0.07665	0	0	0
0.07676	1.4518	0.0864	1.3654
0.07680	1.9469	0.1398	1.8071
0.07686	2.6687	0.2672	2.4015
0.07692	3.5681	0.5903	2.9778
0.07697	4.1734	1.0611	3.1123
0.07701	4.6602	1.5009	3.1593
0.07705	5.2489	1.9317	3.3172
0.07709	5.6792	2.3554	3.3238
0.07714	6.3105	2.8945	3.4160
0.07717	6.7468	3.3368	3.4100

$n^o \Delta x_1^l / m \times 10^4$	x_2^l	$m x_1^l x_2^l / n^o \Delta x_1^l$
0	1.0000	-
2.0961	0.9999	0.4122
2.7755	0.9999	0.5037
3.6916	0.9997	0.7238
4.5809	0.9994	1.2886
4.7911	0.9989	2.2103
4.8660	0.9985	3.0752
5.1118	0.9981	3.7676
5.1247	0.9976	4.5824
5.2703	0.9971	5.4701
5.2628	0.9967	6.3150

TABLE 23: SORPTION OF 1-NAPHTHOL FROM TETRALIN

n°	$x_1^{\circ} \times 10^3$	$x_1^{\ell} \times 10^3$	$\Delta x_1^{\ell} \times 10^3$
0.08814	0	0	0
0.08825	1.2009	0.1232	1.0777
0.08829	1.6844	0.2351	1.4493
0.08835	2.4074	0.4644	1.9430
0.08839	2.8674	0.7683	2.0991
0.08846	3.5685	1.1682	2.4003
0.08852	4.2631	1.6406	2.6225
0.08855	4.6474	2.0181	2.6293
0.08858	5.0125	2.3457	2.6668
0.08862	5.4349	2.7368	2.6981
0.08866	5.8112	3.0614	2.7498

$n^{\circ} \Delta x_1^{\ell} / m \times 10^4$	x_2^{ℓ}	$m x_1^{\ell} x_2^{\ell} / n^{\circ} \Delta x_1^{\ell}$
0	1.0000	-
1.9021	0.9999	0.6477
2.5593	0.9998	0.9186
3.4331	0.9995	1.3527
3.7107	0.9992	2.0705
4.2466	0.9988	2.7454
4.6429	0.9984	3.5230
4.6563	0.9980	4.3211
4.7244	0.9977	4.9502
4.7819	0.9973	5.7003
4.8761	0.9969	6.2533

TABLE 24: SORPTION OF 1-NAPHTHOL FROM

1 - METHYLNAPHTHALENE

n°	$x_1^{\circ} \times 10^3$	$x_1^{\ell} \times 10^3$	$\Delta x_1^{\ell} \times 10^3$
0.08650	0	0	0
0.08659	1.0799	0.1170	0.9629
0.08666	1.8199	0.2832	1.5367
0.08672	2.5677	0.5412	2.0265
0.08680	3.4018	1.0053	2.3965
0.08685	4.0204	1.5489	2.4715
0.08690	4.6587	1.9588	2.6999
0.08694	5.0501	2.3141	2.7360
0.08697	5.4090	2.6433	2.7657

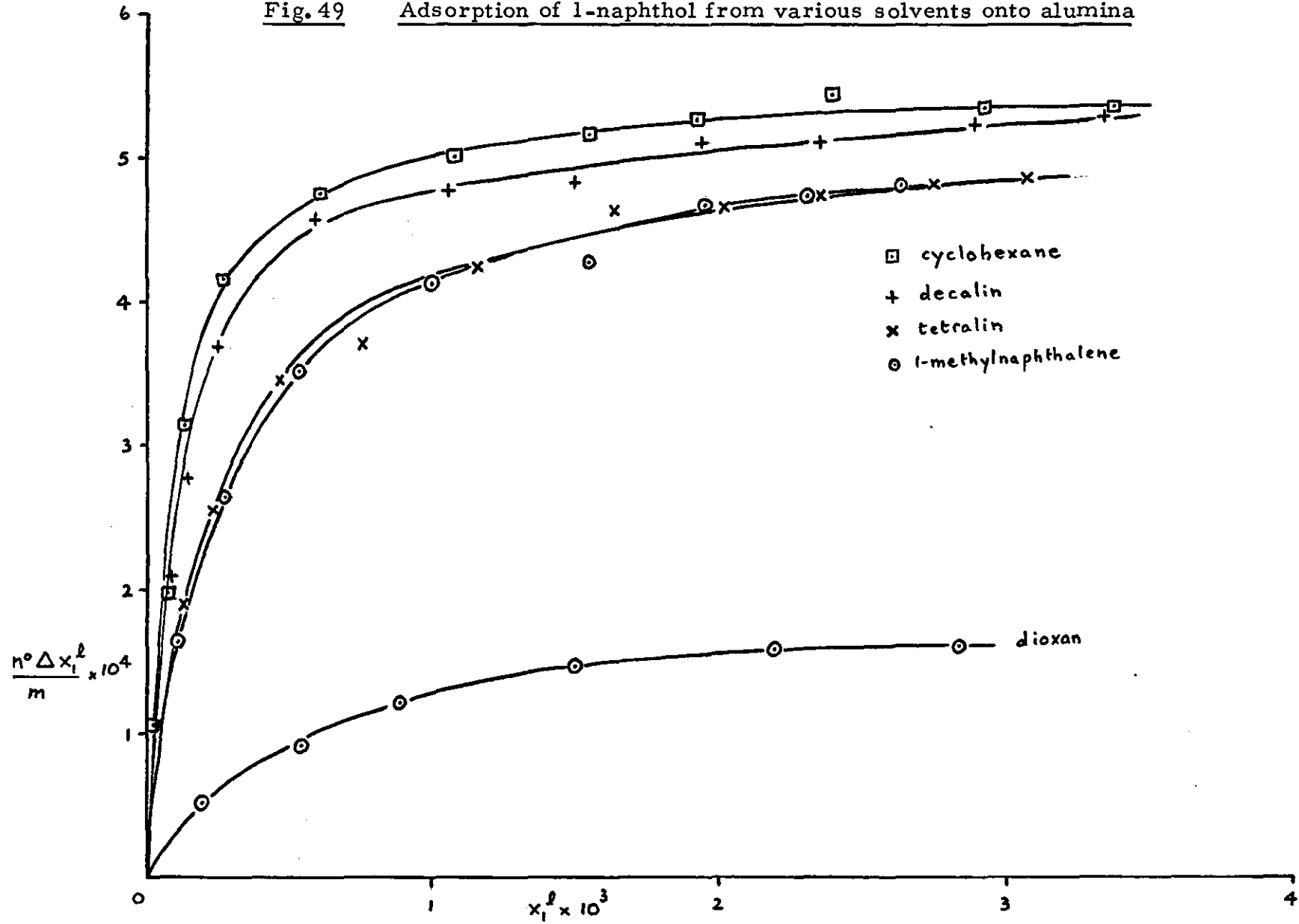
$n^{\circ} \Delta x_1^{\ell} / m \times 10^4$	x_2^{ℓ}	$m x_1^{\ell} x_2^{\ell} / n^{\circ} \Delta x_1^{\ell}$
0	1.0000	-
1.6676	0.9999	0.7016
2.6634	0.9997	1.0633
3.5147	0.9995	1.5398
4.1604	0.9990	2.4115
4.2929	0.9985	3.5972
4.6922	0.9980	4.1621
4.7573	0.9977	4.8497
4.8105	0.9974	5.4729

TABLE 25: SORPTION OF 1-NAPHTHOL FROM
DIOXAN

n°	$x_1^{\circ} \times 10^3$	$x_1^{\ell} \times 10^3$	$\Delta x_1^{\ell} \times 10^3$
0.141017	0	0	0
0.141071	0.3828	0.1982	0.1846
0.141140	0.8715	0.5473	0.3242
0.141206	1.3385	0.9022	0.4363
0.141304	2.0311	1.5298	0.5013
0.141401	2.7157	2.1956	0.5201
0.141499	3.4064	2.8502	0.5562
0.141631	4.3352	3.7630	0.5722
0.141771	5.3184	4.7324	0.5860

$n^{\circ} \Delta x_1^{\ell} / m \times 10^4$	x_2^{ℓ}	$m x_1^{\ell} x_2^{\ell} / n^{\circ} \Delta x_1^{\ell}$
0	1.0000	-
0.5213	0.9998	3.8013
0.9064	0.9995	6.0352
1.2113	0.9991	7.4415
1.4175	0.9985	10.7761
1.4805	0.9978	14.7975
1.5697	0.9971	18.1050
1.6212	0.9962	23.1230
1.6684	0.9953	28.2316

Fig. 49 Adsorption of 1-naphthol from various solvents onto alumina



(b) Adsorption of 4-Substituted-1-Naphthols

A series of 4-substituted-1-naphthols, together with the parent 1-naphthol, were sorbed onto alumina from dioxan solution at 35°C. The derivatives sorbed were 4-t-butyl-, 4-methyl-, 4-bromo-, 4-chloro-, 4-cyano-, and 4-nitro-1-naphthols. Since these compounds were not available commercially at the time of this study, their syntheses (and the purification of all solutes and solvents) are reported in an Appendix.

The adsorption procedure was similar to that described in the previous section; the results are reported (once again in a condensed form, the symbols having their usual significance) in Tables 26 to 31 and Fig. 50 collectively displays the adsorption isotherms.

TABLE 26: SORPTION OF 4-t-BUTYL-1-NAPHTHOL FROM DIOXAN

n^o	$x_1^o \times 10^3$	$x_1^l \times 10^3$	$\Delta x_1^l \times 10^3$
0.141017	0	0	0
0.141061	0.3119	0.1989	0.1130
0.141115	0.6945	0.4733	0.2212
0.141183	1.1758	0.8785	0.2973
0.141258	1.7061	1.3654	0.3407
0.141341	2.2923	1.9120	0.3803
0.141410	2.7792	2.3774	0.4018
0.141488	3.3289	2.9062	0.4227
0.141595	4.0821	3.6483	0.4338

$n^o \Delta x_1^l / m \times 10^4$	x_2^l	$m x_1^l x_2^l / n^o \Delta x_1^l$
0	1.000	-
0.3243	0.9998	6.1320
0.6204	0.9995	7.6251
0.8412	0.9991	10.4340
0.9557	0.9986	14.2669
1.0794	0.9980	17.6781
1.1385	0.9976	20.8317
1.1948	0.9970	24.2508
1.2231	0.9964	29.7209

TABLE 27: SORPTION OF 4-METHYL-1-NAPHTHOL FROM DIOXAN

n^o	$x_1^b \times 10^3$	$x_1^l \times 10^3$	$\Delta x_1^l \times 10^3$
0.141017	0	0	0
0.141074	0.4040	0.2184	0.1856
0.141115	0.6945	0.3968	0.2977
0.141188	1.2112	0.8161	0.3951
0.141255	1.6849	1.2430	0.4419
0.141361	2.4335	1.9412	0.4923
0.141456	3.1034	2.5843	0.5191
0.141563	3.8569	3.3252	0.5317
0.141669	4.6023	4.0610	0.5413

$n^o \Delta x_1^l / m \times 10^4$	x_2^l	$m x_1^l x_2^l / n^o \Delta x_1^l$
0	1.0000	-
0.5302	0.9998	4.1184
0.8398	0.9996	4.7240
1.1091	0.9992	7.3523
1.2522	0.9988	9.9146
1.3875	0.9981	13.9640
1.4604	0.9974	17.6498
1.5122	0.9967	21.9166
1.5274	0.9959	26.4787

TABLE 28: SORPTION OF 4-CHLORO-1-NAPHTHOL FROM DIOXAN

n°	$x_1^{\circ} \times 10^3$	$x_1^{\ell} \times 10^3$	$\Delta x_1^{\ell} \times 10^3$
0.141017	0	0	0
0.141095	0.5528	0.2263	0.3265
0.141138	0.8573	0.4301	0.4272
0.141192	1.2394	0.7383	0.5011
0.141287	1.9110	1.3412	0.5698
0.141392	2.6522	2.0554	0.5968
0.141486	3.3148	2.7030	0.6118
0.141570	3.9062	3.2997	0.6065
0.141651	4.4758	3.8513	0.6245

$n^{\circ} \Delta x_1^{\ell} / m \times 10^4$	x_2^{ℓ}	$m x_1^{\ell} x_2^{\ell} / n^{\circ} \Delta x_1^{\ell}$
0	1.0000	-
0.9211	0.9998	2.4564
1.2004	0.9996	3.5815
1.4094	0.9993	5.2347
1.6062	0.9987	8.3393
1.6815	0.9980	12.1992
1.7221	0.9973	15.6536
1.7268	0.9967	19.0457
1.7612	0.9961	21.7822

TABLE 29: SORPTION OF 4-BROMO-1-NAPHTHOL FROM DIOXAN

n°	$x_1^{\circ} \times 10^3$	$x_1^{\ell} \times 10^3$	$\Delta x_1^{\ell} \times 10^3$
0.141017	0	0	0
0.141119	0.7228	0.3612	0.3616
0.141157	0.9918	0.5502	0.4416
0.141219	1.4304	0.9165	0.5139
0.141323	2.1582	1.5784	0.5798
0.141427	2.8990	2.2996	0.5994
0.141518	3.5402	2.9174	0.6228
0.141593	4.0680	3.4391	0.6289
0.141667	4.5882	3.9504	0.6378

$n^{\circ} \Delta x_1^{\ell} / m \times 10^4$	x_2^{ℓ}	$m x_1^{\ell} x_2^{\ell} / n^{\circ} \Delta x_1^{\ell}$
0	1.0000	-
1.0223	0.9996	3.5318
1.2412	0.9994	4.4301
1.4531	0.9991	6.3015
1.6429	0.9984	9.5920
1.7033	0.9977	13.4698
1.7562	0.9971	16.5638
1.7874	0.9966	19.1754
1.8042	0.9960	21.8080

TABLE 30: SORPTION OF 4-CYANO-1-NAPHTHOL FROM DIOXAN

n°	$x_1^{\circ} \times 10^3$	$x_1^{\ell} \times 10^3$	$\Delta x_1^{\ell} \times 10^3$
0.141017	0	0	0
0.141131	0.8078	0.2864	0.5214
0.141171	0.0909	0.4584	0.6325
0.141278	1.8474	1.0779	0.7695
0.141352	2.3700	1.6015	0.7685
0.141391	2.6451	1.8812	0.7639
0.141469	3.1950	2.3931	0.8019
0.141608	4.1735	3.3562	0.8173
0.141769	5.3044	4.4701	0.8343

$\frac{n^{\circ} \Delta x_1^{\ell}}{m} \times 10^4$	x_2^{ℓ}	$\frac{m x_1^{\ell} x_2^{\ell}}{n^{\circ} \Delta x_1^{\ell}}$
0	1.0000	-
1.4797	0.9993	1.9342
1.7788	0.9995	2.5757
2.1802	0.9989	4.9386
2.1843	0.9984	7.3201
2.1699	0.9981	8.6531
2.2754	0.9976	10.4920
2.3208	0.9966	14.4122
2.3768	0.9955	18.7226

TABLE 31: SORPTION OF 4-NITRO-1-NAPHTHOL FROM DIOXAN

n°	$x_1^{\circ} \times 10^3$	$x_1^l \times 10^3$	$\Delta x_1^l \times 10^3$
0.141017	0	0	0
0.141107	0.6378	0.2954	0.3424
0.141216	1.4092	0.6586	0.7506
0.141323	2.1582	1.3075	0.8507
0.141395	2.6734	1.8004	0.8730
0.141575	3.9414	2.3461	1.5953
0.141599	4.1102	3.2084	1.9018
0.141679	4.6725	3.7825	1.8900
0.141808	5.5780	4.6711	1.9069

$n^{\circ} \Delta x_1^l / m \times 10^4$	x_2^l	$m x_1^l x_2^l / n^{\circ} \Delta x_1^l$
0	1.0000	-
1.7210	0.9997	1.7159
2.1222	0.9993	3.1012
2.4063	0.9987	5.4266
2.4788	0.9982	7.2501
2.5205	0.9977	9.2867
2.5633	0.9968	12.4766
2.5374	0.9962	14.8503
2.5896	0.9953	17.9531

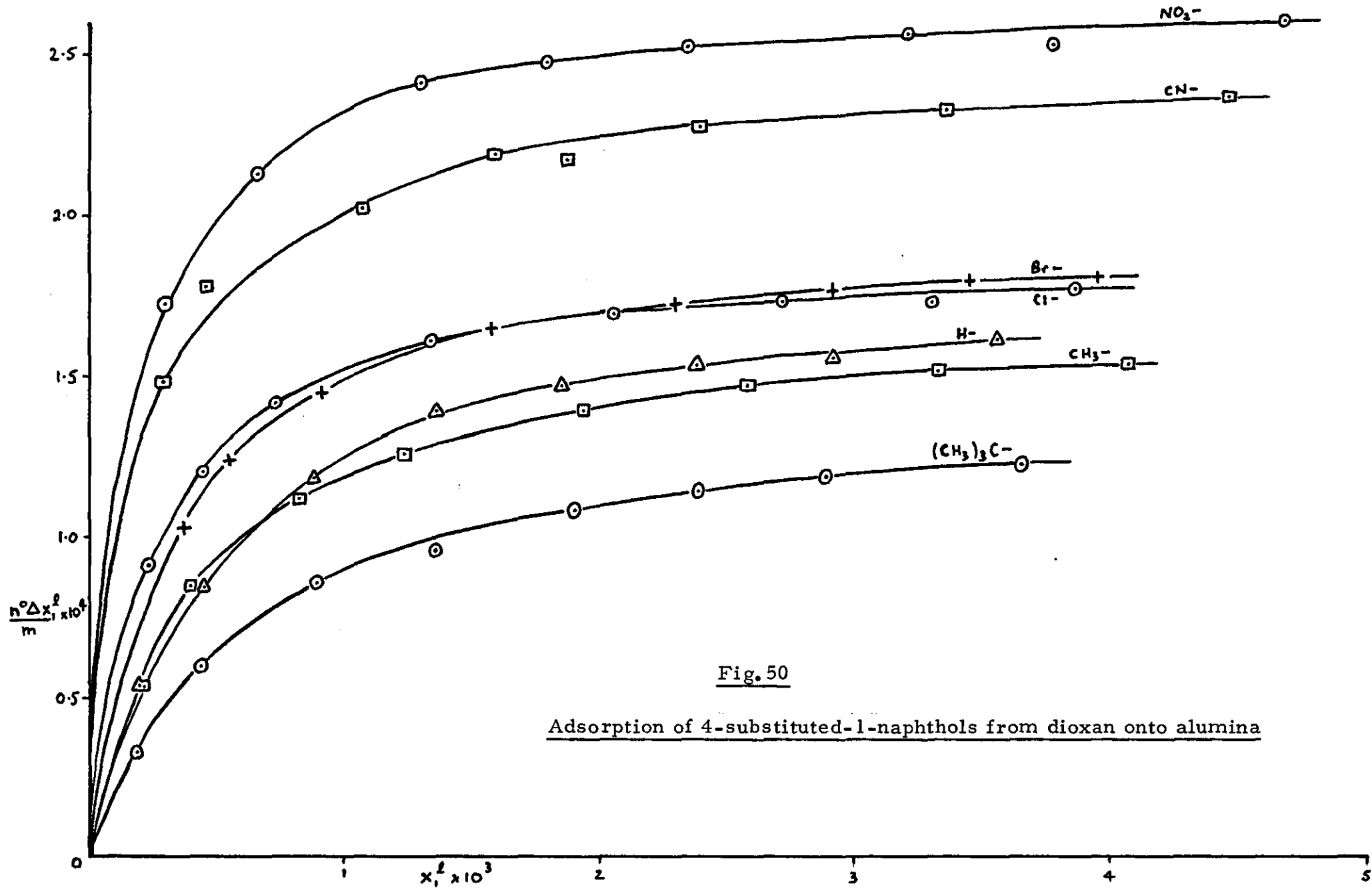


Fig. 50

Adsorption of 4-substituted-1-naphthols from dioxan onto alumina

DISCUSSION OF RESULTS

(A) ASSOCIATION IN SOLUTION

In this study of the 1 - naphthols two solvents have been predominantly employed; cyclohexane and dioxan. They offer an interesting contrast in solvation behaviour; in the former solute-solvent interactions are very weak, there is no specific mechanism identifiable and the solubilities of the naphthols reflect the low energies involved (thus the solubilities are not high and are vanishingly small for 4-cyano- and 4-nitro-1-naphthols). However, dioxan readily hydrogen bonds with hydroxy aromatic compounds and in this solvent solubilities can be so high that difficulty is experienced in measuring them. Comparisons are made, then, between the behaviour of the naphthols in these two solvents and since dilute solutions are employed this amounts to a comparison between properties of the 'free' naphtholic OH and the 'bonded' naphtholic OH group. Amongst the changes discussed in the Introduction which occur upon hydrogen bond formation are changes in the vibrational spectra of A-H and B, particularly changes in the A-H stretching mode :-

- (a) the decrease in the frequency,
- (b) the increase in the band width, and
- (c) the increase in the intensity.

Fig. 51 shows infrared spectra for 1-naphthol in cyclohexane and dioxan solution and all of the above changes can readily be identified.

The change in OH stretching frequency, $\Delta \nu$, on hydrogen bond formation of 1-naphthol to dioxan is inversely related to the overall O-H.....O distance and this in turn is dependent upon the proton-

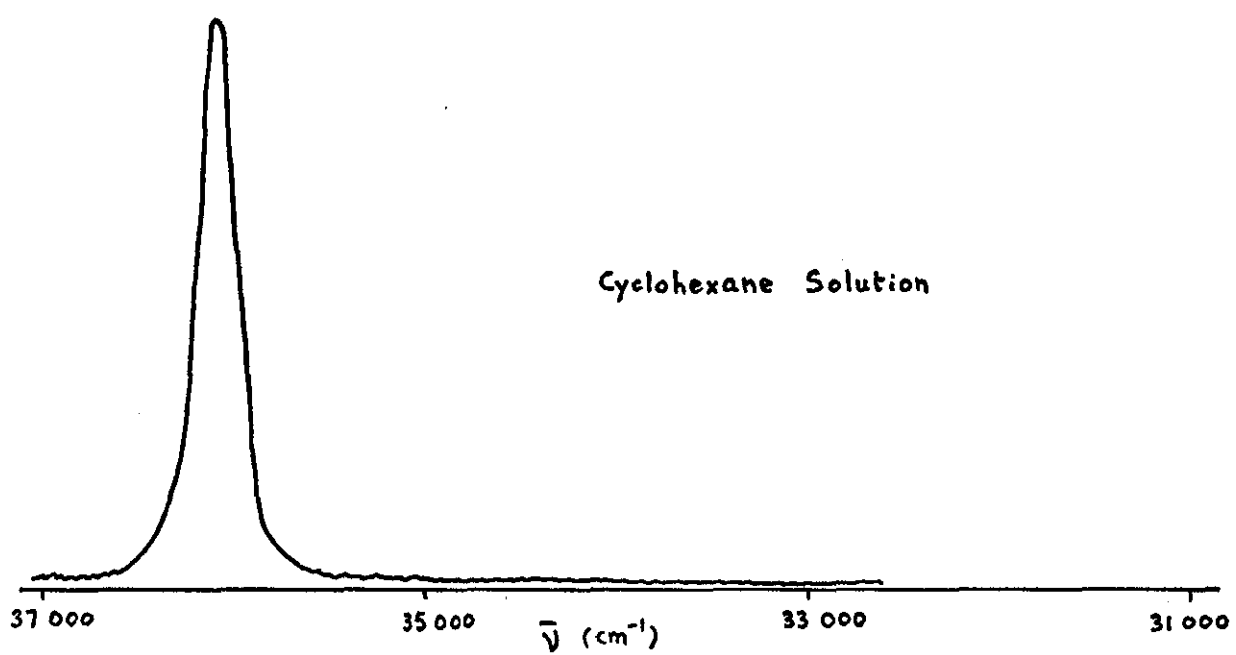
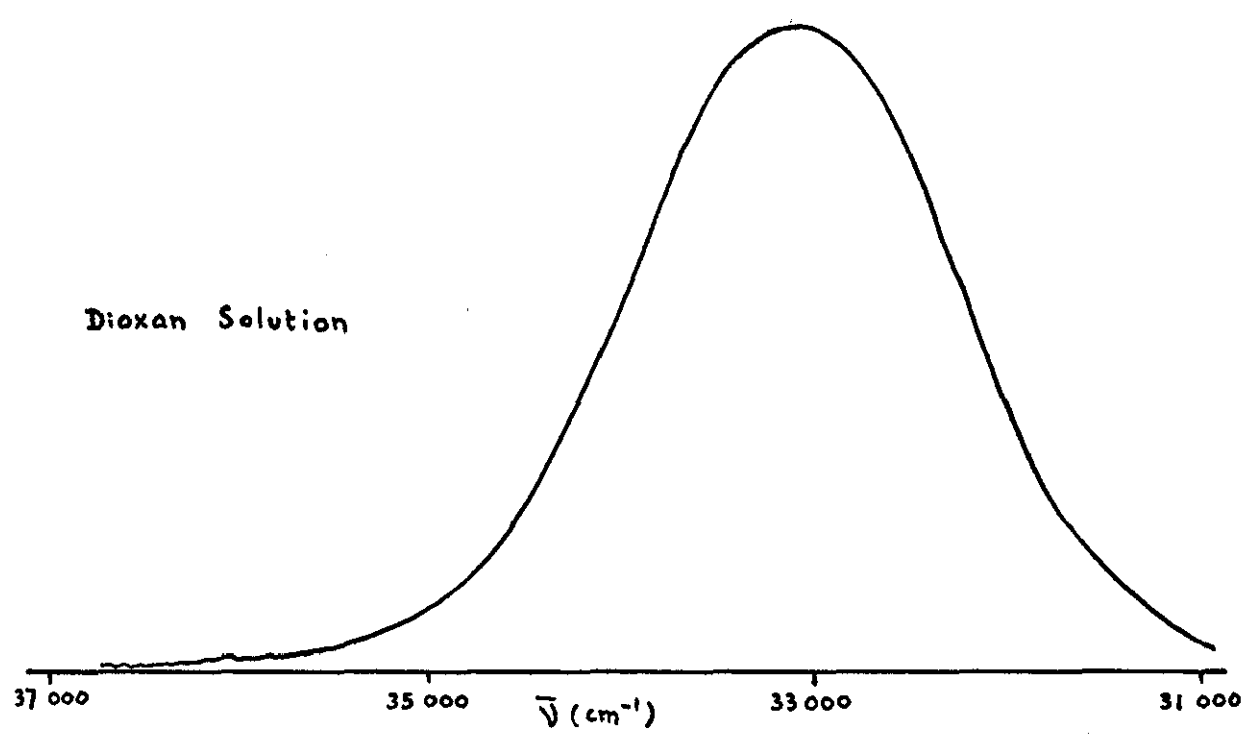


Fig. 51 Absorption bands in the infrared for 1-naphthol in
cyclohexane and dioxan solutions



donor and -acceptor properties of the system. Thus the O.....O distance for a given oxygen containing solvent (i. e. proton acceptor, base) decreases with increasing acidity (as measured for example by its pK_a value) of the proton donor (naphthol in this case) and in the systems studied in this investigation, $\Delta\nu$ can be expected to increase with increasing acidity of the naphthols.

It has been established⁴³ that $\Delta\nu$ values of 4-substituted phenols can be related to the influence of the 4-substituent and in particular to this influence as measured by the Hammett structural parameter: Fig. 52 shows a plot of $\Delta\nu$ for a series of 4-substituted phenols against corresponding (normal) σ_{para} values for the substituents. It can be seen that the presence of electron withdrawing groups increase the acidity of the phenol and from Table 32 that these groups consequently also increase the OH stretching frequency shift, $\Delta\nu$ (i. e. $\Delta\nu = \text{frequency in cyclohexane} - \text{frequency in dioxan}$).

The 4-substituted-1-naphthols appear to follow the same pattern; unfortunately not all of the required pK_a values are to be found in the literature but Fig. 53 shows the roughly linear increase of $\Delta\nu$ (again, the difference between measured stretching frequencies in cyclohexane and dioxan solutions) with $\sigma_{4,1}$. Table 33 recalls the values of $\sigma_{4,1}$ selected for this study and the experimental $\Delta\nu$ values.

Joesten and Drago⁹⁶ have reported a linear relationship between the standard enthalpy of hydrogen bonding (ΔH^\ominus) and the change in OH stretching frequency ($\Delta\nu_{OH}$) when phenol is complexed with 15 different electron donors in carbon tetrachloride solution. This relationship is given as

$$-\Delta H^\ominus \text{ (K cal. mol}^{-1}\text{)} = 0.016 \Delta\nu_{OH} \text{ (cm}^{-1}\text{)} + 0.63.$$

Fig. 52 $\Delta\nu$ values for 4-substituted phenols

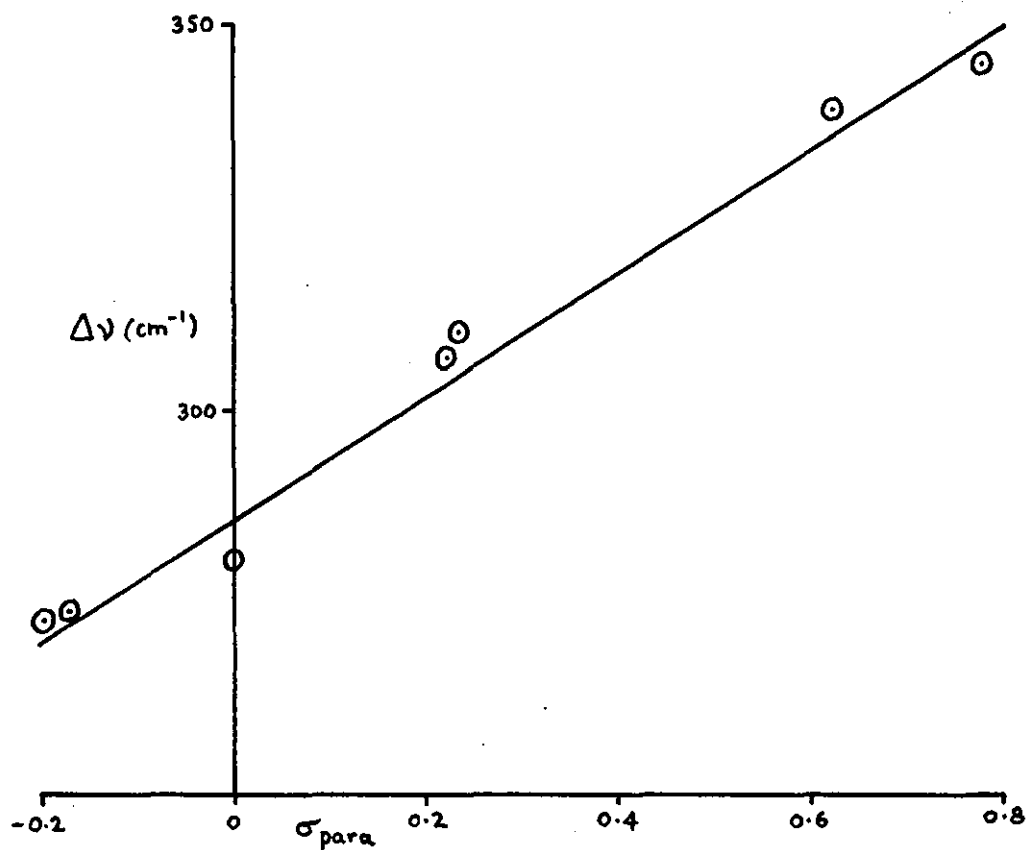


TABLE 32: pK_a and $\Delta\nu$ values for 4-substituted Phenols

4-Substituent	σ_{para}^{10}	pK_a^{95}	$\Delta\nu$ (cm^{-1}) ⁴³
$C(CH_3)_3$	- 0.197	-	270
CH_3	- 0.170	10.26	272
H	0	9.92	282
Cl	0.227	9.38	307
Br	0.232	9.34	311
CN	0.628	7.95	339
NO_2	0.778	7.15	345

Fig. 53 $\Delta\nu$ values for 4-substituted-1-naphthols

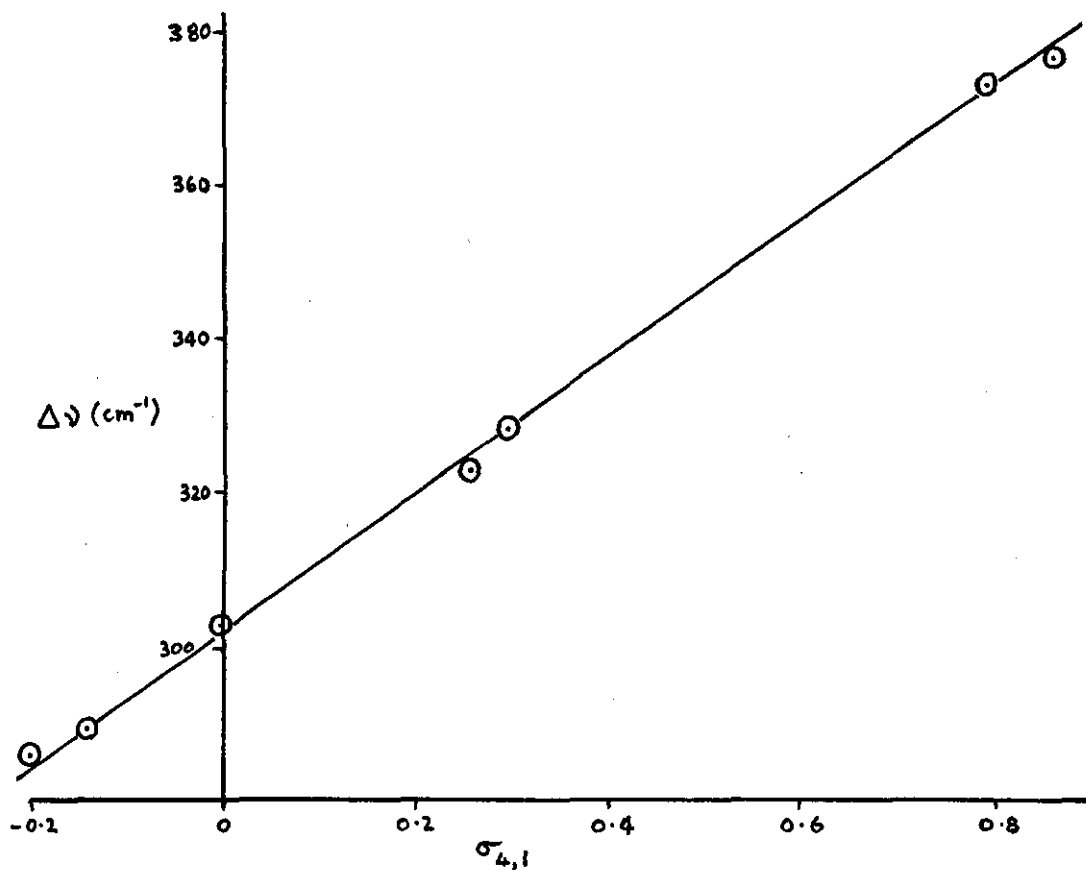
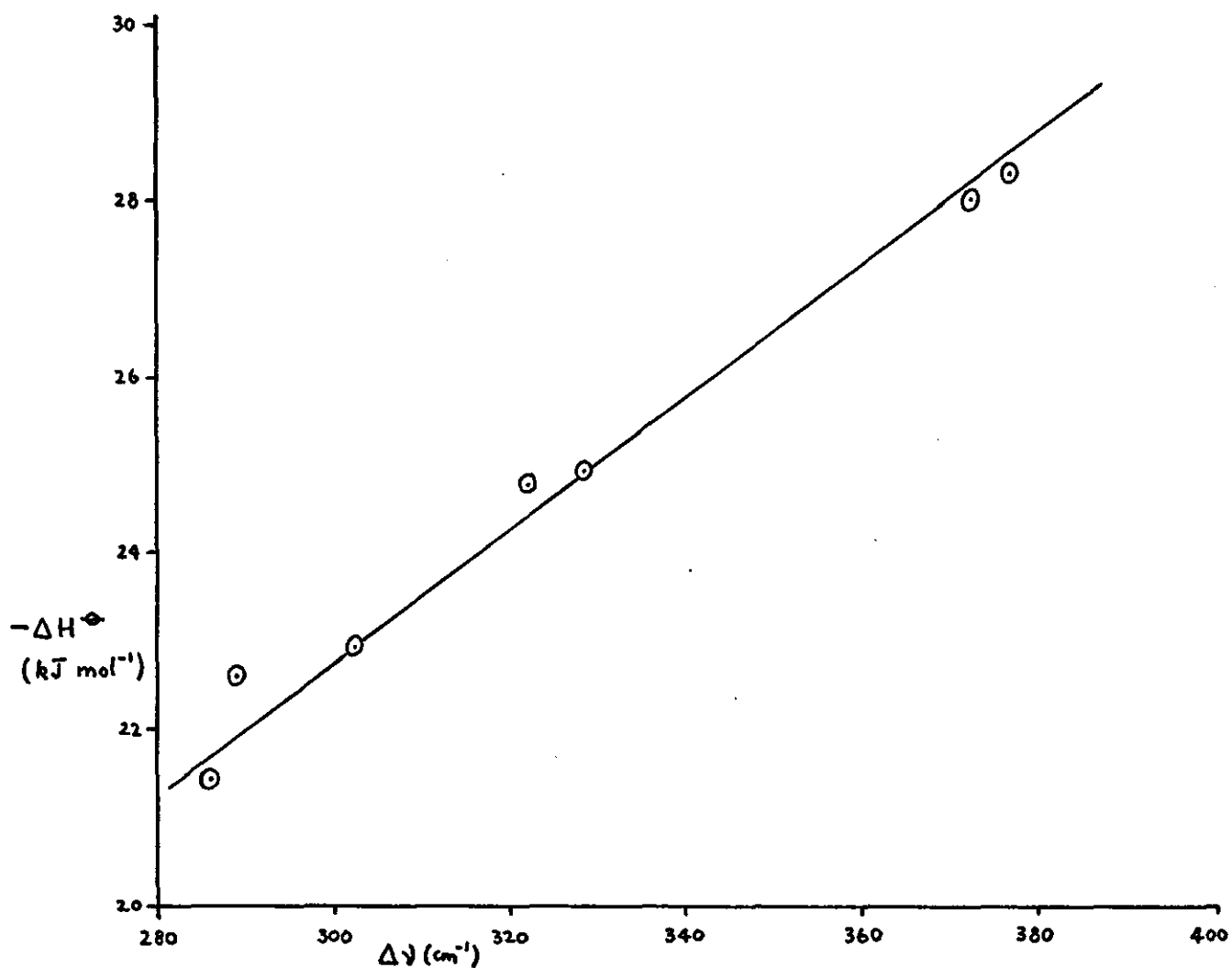


TABLE 33: Frequency Shifts for 4-Substituted-1-Naphthols

<u>Substituent</u>	<u>$\sigma_{4,1}$</u>	<u>$\Delta\nu$ (cm^{-1})</u>
$\text{C}(\text{CH}_3)_3$	- 0.2	286
CH_3	- 0.14	289
H	0	303
Cl	0.26	323
Br	0.30	328
CN	0.79	373
NO_2	0.86	377

It is of interest to investigate the possibility of a parallel relationship for the naphthols in cyclohexane solution and complexed with the same electron donor molecule such as dioxan. Fig. 54 shows a plot of $\Delta\nu$ for the naphthols against ΔH^\ominus values calculated from smoothed values of K detailed in the 'Association Constant' section which follows. It is thus possible, in principle, to calculate a standard enthalpy of hydrogen bond formation from a stretching frequency shift measured in the near infrared.

Fig. 54 Enthalpy and $\Delta\nu$ values for naphthols



1. The Association Constant

Whilst the infrared shifts show the presence of, and point to the magnitude of interaction between naphthols and dioxan, for a quantitative assessment of the equilibrium constant it is more apposite to measure changes occurring in the ultraviolet region of the spectrum upon complex formation. The results of such an investigation have already been summarised in Table 15.

However, a study of the literature reveals some ambiguity in spectroscopic parameters (notably, extinction coefficients in UV measurements and limiting chemical shifts in N.M.R. measurements) of various charge transfer complexes according to which of three concentration scales is employed in calculation: molarity, molality or mole fraction. The confusion arises in the use of the Benesi-Hildebrand equation¹⁵ (of which Equation (27) in the Introduction is a form) which may be written, for the molar scale :-

$$\frac{C_A \cdot \ell}{(A - A^0)} = \frac{1}{K_c} \cdot \frac{1}{(\epsilon_c - \epsilon_A)} \cdot \frac{1}{C_D} + \frac{1}{(\epsilon_c - \epsilon_A)} \quad (63)$$

where ℓ is the path length,

ϵ_A , ϵ_c are the extinction coefficients of acceptor and complex,

A^0 , A are the absorbances of acceptor alone and acceptor plus complex,

C_A , C_D are the initial concentrations of acceptor and donor.

It is judicious to consider the concentration scale dependence of this equation before attaching significance to results obtained by its use since Trotter and Hanna⁹⁷ report that variation arises when the concentration of donor is so high that the concentrations on the three scales are no longer proportional to each other and conclude that solution ideality only exists on one concentration scale. Kuntz et al⁹⁸ suggest how the concentration scale most appropriate to a given system can be determined experimentally and conclude that the molar scale seems to give the most consistent results for such as those under discussion (it is usual in spectroscopic measurements to express concentrations in mol dm⁻³, compatible units for path length and extinction coefficient being dm and dm² mol⁻¹ respectively.)

If there are n_D moles of donor, molecular weight M_D in n_S moles of solvent, molecular weight M_S , giving a solution of density d , then the following relationships can be set up :-

$$\frac{x_D}{c_D} = \frac{(n_S M_S + n_D M_D)}{d(n_D + n_S)} \quad (64)$$

$$\frac{m_D}{c_D} = \frac{(n_S M_S + n_D M_D)}{n_S M_S d} \quad (65)$$

where x_D , m_D , c_D are concentrations on the mole fraction, molality and molarity scales respectively.

There is reason to believe that it is more fundamental to define the chemical potential of a component of an ideal solution in terms of its mole fraction, and it follows from this definition that

$$\frac{e^{x_C}}{e^{x_A} \cdot e^{x_D}} = \text{constant} \quad (66)$$

This quotient is symbolised by K_x , subscript 'e' to the values implying equilibrium mole fractions. Combining Equations (64) and (66) gives

$$K_x = \frac{e^c c}{e^c A \cdot e^c D} \cdot \frac{d(n_D + n_S)}{(n_S M_S + n_D M_D)}$$

$$\text{i.e. } K_x = \frac{K_c \cdot d(n_D + n_S)^r}{(n_S M_S + n_D M_D)} \quad (67)$$

the assumptions being made that acceptor and complex concentrations are sufficiently small for proportionality to exist between 'c' and 'x' in each case.

If the solution is thermodynamically ideal and so dilute that $n_S \gg n_D$, Equations (64), (65) and (67) reduce to

$$\frac{x_D}{c_D} = \frac{M_S}{d} ; \quad \frac{m_D}{c_D} = \frac{1}{d} ; \quad K_x = \frac{K_c \cdot d}{M_S}$$

Substituting these expressions in Equation (63) gives

$$(i) \quad \frac{C_A \cdot \ell}{(A-A^0)} = \frac{d}{M_S K_x (\epsilon_c - \epsilon_A)} \cdot \frac{1}{C_D} + \frac{1}{(\epsilon_c - \epsilon_A)} \quad (68)$$

$$(ii) \quad \frac{C_A \cdot \ell}{(A-A^0)} = \frac{1}{M_S K_x (\epsilon_c - \epsilon_A)} \cdot \frac{1}{m_D} + \frac{1}{(\epsilon_c - \epsilon_A)} \quad (69)$$

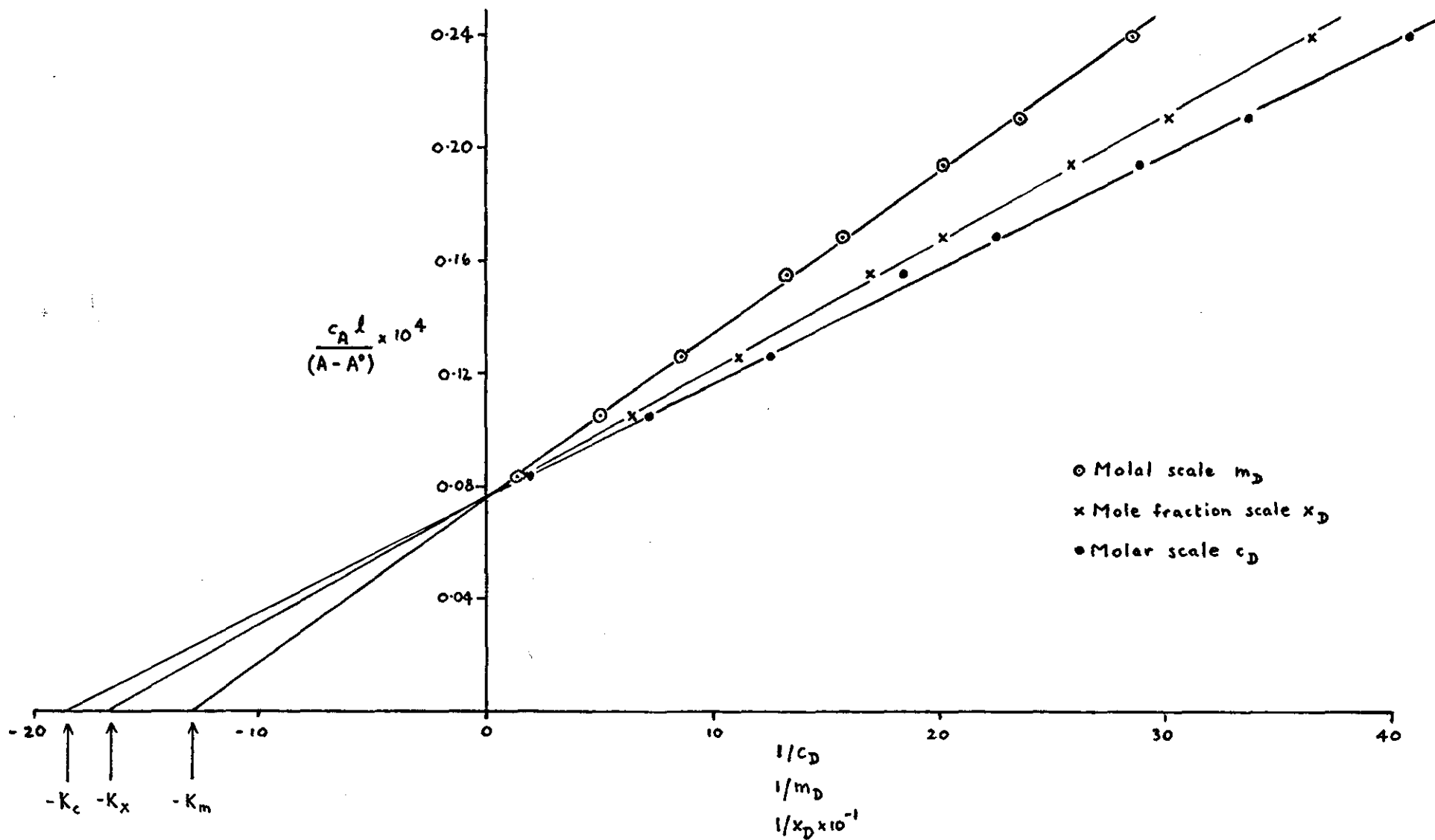
$$(iii) \quad \frac{C_A \cdot \ell}{(A-A^0)} = \frac{1}{K_x (\epsilon_c - \epsilon_A)} \cdot \frac{1}{x_D} + \frac{1}{(\epsilon_c - \epsilon_A)} \quad (70)$$

Thus when $n_S \gg n_D$ and the solutions are ideal, the three concentration scales are directly proportional to each other and Equations (68), (69) and (70) will be linear having a common intercept of $1/(\epsilon_c - \epsilon_A)$. The experimental results obtained for

Fig. 55

Various scales for association constants : 1-naphthol/dioxan in cyclohexane solution

151



the association of 1-naphthol to dioxan in cyclohexane solution (Table 7) have been assessed on the three concentration scales (Fig. 55) and the extinction coefficient, ϵ_c , and association constant, K_x , calculated from Equations (68), (69) and (70) are given in Table 34.

TABLE 34. Association of 1-Naphthol to Dioxan
In Cyclohexane at 25°C

<u>Concentration Scale</u>	<u>$\epsilon_c / (\text{dm}^2 \text{mol}^{-1})$</u>	<u>K_x</u>
Mole fraction	77,665	0.1701
Molar	77,650	0.1706
Molal	77,560	0.1715

It is concluded that the solutions used for the systems studied in this thesis approach ideality so closely and are sufficiently dilute ($n_s \gg n_D$) for the choice of concentration scale not to be critical.

When the solutions are ideal but not so dilute ($n_s \gg n_D$), Equations (64) and (65) show that the three concentration scales are no longer proportional to each other and Equations (68) and (69) are no longer applicable and must be replaced by Equations (71) and (72) respectively :-

$$\frac{C_A \cdot l}{(A - A^0)} = \frac{d}{K_x M_s (\epsilon_c - \epsilon_A)} \cdot \frac{1}{C_D} + \frac{1}{(\epsilon_c - \epsilon_A)} \times \left[1 - \frac{(M_D - M_s)}{M_s} \cdot \frac{1}{K_x} \right] \quad (71)$$

$$\frac{C_A \cdot l}{(A-A^0)} = \frac{1}{K_x M_s (\epsilon_c - \epsilon_A)} \cdot \frac{1}{m_D} + \frac{1}{(\epsilon_c - \epsilon_A)^x} \left[1 + \frac{1}{K_x} \right] \quad (72)$$

These equations are obtained by substituting Equations (64), (65) and (67) into Equation (63). It is seen that under these conditions linear plots of differing slopes and intercepts will be obtained.

Having established the validity of the association constant calculations it is now possible to explore correlations with the Hammett σ parameter and hence with the effect of 4-substitution. In this context it should be mentioned that the $\sigma_{4,1}$ value for the 4-t-butyl substituent, being inaccessible from the literature, has been interpolated at a nominal -0.2 from comparison with σ_{para} values for benzene systems. Since the Hammett equation derives from a linear free energy relationship, as demonstrated in the Introduction, and since free energy changes (ΔG^\ddagger) can be related to equilibrium constants by the general expression

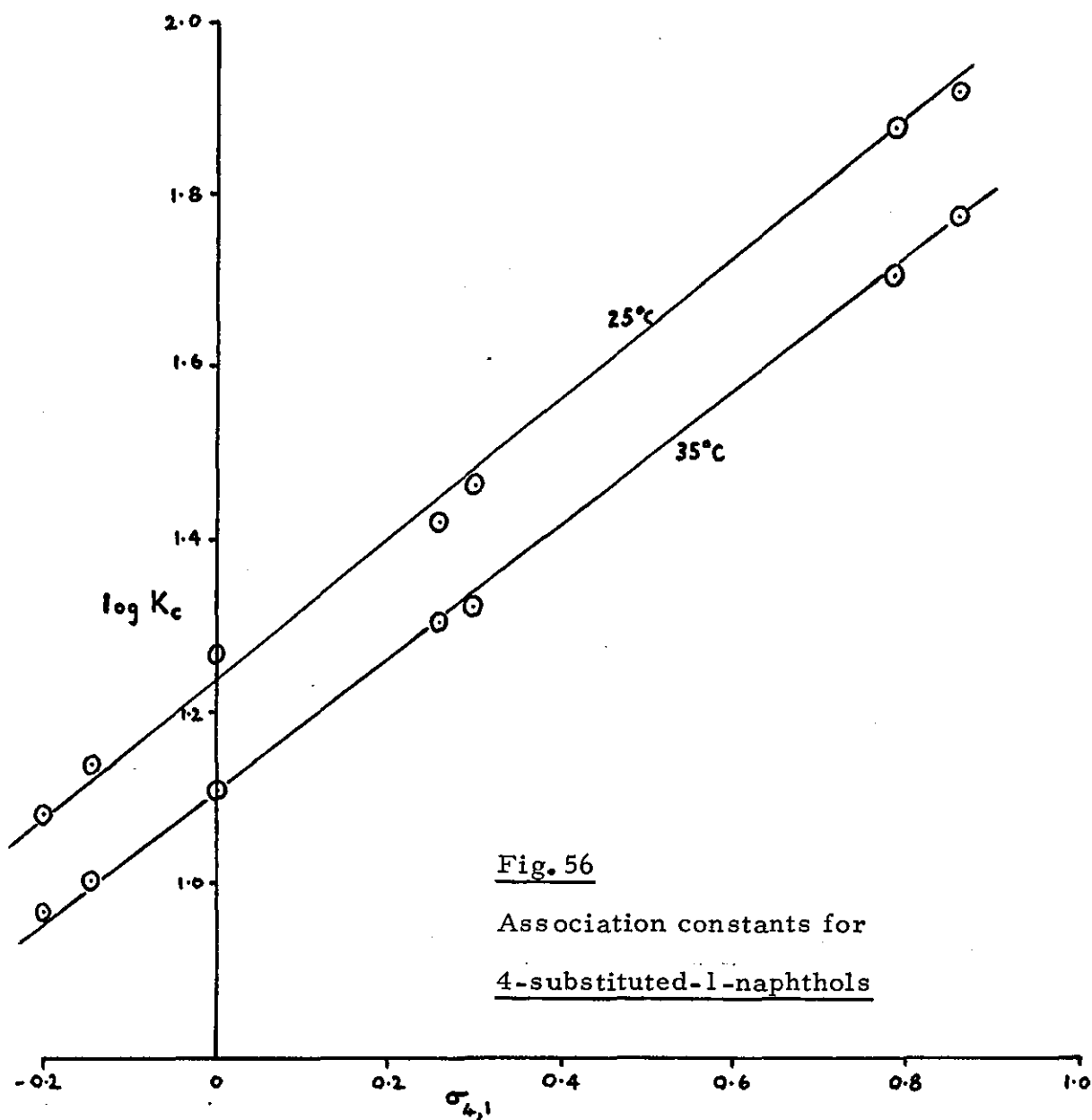
$$\Delta G^\ddagger = -RT \ln K_c$$

it is clearly necessary to compare σ with the logarithm of the equilibrium constant.

The relevant co-ordinates are recorded in Table 35 from which it is seen that the temperature coefficient of the association constant is as expected, K_c decreasing with increasing temperature and also that electron donating groups give rise to a decrease and electron withdrawing groups an increase in K_c over that observed for the parent 1-naphthol. Fig. 56 shows plots of

TABLE 35: Association Constants for 4-Substituted-1-Naphthols

<u>4-Substituent</u>	<u>$\sigma_{4,1}$</u>	<u>$K_c(25^\circ\text{C})$</u>	<u>$\log K_c(25^\circ\text{C})$</u>	<u>$K_c(35^\circ\text{C})$</u>	<u>$\log K_c(35^\circ\text{C})$</u>
$\text{C}(\text{CH}_3)_3$	- 0.20	12.14	1.0844	9.17	0.9623
CH_3	- 0.14	13.75	1.1383	10.23	1.0098
H	0	18.45	1.2660	12.95	1.1123
Cl	+ 0.26	26.50	1.4232	20.15	1.3043
Br	+ 0.30	29.32	1.4672	21.21	1.3266
CN	+ 0.79	75.91	1.8803	51.42	1.7112
NO_2	+ 0.86	83.49	1.9216	59.81	1.7768



$\sigma_{4,1}$ against $\log_{10} K_c$ at 25°C and 35°C and the dominating influence of the 4-substituent upon complex formation is at once apparent: the two 'least squares' straight lines have been calculated and drawn through the points (departures from these lines are probably due to experimental inaccuracies or even to uncertainty in precise $\sigma_{4,1}$ values for naphthalene systems).

2. Changes in Thermodynamic Functions upon Association

The van't Hoff isochore, Equation (73), enables standard molar enthalpy changes to be estimated from equilibrium data :-

$$\frac{d \ln K_c}{dt} = \frac{\Delta H^\ominus}{RT^2} \quad (73)$$

Since measurements have been made at two temperatures only, an integrated form of the equation is more appropriate :-

$$\log (K_2/K_1) = \frac{\Delta H^\ominus (T_2 - T_1)}{2.303 RT_1 T_2} \quad (74)$$

where K_1 and K_2 are the association constants at T_1 K and T_2 K (i. e. 298K and 308K respectively)

ΔH^\ominus is the standard enthalpy change, assumed constant over the range $T_1 - T_2$ K

R is the universal gas constant.

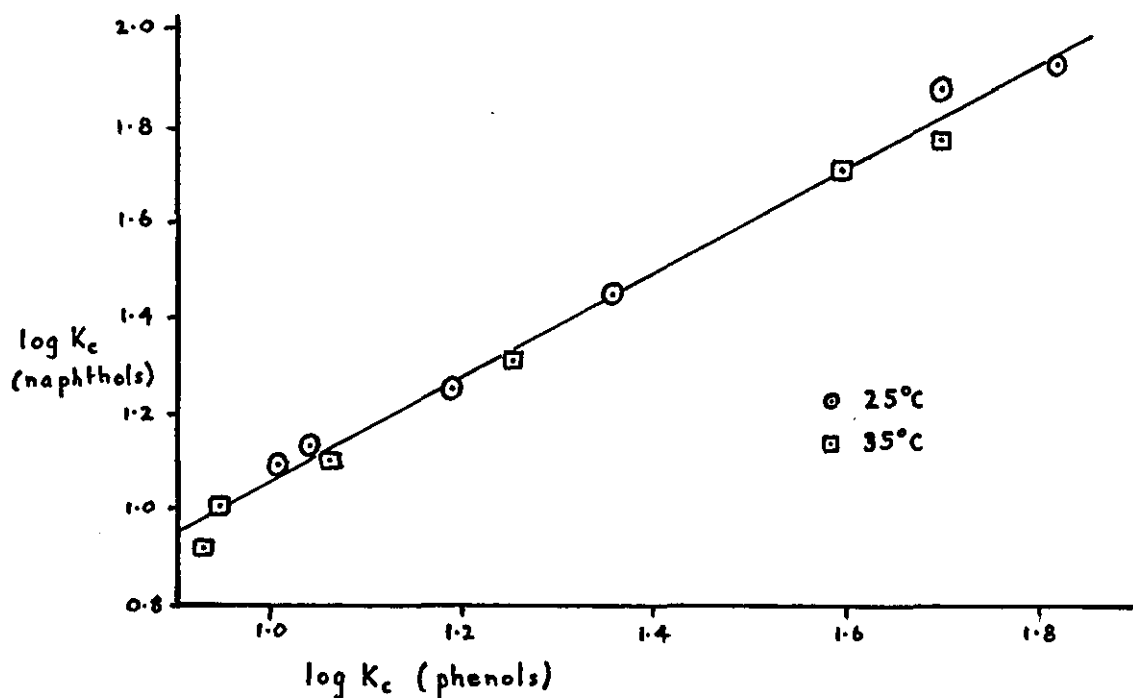
In an attempt to avoid distortion of the overall picture by local variation (probably due to experimental error) smoothed values taken from equations for the straight lines in Fig. 56 were substituted into Equation (74) and the ΔH^\ominus values so obtained are recorded in Table 36 together with results derived in a similar manner from the author's earlier work on 4-substituted phenols.

The variation in ΔH^\ominus for either series is small although a continuous trend is shown and the greater the electron withdrawing effect of the 4-substituent the stronger the hydrogen bond between the enolic OH group and the oxygen of the dioxan. Further, it would appear that a marginally stronger hydrogen bond is made by a 4-substituted naphthol with dioxan than that made by the corresponding 4-substituted phenol and this is again demonstrated by the plot of $\log K_c$ for naphthols against corresponding $\log K_c$ values for phenols at both 25 and 35°C. Fig. 57 shows that the relationship is essentially linear, that the relationship is temperature independent and that the slope of 1.11 implies a slightly greater hydrogen bonding tendency of the naphthols for dioxan than the phenols.

TABLE 36: Standard Enthalpy Changes for Naphthols and Phenols

4-Substituent	ΔH^\ominus (naphthol) /kJ mol ⁻¹	ΔH^\ominus (phenol) /kJ mol ⁻¹
C(CH ₃) ₃	- 21.46	- 16.34
CH ₃	- 22.67	- 16.61
H	- 22.85	- 18.03
Cl	- 24.78	- 19.87
Br	- 24.96	-
CN	- 27.94	- 23.14
NO ₂	- 28.30	- 24.35

Fig. 57 Association constants for naphthols and phenols



The standard free energy and standard entropy changes (ΔG^\ominus and ΔS^\ominus) upon association can readily be calculated from the reported data at 25°C by means of Equations (75) and (76) :-

$$\Delta G^\ominus = -RT \ln K_c \quad (75)$$

$$\Delta G^\ominus = \Delta H^\ominus - T \Delta S^\ominus \quad (76)$$

Table 37 records the results of such computations from the author's work for both naphthols and phenols. Once again, a steady increase in standard free energy change is observed in both cases but the standard entropy changes do not lend themselves to such an obvious comment.

The magnitude of the changes in free energy (and hence the variation in association constant) represent a balance between changes in enthalpy and entropy upon association. Theoretically, the change in entropy occurring upon complex formation will be largely the result of a decrease in the number of degrees of freedom, leading to an increase in the 'order' of the system. Thus negative values of ΔS^\ominus for the systems considered can be predicted and are, in fact, realised in practice. As the number of degrees of freedom of a molecule increases with its structural complexity, then the negative standard entropy change upon association would be expected to increase as the reacting molecules became more complex. However, in the naphthol-dioxan complexes encountered in this study the only variation is in the 4-substituent of the naphthol and therefore only small differences in entropy changes might be anticipated : an examination of Table 37 shows this to be the case, and in the phenol-dioxan system, too, entropy changes are of similar magnitude within the series. Nonetheless, it is noteworthy that the negative standard entropy changes upon complex formation for the series of naphthols are, without exception, greater in magnitude than those for the corresponding phenols. This observation supports the remark made above : the greater complexity of naphthol molecules over that of the corresponding phenol molecules provides a greater number of possible distributions of the internal energy of the molecules and consequently entropy changes upon association are larger numerically for the naphthols than for the phenols.

TABLE 37: Standard Free Energy and Entropy Changes for Naphthols and Phenols

<u>4-Substituent</u>	NAPHTHOLS		PHENOLS	
	$-\Delta G^\ominus$ /kJ mol ⁻¹	$-\Delta S^\ominus$ /J mol ⁻¹ K ⁻¹	$-\Delta G^\ominus$ /kJ mol ⁻¹	$-\Delta S^\ominus$ /J mol ⁻¹ K ⁻¹
C(CH ₃) ₃	6.19	51.24	5.83	35.27
CH ₃	6.46	54.40	5.93	35.84
H	7.09	52.89	6.75	37.85
Cl	8.27	55.40	7.92	40.10
Br	8.46	55.37	-	-
CN	10.71	57.82	9.70	45.10
NO ₂	11.03	57.95	10.41	46.78

In conclusion, it would appear that changes in free energy of association are controlled by the magnitude of the enthalpy changes rather than the entropy changes. This discovery is in interesting contrast to that reported by another worker who has studied the association in cyclohexane of unsubstituted phenol with a series of donors of widely different structure.⁹⁹ In these circumstances it was found that the enthalpy changes were virtually constant and so changes in free energy of association were principally governed by entropy changes, which is not surprising considering the large variation in phenol-donor complex structure.

B. ADSORPTION ON ALUMINA

1. The Sorbent

The use of activated aluminas as industrial catalysts and catalyst supports has promoted their intense study and in consequence the literature abounds with references to the many modifications which appear to exist, although rather less information is available concerning the rates of interconversion, as a function of temperature, between the various forms. In consequence, a particular sample may well prove to be a mixture of partial decomposition and conversion products and even with a knowledge of its history, a complete characterisation can still present considerable problems. Nevertheless it seems most likely that the sorbent used in this study comprises approximately 90% γ -alumina with admixture of roughly 10% undecomposed boehmite, and before any quantitative discussion of adsorption data can take place a value for the specific surface area must be resolved.

The Extent of the Accessible Surface

With outer orbits of electrons complete, the noble gases are attractive adsorbates for area measurements: argon, krypton and xenon have been used for this purpose and in this context it is significant that argon, with the smallest molecules of the three, has the lowest polarisability. It would seem less likely than the others, therefore, to show an appreciable variation in enthalpy of adsorption from one solid to another, or to exhibit pronounced localised adsorption: suitable criteria for its selection for determination of surface areas. The monolayer capacities (cm^3 of gas at S.T.P.) for argon at 78.7 K determined for this alumina have been reported

in Table 15 and a value for the surface area requirement (i. e. the apparent atomic cross-sectional area) of an argon atom ($A_m \text{ nm}^2$) is required before the total accessible sorbent surface area can be calculated.

Whilst the area requirement for a nitrogen molecule has been widely accepted as 0.162 nm^2 on a wide variety of sorbents since the pioneer work of Davies et al¹⁰⁰, there is much less accord in the literature upon a corresponding figure for argon. The value for nitrogen was calculated from liquid nitrogen data using Equation 54 and in their early work Brunauer and Emmett¹⁰¹ adopted 0.138 nm^2 as the A_m value for argon at 77 K, calculated from the liquid density in a similar manner. However, consistently low results for surface areas have been reported by some workers¹⁰² using this value and various arbitrary adjustments have been suggested, 0.166 nm^2 ¹⁰³ and even higher (e. g. 0.20 nm^2 ¹⁰⁴) in order to correlate results from nitrogen and argon adsorption. From data published for argon sorptions the fact emerges that on some adsorbents (notably where the energy of interaction between adsorbate and adsorbent is relatively high) the close packed argon monolayer resembles the liquid state in packing; on most adsorbents, however, the monolayer of argon has a more open structure than that of nitrogen. In those cases where the surface packing is similar to that in the liquid phase, Aristov and Kiselev¹⁰⁵ have proposed that the A_m value for nitrogen should be adjusted from its usual value of 0.162 nm^2 , the A_m value for argon being held constant at 0.137 nm^2 . The argument in favour of taking a constant value of A_m for argon is based on the principle

that the interaction of argon with all surfaces is non-polar - it involves only dispersion forces - whereas nitrogen exhibits strongly polar interaction (from quadrupoles) with some surfaces but not with others. Essentially, the area occupied by an adsorbed molecule in a completed monolayer is a compromise between the effects of two factors: the lattice parameter, tending to localise the molecule over the surface potential energy 'well', and thermal agitation, tending to break up the ordered arrangement and produce the almost random packing of a liquid. Only if the localisation effect is negligible can a value of A_m be found using Equation 54; at the other extreme, where localisation is complete (e.g. chemisorption - see the discussion of thermogravimetric analysis presented later), the effective cross-sectional area will be a function of the lattice parameters of the solid. Indeed, if the surface is strongly heterogeneous (i.e. endowed with 'active sites') or if attachment to the surface is by specific mechanism (e.g. hydrogen bonding) localised adsorption on a portion only of the surface produces a well-defined 'point B', but it now corresponds to a 'monolayer' of active sites.

Between these two extremes, there will be a greater or lesser tendency towards localisation according to the size of the constant 'C', which is, in turn, related to the net enthalpy of adsorption, and the value of A_m will then be somewhere between that calculated by Equation 54 and that calculated from the lattice parameters of the solid. The unfortunate conclusion emerges that since a high 'C' value leads to an isotherm with a sharp knee, the very factor which makes it possible to calculate a reliable value of the monolayer capacity also tends to produce a divergence from a unique value of A_m .

From the B.E.T. theory :⁸³

$$C = \frac{a_1 \nu_2}{a_2 \nu_1} \cdot e^{(E_1-L)/RT} \quad (77)$$

where a_1 is a condensation coefficient in the first adsorbed layer,
(similarly a_2 for the second and subsequent layers),

ν_1 is the frequency of oscillation of the adsorbed molecules
in the first adsorbed layer (similarly ν_2 for other
layers),

E_1 is the energy of activation of desorption,

L is the latent heat of condensation (assumed equivalent to
the enthalpy of adsorption in all layers after the first).

Equation(77) can be restated approximately as:

$$C = e^{(E_1-L)/RT} \quad (78)$$

in which (E_1-L) is frequently referred to as the 'net
enthalpy of adsorption'.

On polar adsorbents the net enthalpy of adsorption is high
enough to give an isotherm with a sharp knee but not sufficiently
high to cause excessive localisation and in these circumstances a
value of A_m from liquid data would be appropriate, but where
interactions are weaker thermal agitation probably becomes a
controlling factor and the A_m value rises.

The reasonably high experimental 'C' value for the
adsorption of argon on this alumina implies a reasonably strong
interaction between argon atoms and the surface which in turn
justifies the assumption of a close packed monolayer at the

'B point' and hence a value of 0.138 nm^2 for the apparent cross-sectional area, A_m , of the argon atom. Table 38 records values of the specific surface area from data reported in Table 18. Since the 'normal' range for linearity of the B.E.T. plot is traditionally $0.05 < p/p_0 < 0.35$ it is reasonable to adopt for the specific surface area of the alumina used in this study a value of $103.5 \text{ m}^2 \text{ g}^{-1}$.

In principle it would be possible to carry out an analysis of the desorption branch of the argon isotherm, apply t-curve and V_s calculation techniques summarised earlier to construct cumulative area and pore size distribution plots. Unfortunately, the necessary data (in the form of experimental master curves etc.) whilst available for nitrogen and alumina has not yet appeared in the literature for argon-alumina systems and so such analyses cannot be carried out at this point.

TABLE 38: SPECIFIC SURFACE AREA ESTIMATES

<u>Range of p/p_0 values</u>	<u>V_m (cm³)</u>	<u>Area (m² g⁻¹)</u>
0 - 0.250	27.597	102.3
0 - 0.275	27.677	102.6
0 - 0.300	27.904	103.5
0 - 0.325	27.904	103.5
0 - 0.350	28.154	104.4
0 - 0.375	28.762	106.7
0 - 0.400	28.825	106.9

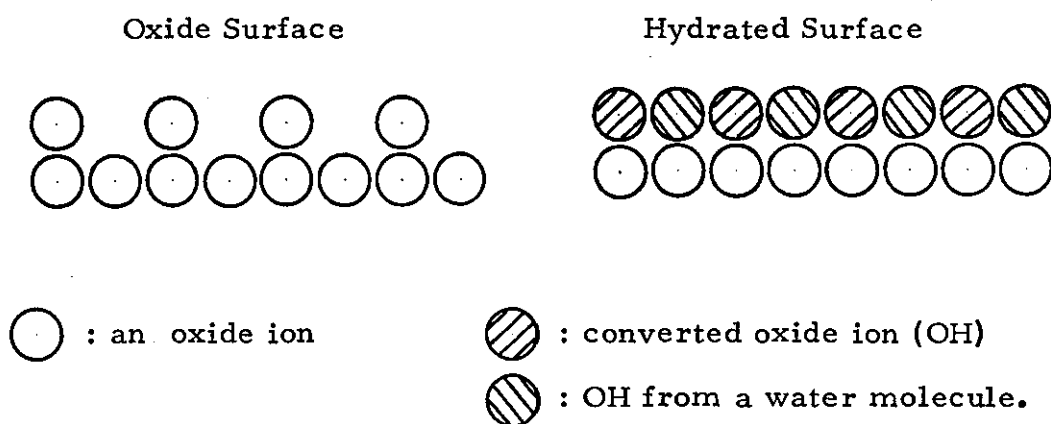
The established facts, then, relevant to this alumina surface are that approximately $90 \text{ m}^2 \text{ g}^{-1}$ of the total area ($103.5 \text{ m}^2 \text{ g}^{-1}$) is due to the presence of slit-shaped pores having a width in excess of 2 nm and the majority of pores have a diameter between 2.7 and 3.2 nm. Thus true microporosity is absent and all of the 103.5 m^2 will be accessible to any of the solute or solvent molecules encountered in this study: no 'molecular sieve' effects are likely to operate.

The Nature of the Surface

γ -Alumina has been shown to possess a pseudo-spinel structure⁷³ with unit cell edge of 0.795 nm ⁶⁹, and a considerable part of the surface formed by the 100, 010, 001 planes of the spinel lattice.¹⁰⁶ This is not surprising in view of the very good 100 cleavage shown by boehmite (γ -Al₂O₃·xH₂O, from which γ -alumina derives) caused by the weak hydrogen bonds joining layers of octahedra.¹⁰⁷ Arguments for the preferred exposure of the 111 face⁷² based on the greater density of packing of oxide ions in this face of anhydrous alumina are unconvincing since actual exposure may still reflect the relative stabilities of hydrated faces (hydroxyl) packing rather than those of dehydrated faces. Earlier workers^{82, 108} have supposed that chemisorption of water is closely related to the spacing of oxide ions on exposed faces of a cubic, close packed oxide lattice. Each oxide ion in a 111 plane would occupy 0.0674 nm^2 whereas on a 100 face the area per oxide ion would be 0.0790 nm^2 .

Establishing the extent of the surface permits of a more detailed interpretation of the results of the thermogravimetric analysis reported in the Experimental Section. The total loss of water upon heating to 1000°C amounted to 8.1% and roughly 2.0% of this is chemisorbed water; this implies, on average, 6.47 molecules of water per nm^2 which is in very good agreement with Peri's value of 6.25.⁸⁰ Thus each chemisorbed water molecule occupies 0.1546 nm^2 of the surface and this represents the area requirement of the two hydroxyl groups produced by the chemisorption of one water molecule onto an oxide surface, possibly as illustrated in Fig. 58.

Fig. 58 : Chemisorption of Water.



This result agrees very well with the area requirement predicted theoretically, viz. $2 \times 0.079 = 0.158 \text{ nm}^2$, and so once again points to the preferential exposure of 100 faces (as do the 'B points' observed in 100°C adsorption isotherms⁸⁰).

The second source of eliminated water, estimated at 1.5%, arises from the bulk decomposition of the residual bochmite (roughly 10% of the original sample) leaving a nominal 4.6% for the physically adsorbed water. This corresponds to 14.88 molecules of water per nm^2 , each molecule occupying 0.0672 nm^2 if they are all in the same layer. Clearly this very low area requirement shows that there must be more than one layer involved since the usual A_m value for a water molecule is 0.16 nm^2 ⁸⁰ (simple calculation shows that at 4°C a water molecule in the most condensed phase has an area requirement of at least 0.096 nm^2). Kipling and Peakall⁸² report that a monolayer of physically adsorbed water is complete when a total of 12.5 - 13.0 molecules per nm^2 have been adsorbed which indicates that one water molecule is situated over the same area as two surface hydroxyl groups.

Bearing in mind that the divisions in the thermogravimetric data are somewhat arbitrary, the 'average' situation on the 'wet' alumina could be interpolated as :-

Layer	State	Component	Water Molecules per nm^2	% Weight
1st	complete	hydroxyl groups	6.47	2.0
2nd	complete	water molecules	6.47	2.0
3rd	complete	water molecules	6.47	2.0
4th	incomplete	water molecules	1.94	0.6

After heating this very 'wet' alumina at 120°C there is a 3.4% loss in weight at which point an 'average' situation might be:-

Layer	State	Component	Water Molecule per nm ²	% Weight
1st	complete	hydroxyl groups	6.47	2.0
2nd	incomplete	water molecules	3.88	1.2

The state of the alumina surface, then, after the standard treatment immediately prior to sorption approximates to roughly half a monolayer of water molecules physically adsorbed onto a complete monolayer of hydroxyl groups.

2. Adsorption of Organic Vapours

Of the solvents employed in the sorption work only cyclohexane and dioxan had vapour pressures sufficiently high at room temperature to permit vapour sorptions: decalin, tetralin and 1-methylnaphthalene (all high boiling liquids) had vapour pressures too low to be accurately measured on the gas sorption apparatus available.

The dioxan isotherm shown in Fig. 43 is B.E.T. Type 11 in shape although the knee is quite rounded, implying a lower value of 'C' (and therefore of net enthalpy of adsorption) than that for either the argon or nitrogen isotherms. However, a reasonable B.E.T. plot is given and enables a value of v_m to be found (8.996 cm³ of dioxan vapour at S.T.P.).

The problem of assigning a value for A_m for dioxan is acute: the molecule is not spherically symmetrical and so a decision with regard to its orientation on the surface must be taken. Since both

of the oxygen atoms could form hydrogen bonds with hydroxyl groups on the surface, it would seem most reasonable to assume the molecules lie parallel to the surface in which case the minimum possible area requirement would be the molecular cross-sectional area, calculated from the geometry of the molecule and van der Waals radii to be 0.336 nm^2 . However, in view of hydrogen bonding possibilities, localisation effects are likely to play an important role and experience suggests that the area requirement in practice may be in considerable excess of the geometrical cross-section.

Considering these uncertainties (and the rather rounded knee of the isotherm) it would be imprudent to use the dioxan data to calculate a specific surface area. A more constructive and useful exercise is to assume the argon result as the area available to the dioxan molecules. From this, and the dioxan monolayer capacity, ^{it is possible} to calculate a practical A_m value for dioxan: a quantity also of significance in later discussions of sorptions from dioxan solutions. The result obtained is 0.428 nm^2 for the surface area requirement of a dioxan molecule: considerably higher than the minimum geometrical area, as anticipated, and this value lends strong support to the earlier supposition that dioxan molecules lie 'flat' on the surface (each covers, on average, 5.4 ion sites - hydroxyl groups - of the alumina lattice). Further support for rationality of this A_m value lies in the experimental A_m values for the similar sized benzene molecule: ranging $0.38 - 0.40 \text{ nm}^2$.

When an adsorption isotherm for cyclohexane vapour is constructed (Fig. 45) a very different situation is revealed.

Since cyclohexane cannot form hydrogen bonds with surface groups localisation effects should be minimal but so will be the overall energy of interaction with the surface, therefore the 'C' value will be small and this is confirmed by the shape of the isotherm:

B.E.T. Type 111 with no knee at all.

If the B.E.T. equation (Equation 53) is examined it will be seen that as 'C' falls to unity the relationship converges to

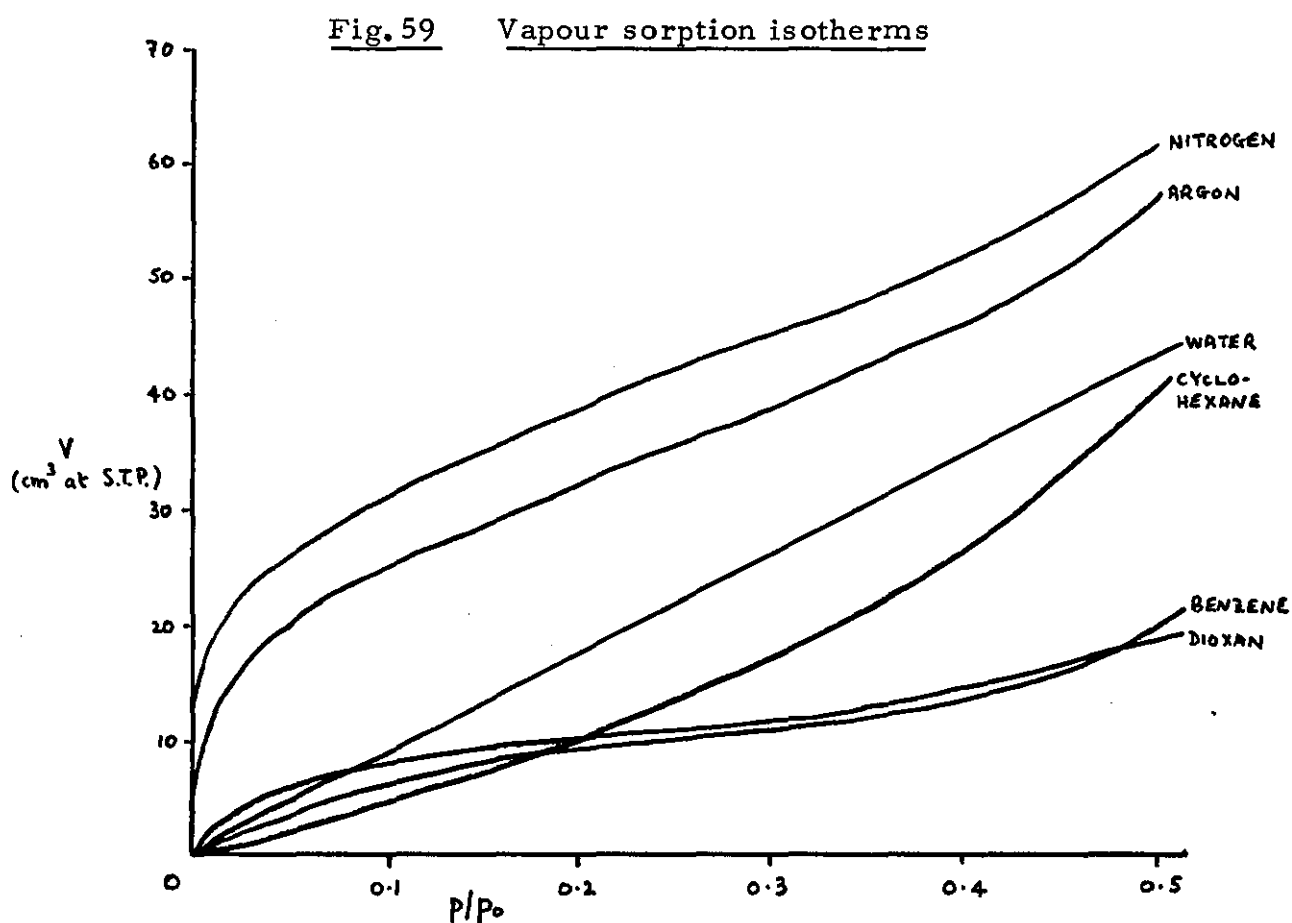
$$\frac{p}{v(p_0-p)} = \frac{1}{v_m} \quad (79)$$

Thus the B.E.T. plot of $p/v(p_0-p)$ against p/p_0 becomes a straight line parallel to the p/p_0 axis and at a distance of $1/v_m$ from it. In the adsorption of cyclohexane onto the alumina used in these sorption studies such a situation is all but realised (Fig. 46); the net enthalpy of adsorption must be very low (i.e. the adsorbate-surface interactions are of closely similar magnitude to the adsorbate-adsorbate interactions) and 'C' is close to unity. Nonetheless, a value for the monolayer capacity could be obtained, in principle, from Equation (79). However, the conclusions from a study⁹⁴ of the B.E.T. procedure for calculating monolayer capacities from Type 111 isotherms are discouraging: Gregg and Sing conclude that there is no strong a priori reason for supposing that the B.E.T. or any similar method is capable of yielding a reliable value for the monolayer capacity from a Type 111 isotherm. Appropriate discretion is accordingly exercised in this study and no quantitative data are deduced from the cyclohexane isotherm.

Finally, parameters calculated from the vapour sorption data of the author and other workers for the alumina under investigation are summarised in Table 39, and Fig. 59 illustrates the variation of the isotherm shape and type with the value of 'C'.

TABLE 39: PARAMETERS FROM VAPOUR SORPTIONS

Adsorbate	A_m	Temp.	v_m	c	net enthalpy of adsorption	enthalpy change upon monolayer formation
	$/nm^2$	$/K$	$/cm^3$		$/kJ mol^{-1}$	$/J$
Nitrogen ³⁴	0.162	77.4	30.3	75.32	2.78	3.76
Argon	0.138	78.7	27.9	39.49	2.41	3.00
Dioxan	0.428	293	9.0	20.57	7.37	2.96
Tetrahydrofuran ⁶⁸	0.428	293	8.9	18.34	7.09	2.83
Benzene ³⁴	0.400	293	9.5	12.03	6.06	2.58
Water ³⁴	0.160	293	21.1	10.41	5.71	5.39
Cyclohexane	-	293	-	1-2	0-0.17	-



3. Adsorption at the Solution-Solid Interface

The sorptions from the gaseous phase discussed in the previous section are elementary in that only one adsorbate is involved, but sorptions from solution are more complex in that there are two possible adsorbates, both of which may be simultaneously adsorbed at all concentrations, and the situation at any point is a compromise between their respective affinities for surface sites. Thus the process of sorption from solution is essentially one of phase change as the accessible surface is at all times completely occupied by molecules of sorptive and solvent. If the total number of molecules in the surface phase remains constant, then this phase change can be represented



where (as before) 1 and 2 represent one molecule each of solute and solvent and s and l denote surface and liquid phases respectively.

The Everett relationship derived in the Introduction is based on such an exchange equilibrium together with the further conditions that

- (i) sorption is monomolecular,
- (ii) the sorbed phase rests on identical surface sites,
- (iii) the solution and sorbed phases behave in a thermodynamically ideal manner.

The adsorption equilibrium constant (K) in the above process has been represented :-

$$K = \frac{x_1^s \cdot x_2^l}{x_1^l \cdot x_2^s} \quad (39)$$

and this has been arranged into the linear form :-

$$\frac{m x_1^l (1 - x_1^l)}{n^o \Delta x_1^l} = \frac{1}{n^s} \left[x_1^l + \frac{1}{(K-1)} \right] \quad (45)$$

where (as before) x_1^l is the equilibrium mole fraction of component 1 in the liquid phase

n^o is the total moles present before sorption onto m g of sorbent

n^s is the total moles of solute and solvent on the surface.

For perfect systems the left hand side plotted against x_1^l should give a linear graph of slope $1/n^s$ and intercept (when $x_1^l = 0$) of $1/n^s (K-1)$ so enabling adsorption equilibrium constants to be evaluated and ^{also} the total number of moles of solute and solvent on the surface.

Another important quantity is the maximum value of uptake as this is thought to represent a monolayer of solute molecules (or an equilibrium monolayer of solute and solvent molecules in those cases where comparable affinities lead to competition for the surface): its significance in interpreting liquid sorption data is patent. Since all the isotherms obtained from solution sorptions in this study appear to rise towards a definite plateau, it is necessary to devise some standard method of extrapolation to calculate these limiting sorption values.

The Assessment of Limiting Sorption Values

A curve fitting technique using the empirical Jowett equation¹⁰⁹ over the latter part of the isotherm has commonly been employed for this purpose and a suitable form of the equation is shown in Equation (80):

$$\frac{n_1^s}{m} = A - (A-a) e^{-bx_1^l} \quad (80)$$

where n_1^s is the number of moles of solute adsorbed by m g of sorbent,

x_1^l is the equilibrium mole fraction of solute,

A is the limiting adsorption value,

a and b are proportionality constant.

Unfortunately, the Jowett equation is purely empirical, it can only fit the isotherm closely over part of the curve: thus it will be noted, for example, that a 'Jowett curve' does not pass through the origin as true isotherms do.

Accordingly, an alternative method for calculating limiting sorption values has been devised and based upon the observation that, mathematically, experimental data satisfy a particular type of empirical equation of the second degree. Every equation of the second degree represents a conic and using standard mathematical notation may be written in the form:

$$ax^2 + 2hxy + by^2 + 2gx + 2fy + c = 0 \quad (81)$$

Equation (81) can represent a circle, an ellipse, a parabola, an hyperbola or a pair of straight lines according as

$$h^2 - ab \begin{cases} > \\ = \\ < \end{cases} 0.$$

It is found that part of a curve of the form

$$x^2 + pxy - x + qy = 0 \quad (82)$$

fits experimental sorption data very closely when x corresponds to x_1^l , y to $n^o \Delta x_1^l / m$ and p, q are positive constants. For Equation (82), $(h^2 - ab)$ of the general conic (81) corresponds to

$p^2/4$ and since this is always greater than zero, the curve yielded on plotting Equation (82) is hyperbolic in shape. This equation has a further interesting and useful property in that it can be readily rearranged into a straight line form :

$$\frac{x(1-x)}{y} = px + q \quad (83)$$

which enables an estimate of the sharpness of fit of data to Equation (82) to be conveniently made, and in practice a very close fit is found.

The centre and asymptotes of the curve can be found from these for the general conic :-

$$\begin{aligned} \text{centre : } & \left(\frac{hf - bg}{ab - h^2} \right), \left(\frac{gh - af}{ab - h^2} \right) \\ \text{asymptotes : } & ax^2 + 2hxy + by^2 + 2gx + 2fy + c = \\ & \frac{(abc + 2fgh - af^2 - bg^2 - ch^2)}{(ab - h^2)} \end{aligned} \quad (84)$$

Thus for Equation (82) :

$$\begin{aligned} \text{centre : } & \left(\frac{-q}{p} \right), \left(\frac{p+2q}{p^2} \right) \\ \text{asymptotes : } & x^2 + pxy - x + qy = \frac{q(p+q)}{p^2} \end{aligned}$$

and the latter equation will factorise :

$$\left(x + py - \frac{p+q}{p} \right) \left(x + \frac{q}{p} \right) = 0 \quad (85)$$

Equation (85) gives the pair of asymptotes :

$$y = -\frac{1}{p} \cdot x + \frac{p+q}{p^2} \quad \text{and} \quad x = -\frac{q}{p}.$$

The mathematical environment of the relevant portion of Equation (82) can now be seen in Fig. 60.

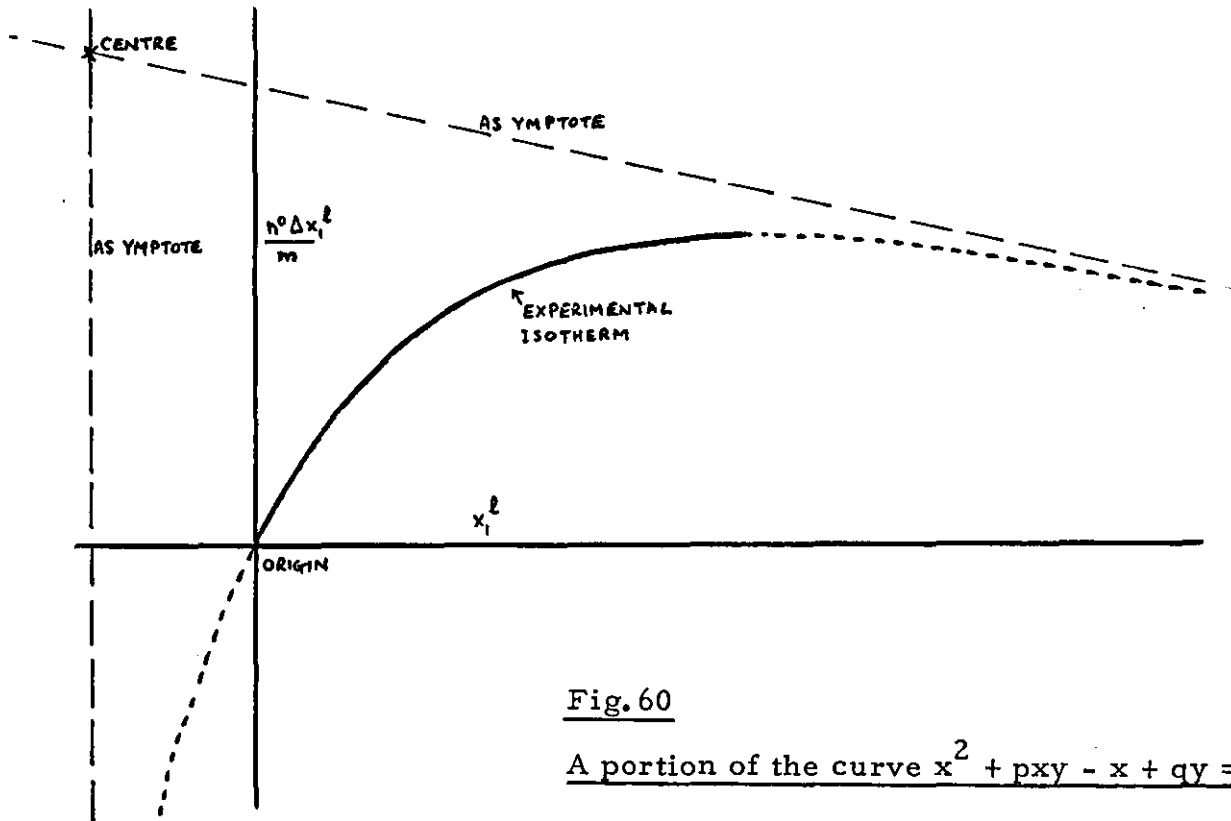


Fig. 60

A portion of the curve $x^2 + pxy - x + qy = 0$

Now the highest value of the ordinate of the empirical second degree equation corresponds to the limiting sorption value of the isotherm (provided the data fits the curve) and should agree with the limiting sorption value calculated by use of the Jowett equation. Further, this 'highest value' will occur when the slope of the isotherm is zero and so in principle these maximum values can be found from Equation (82) as follows :-

the differential with respect to x of Equation (82) is

$$2x + p \left(x \cdot \frac{dy}{dx} + y \right) - 1 + q \cdot \frac{dy}{dx} = 0$$

whence $\frac{dy}{dx} = \frac{(1-py-2x)}{(px+q)}$ (86)

If the point (x_1, y_1) is the highest point on the curve then from Equation (86), $dy/dx = 0$ and so

$$1 - py_1 - 2x_1 = 0 \quad (87)$$

But (x_1, y_1) lies on the curve so that, from Equation (82) :

$$x_1^2 + px_1y_1 - x_1 + qy_1 = 0 \quad (88)$$

Solving simultaneously Equations (87) and (88) gives

$$x_1 = \frac{-q + (q^2 + pq)^{\frac{1}{2}}}{p} \quad \text{and} \quad y_1 = \frac{1}{p} \times \left[p + 2 \left\{ q - (q^2 + pq)^{\frac{1}{2}} \right\} \right] \quad (89)$$

A suitable procedure, then, would be firstly to plot the experimental data in the straight line form of Equation (83) and provided the points lie on the line, values for the constants p and q could be assigned. Application of relationship (89) would then enable y_1 to be calculated and this would be the extrapolated value of maximum uptake - the limiting sorption value - n_1^s .

(a) The Adsorption of 1-Naphthol from Various Solvents

The experimental data from the sorption of 1-naphthol from cyclohexane, decalin, tetralin, 1-methylnaphthalene and dioxan are listed in Tables 21 to 25 and the isotherms are to be found in Fig. 49. The Everett plots of $mx_1^l x_2^l / n^o \Delta x_1^l$ against x_1^l are shown collectively in Fig. 61 although only part of the dioxan plot can be shown. Table 40 records parameters calculated from Equation (82) and from the Jowett equation (80); the area requirements per naphthol molecule (A_m) have been calculated from the specific surface area of the alumina established earlier ($103.5 \text{ m}^2 \text{ g}^{-1}$). An examination of these data gives an insight

Fig. 61

Everett plots for 1-naphthol on alumina from various solvents

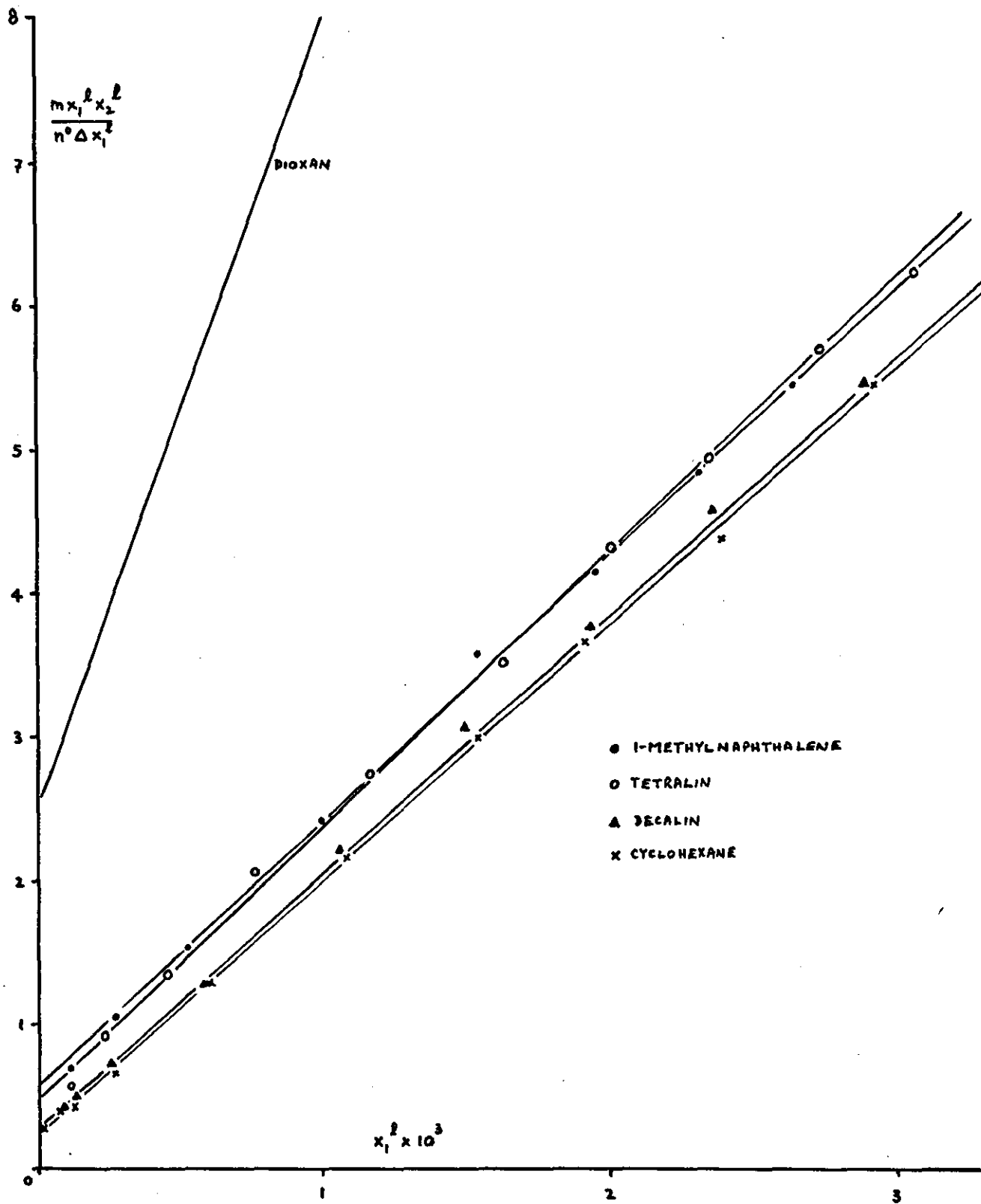


TABLE 40: ADSORPTION OF 1-NAPHTHOL

From the Everett Equation (45) :-

<u>Solvent</u>	<u>Slope</u>	<u>Intercept</u>	<u>K</u>	<u>$n^s \times 10^4$/moles</u>
Cyclohexane	1783	0.245	7278	5.609
Decalin	1800	0.255	7059	5.556
Tetralin	1889	0.478	3953	5.294
1-Methyl-naphthalene	1863	0.552	3376	5.368
Dioxan	5495	2.497	2201	1.820

From the Jowett Equation (80) and Equation (82) :-

<u>Solvent</u>	<u>Jowett Equation (80)</u>		<u>Equation (82)</u>	
	$(n_1^s)_{\max} \times 10^4 /$	A_m / nm^2	$(n_1^s)_{\max} \times 10^4 /$	A_m / nm^2
	<u>moles</u>		<u>moles</u>	
Cyclohexane	5.465	0.3144	5.479	0.3136
Decalin	5.411	0.3176	5.425	0.3167
Tetralin	4.962	0.3463	5.128	0.3351
1-Methyl-naphthalene	4.930	0.3486	5.186	0.3314
Dioxan	1.671	1.0284	1.744	0.9853

into the mechanism of the adsorption process, the orientation of the adsorbed molecules and the applicability of Everett's theory to these systems ; these are discussed below and later with respect to the adsorption of 4-substituted-1-naphthols from dioxan.

Mechanism of the Adsorption Process

McDonald¹¹⁰ has shown that the noble gases, nitrogen and oxygen which only physically adsorb on silica surfaces at low temperatures interact with surface hydroxyl groups to cause a broadening and displacement of the associated infrared absorption band to lower frequencies. These effects indicate the presence of hydrogen bond type interactions between surface hydroxyls and adsorbed molecules. The intensity of the free OH band progressively decreased with increasing adsorption, while a new band associated with these groups interacting with adsorbed molecules grew in intensity at lower frequencies. Frohnsdorff and Kington¹¹¹ consider that the relatively large frequency displacement effected by nitrogen, 24 cm^{-1} (compared with argon : 8 cm^{-1} , krypton: 16 cm^{-1} , xenon : 19 cm^{-1} and oxygen : 12 cm^{-1}), is consistent with the large value for the quadrupole moment of this gas which interacts with the surface hydroxyl groups.

McDonald noted further that all free hydroxyl groups were interacting with adsorbed nitrogen as indicated by the disappearance of the 3749 cm^{-1} band (a sharp peak with a narrow band width, 15 cm^{-1} , due to the O - H stretching vibration of free hydroxyl groups) when the surface coverage by nitrogen was considerably

less than the monolayer capacity determined from gas adsorption isotherms. He concluded that the silica surface was heterogeneous and that OH groups were preferred physical adsorption sites for nitrogen molecules. Kiselev and Khrapova¹¹² found that the nitrogen adsorption capacity was decreased after dehydration of silica surfaces, the result being in accord with the view that there is appreciable interaction between the nitrogen adsorbate and the surface hydroxyl groups.

Having established the deep involvement of the surface groups, the reports of Kipling and Wright¹¹³ and deBoer⁷² upon the adsorption of fatty acids onto alumina are significant since these workers conclude that the mechanism is one of hydrogen bonding and their findings are likely to apply to the sorption of 1-naphthol. The affinity of this compound for the surface is shown by the sharply curving isotherms, although the difference in character of the dioxan isotherm is striking: the only significant difference between dioxan and the other solvents is its potential for hydrogen bond formation with the hydroxylated alumina surface, and the fact that this so influences the extent of adsorption of 1-naphthol supports the view that the latter is adsorbed by a similar hydrogen bonding mechanism - to which dioxan can evidently provide very effective competition.

The limiting sorption values (at monolayer coverage) of the composite isotherms of Fig. 49 show little variation other than that with dioxan as solvent. Cyclohexane has been shown to have a low energy of interaction with the surface (B.E.T. Type 111 vapour isotherm^{and} very low 'C' value and so it is doubtful

whether this solvent can offer any serious resistance whatever to the adsorption of 1-naphthol) the very sharp curve of the isotherm (and hence the high K value) supports this. It can be imagined that sorption from decalin solution is exactly analogous: in both cases the absence of polarity in the solvent molecules and any specific interaction with the surface leave only weak dispersion forces responsible for adsorption. It is reasonable to assume, therefore, that the limiting sorption values from these two solvents represent monolayers of 1-naphthol molecules, each occupying, on average, $0.31 - 0.32 \text{ nm}^2$ of surface and so a reasonable area requirement for a molecule of 1-naphthol on this alumina could be assigned as 0.315 nm^2 .

When the aromatic solvents, tetralin and 1-methylnaphthalene, were employed the limiting sorption values were slightly lower. This is not surprising since their delocalised π electrons would interact to some extent with the polar alumina surface and had sorption of their vapours been practicable then isotherms similar to the B.E.T. Type 11 obtained with benzene would have been procured with 'C' values in the region of 10. However, the tetralin and 1-methylnaphthalene molecules can scarcely compete with the stronger hydrogen bonding interactions of the naphthol and at surface saturation the ratio of naphthol to solvent molecules is of the order of 26 : 1 (assuming that the solvent molecules lie 'flat' on roughly 0.8 nm^2).

However, when dioxan is used as solvent the situation changes again, but this time more dramatically. The vapour sorption described earlier has shown that dioxan interacts strongly

with the alumina surface, the mechanism is hydrogen bonding with surface hydroxyl groups and the calculated area requirement of approximately 1 nm^2 per naphthol molecule suggests that dioxan is present in quantity on the surface at equilibrium saturation and, moreover, is able to interact with the surface rather more successfully than 1-naphthol: the ratio of naphthol to solvent molecules is now in the region of 1 : 2.

Where cyclohexane, decalin, tetralin and 1-methylnaphthalene are used as solvents the solute-solvent interactions in the liquid phase are so weak and the affinity of the solute for the surface so strong in comparison that there can be no question of the naphthol being adsorbed as a naphthol-solvent complex. However, the 1 : 1 naphthol dioxan complex which exists in the dilute sorption solution (see 'Association in the Liquid Phase') could well be attached to the surface via the free oxygen atom of the dioxan. If this were the case then the molecular layer immediately adjacent to the surface would comprise dioxan molecules and dioxan-naphthol complex molecules. Since dioxan has no delocalised electron system through which mesomeric effects might be transmitted, only inductive and field effects could cause a naphthol molecule hydrogen bonded to one oxygen atom of a dioxan molecule to influence the other oxygen atom of the same dioxan molecule and because such effects decrease rapidly with distance their influence can be expected to be minimal. Thus no particular preference for the surface should be shown by a naphthol-dioxan complex and the amount sorbed should reflect the statistical frequency of complex molecules in the liquid phase.

The possibility of constructing an adsorption isotherm with such a sharp curve as the one obtained in practice suggests that complex molecules are not involved and therefore that the naphthol molecules are adsorbed as discrete entities.

It thus appears that the mechanism of adsorption is hydrogen bonding of 1-naphthol to the hydroxylated alumina surface and that even though hydrogen bonded naphthol-solvent complexes can occur in solution the naphthol molecules are adsorbed discretely, involving the destruction of a hydrogen bond with the solvent and the creation of a new one with the surface.

Individual Isotherms

The construction of individual isotherms reveals the full role of the solvent in adsorption for, although in the case of adsorption from dilute solution the composite isotherm is almost identical to that of the individual isotherm of the solute, solvent adsorption may still be appreciable over the concentration range studied.

To calculate the isotherms it is usual to assume monolayer adsorption and obtain n_1^s and n_2^s by application of the following equations, discussed in the 'Introduction' :-

$$\frac{n^o \Delta x_1^l}{m} = n_1^s x_2^l - n_2^s x_1^l \quad (30)$$

$$\text{and } \frac{n_1^s}{(n_1^s)m} + \frac{n_2^s}{(n_2^s)m} = 1 \quad (34)$$

Unfortunately, the values of $(n_2^s)m$ for some of the solvents can only be given approximately in the absence of vapour phase adsorption data; in these cases nominal values have been assigned as in Table 41.

The individual isotherms displayed in Fig. 62 whilst being only approximate by virtue of assumptions made in the calculations, nonetheless show well the degree of competition between solute and solvent for the adsorbing surface - striking in the case of dioxan. Table 41 also includes estimates of percentage surface coverages in the equilibrium monolayer of solute and solvent as estimated from the Jowett limiting sorption values and suggests that the increasing order of solvent - surface interaction is

cyclohexane \approx decalin $<$ tetralin \approx 1-methylnaphthalene \ll dioxan.

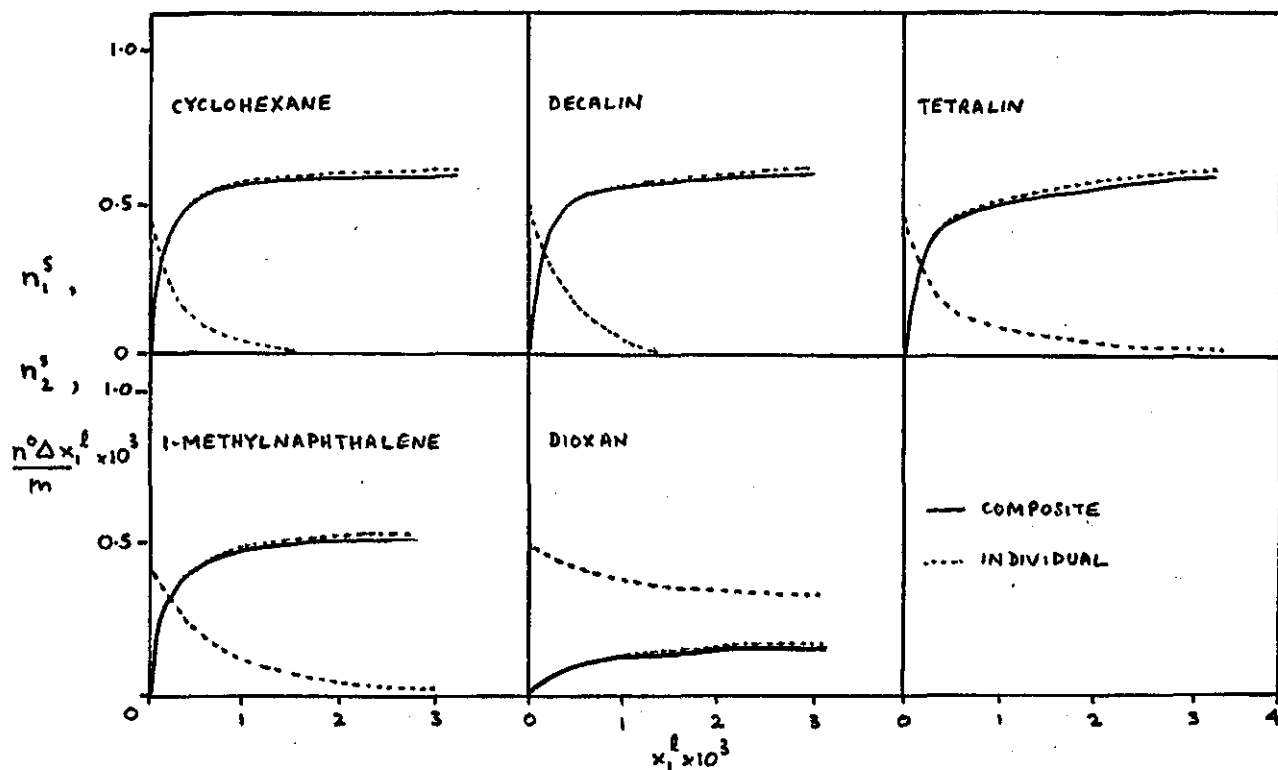
TABLE 41: INDIVIDUAL ISOTHERM DATA

Solvent	A_m	$(n_2^s)_m \times 10^3$	% Surface Coverages	
	<u>/nm²</u>	<u>/mol</u>	<u>Solute</u>	<u>Solvent</u>
Cyclohexane	0.39 ¹¹⁴	0.44	100	0
Decalin	0.8*	0.22	99	1
Tetralin	0.8*	0.22	91	9
1-Methyl-naphthalene	0.9*	0.19	90	10
Dioxan	0.43**	0.40	31	69

* Areas by comparison of molecular models with benzene taken as 0.40 nm².

** Determined experimentally by vapour phase adsorption.

Fig. 62 Individual Isotherms



Orientation of 1-Naphthol Molecules on the Alumina Surface

In their study of the sorption of stearic acid from cyclohexane solution onto activated aluminas, Kipling and Wright¹¹³ concluded that hydrogen bonding to the sorbent surface was the essential sorption mechanism, the sorptive being perpendicularly aligned to the surface. From obvious plateaus in the isotherms these workers estimated limiting sorption values and compared these values with calculated monolayer values based on the two possible orientations of stearic acid, with molecular areas (expressed in terms of monomeric molecules) of 1.14 nm^2 for the parallel orientation and 0.205 nm^2 for the perpendicular

orientation. From the ratio of observed to calculated limiting values, it was clear that the perpendicular orientation was adopted. On the one alumina sample for which this ratio was appreciably less than unity (0.47) the adsorption was too great to correspond to the parallel position although much less than for a close-packed monolayer in the perpendicular orientation. Kipling and Wright reasonably supposed that sorption to give less than a close-packed monolayer is unlikely to be due to competition from the solvent if the solute was so strongly attracted to the surface that it adopted the perpendicular orientation. They suggested that in such a case it is more likely that closeness of packing of the sorbed molecules was the dominant factor and that this was determined by the spacing of the sites, i. e. that sorption was localised. Again de Boer et al⁷² have concluded that Lauric acid is sorbed perpendicularly to an alumina surface from pentane solution, one molecule of lauric acid being sorbed upon the equivalent area of four surface oxide ions.

The orientation of aromatic molecules appears to be largely decided by the presence and nature of substituent groups. Unsubstituted benzene adopts a parallel orientation permitting the maximum interaction between the π electron system and the surface and occupies roughly 0.40 nm^2 .¹¹⁴ It would thus seem reasonable to ascribe area requirements of $0.8 - 0.9 \text{ nm}^2$ for tetralin and 1-methylnaphthalene molecules for these, too, would align themselves parallel to the surface. The A_m value for dioxan from vapour sorption (0.428 nm^2) indicates again a parallel

orientation - not surprising in view of hydrogen bonding possibilities. 1-Naphthol, then, has two alternatives: to assume a parallel position when the main interaction would be through the π electron system of the aromatic nucleus, or a parallel one when the OH group could align itself with a surface hydroxyl to give a linear O..... H-O- assembly and hence the straight hydrogen bond (an examination of models shows that a simultaneous realisation of these possibilities would be most unlikely).

The work of Giles and Nakhwa¹¹⁵ has shown that 4-nitrophenol is adsorbed 'end-on' at polar surfaces and they quote the following apparent cross-sectional areas for an adsorbed 4-nitrophenol molecule: 0.15 and 0.25 nm² for perpendicular adsorption from benzene and water respectively and 0.53 nm² for parallel orientation. These values, together with experimentally determined monolayer capacities, are used to calculate specific surface areas which are then compared with results from low temperature nitrogen sorptions. These workers suggest that the much higher areas obtained by the latter technique are due to microporosity of the alumina surfaces, permitting penetration of nitrogen molecules into the fine capillaries but excluding the larger 4-nitrophenol molecules. The author's earlier work³² included a sorption of 4-nitrophenol from benzene onto the alumina used in this study which yielded an A_m value of 0.36 nm² which points to a perpendicular orientation rather than a parallel one and when Giles' surface areas are recalculated using this value they show much closer agreement with the results from

nitrogen sorptions: the Giles value of 0.15 nm^2 for the apparent cross-sectional area of a 4-nitrophenol molecule seems a little optimistic!

In the same earlier work³², the author reported the sorption of a series of 4-substituted phenols from dioxan and once again came to the conclusion that the phenol molecules were adsorbed 'end-on' and the dioxan molecules parallel to the surface. As with the phenols, so with the naphthols the A_m value of 0.315 nm^2 for 1-naphthol from cyclohexane precludes any possibility of parallel orientation for which at least 0.8 nm^2 per molecule could be anticipated. The interaction of the aromatic nucleus with the hydroxylated surface is much weaker than the hydrogen bond formed between the naphtholic OH and the surface (as evidenced by B.E.T. 'C' values for benzene and dioxan and adsorptions from tetralin and 1-methylnaphthalene solutions) and so the deduction of a perpendicular orientation is a justifiable one.

It is interesting to examine other surface area requirements: Adam¹¹⁶ reported a value of 0.24 nm^2 for an aromatic molecule in a thin film on water and this probably represents a minimum reasonable figure, Deuchar⁹⁹ reports a mean molecular surface area requirement for 4-substituted phenols from benzene (when the 4-substituent is small) on alumina of 0.27 nm^2 . The value assigned to 1-naphthol in this study (0.315 nm^2) is only a small increase on these figures even though this molecule is twice the size of the others: the only explanation lies in assuming a perpendicular orientation, when the area requirement at the immediate interface would be roughly the same (perhaps slightly

larger to allow for thermal agitations) but the thickness of a layer of 1-naphthol would be roughly twice that of a layer of phenol. Returning to the supposition that 100 faces are preferentially exposed on this alumina and the area of 0.795 nm^2 per oxide ion site it is interesting to find that each 1-naphthol molecule lies over the equivalent of 3.96 oxide sites (a result complementary to the work on phenols in which four such sites were allotted to a phenol molecule).

In conclusion, then, when adsorbed from a weakly interacting solvent 1-naphthol forms a close-packed monolayer on the alumina, adopting a perpendicular orientation and covering the area of four surface hydroxyl groups.

The Applicability of Everett's Theory of Adsorption

In developing his theory Everett gave no regard to adsorbed layers other than the first and further assumed that the total number of molecules in this phase was independent of its composition. In the systems studied in this investigation it is conceivable that adsorption is effectively mono molecular, but that the solute and solvent molecules occupy the same area as each other has already been shown not to be so, although with the larger area requirement of 1-naphthol they approach this ideal a little more closely than phenol systems. Everett also specified that the sorbed phase should rest on identical surface sites: the completely hydroxylated alumina surface whilst in the main regular, could not be considered as energetically uniform as, say, a graphon surface, and in addition to hydroxyl groups there is some residual physically adsorbed water (see results of thermo-

gravimetric experiments). The strong possibility of localised sorption, too, cannot be overlooked which would tend to make adsorption relate to the spacing of surface groups of ions.

Lastly, Everett stipulates that the solution and sorbed phases should behave ideally: again, conditions far removed from those to be expected in most of the system studied.

Notwithstanding these problems, the Everett plots shown in Fig. 61 are convincing straight lines although clearly great care must be exercised in drawing conclusions from this discovery.

It is a familiar observation that low solute-solvent interaction in the liquid phase give rise to solution adsorption isotherms with sharp curves and definite plateaus but as the interactions increase with change of solvent the isotherms become more rounded in shape and the ascent to the plateaus (i. e. limiting sorption values) more gradual. These observations have been noted in the systems under discussion and this is reflected in the K values calculated from Everett's equation. For reasons of non-ideality mentioned above it is doubtful whether these values can be taken as precise equilibrium constants for the exchange process



but they do display the anticipated trend.

The values of n^S (the total number of moles in the surface phase) cannot be expected in practice to remain constant since the molecular area requirements of solute and solvent are in every case different. The large discrepancy between the dioxan n^S value and the others is discouraging and probably underlines the lack of provision made for strong interactions in the liquid

phase and lateral interactions in the surface phase in Everett's thermodynamic theory of adsorption from solution for perfect systems.

In an attempt to compensate for varying area requirements of adsorbed molecules, mean molecular area requirements (A_M) have been calculated from Equation (90).

$$A_M = \frac{n_1 A_1 + n_2 A_2}{n_1 + n_2} \quad (90)$$

where A_1 is the molecular area requirement of 1-naphthol on the alumina surface (0.315 nm^2),

A_2 is the molecular area requirement of solvent on the alumina surface,

n_1 , n_2 are the moles of solute and solvent respectively, on the alumina surface at saturation.

The calculated A_M values are listed in Table 42 together with the appropriate n^s values. The table also shows values for the specific surface area of the alumina estimated from these values.

TABLE 42: SPECIFIC SURFACE AREAS FROM EVERETT'S EQUATION

<u>Solvent</u>	<u>$n^s \times 10^4 / \text{mol}$</u>	<u>A_M / nm^2</u>	<u>$S / \text{m}^2 \text{g}^{-1}$</u>
Cyclohexane	5.609	0.315	106.0
Decalin	5.556	0.317	105.7
Tetralin	5.294	0.334	106.1
1-Methylnaphthalene	5.368	0.336	108.2
Dioxan	1.820	0.386	42.2

Once again, from relatively non-polar solvents, where adsorption of solvent is not a major feature, total surface areas agree well with the earlier assigned value ($103.5 \text{ m}^2 \text{ g}^{-1}$) but where strong specific interactions occur (e. g. when dioxan is used as solvent) large deviations from the Everett conditions lead to poor agreement.

(b) The Adsorption of 4-Substituted-1-Naphthols from Dioxan Solution

The experimental data for the sorption of a series of 4-substituted-1-naphthols from dioxan are listed in Tables 26 to 31 and the isotherms are displayed in Fig. 50. The Everett straight line plots of $m x_1^l x_2^l / n^0 \Delta x_1^l$ against x_1^l have been constructed and are shown in Fig. 63. Once again parameters have been calculated from the Everett Equation (45), the Jowett Equation (80) and Equation (82),^{and} the area requirements per naphthol molecule (A_m), giving no regard to adsorbed solvent at saturation, have been calculated from the specific surface area of the alumina, $103.5 \text{ m}^2 \text{ g}^{-1}$. All these data are summarised in Table 43 and are used in the following discussion of mechanism and orientation in the sorption process and the applicability of Everett's theory to these systems.

Mechanism of Sorption and Orientation of Adsorbed Molecules

The sorptions of 4-substituted-1-naphthols from dioxan solution follow closely the pattern for the parent 1-naphthol discussed in an earlier section. Dioxan interacts strongly with the alumina surface and so the limiting sorption values of Table 43 fall well below those of 1-naphthol from cyclohexane, decalin, tetralin and 1-methylnaphthalene thereby suggesting the presence of solvent in the adsorbed layer at equilibrium.

Fig. 63

Everett plots for 4-substituted-1-naphthols on
alumina from dioxan

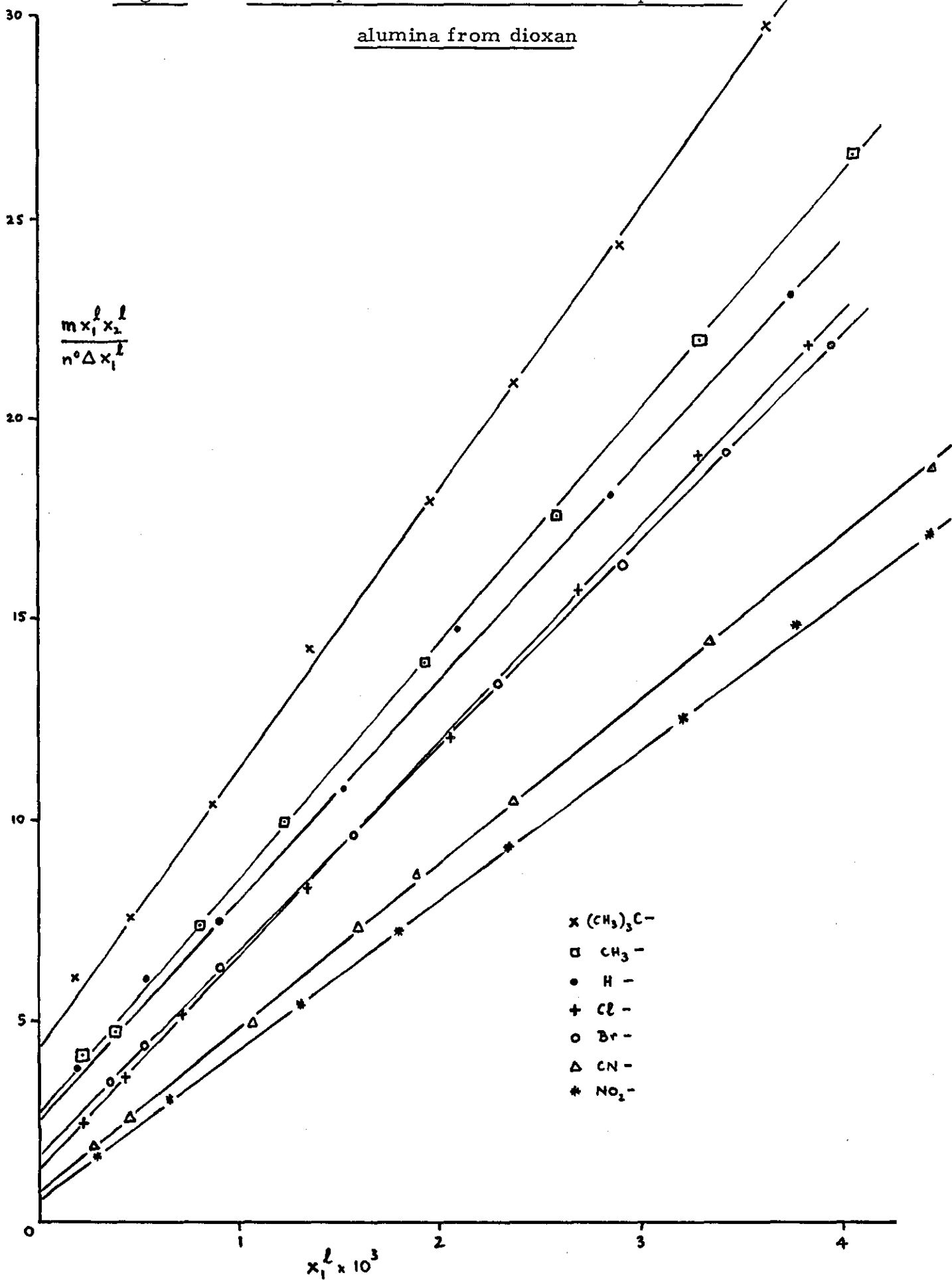


TABLE 43: ADSORPTION DATA FOR 4-SUBSTITUTED-1-NAPHTHOLS

<u>4-Substituent</u>	<u>Intercept</u>	<u>Slope</u>	<u>K</u>	<u>$n^s \times 10^4 / \text{moles}$</u>
$(\text{CH}_3)_3\text{C}$	4.27	6973	1633	1.434
CH_3	2.62	5846	2231	1.710
H	2.50	5495	2201	1.820
Cl	1.28	5318	4155	1.880
Br	1.65	5088	3084	1.966
CN	0.74	4074	5505	2.455
NO_2	0.55	3716	6756	2.691

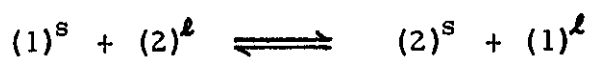
LIMITING SORPTION VALUES

<u>4-Substituent</u>	<u>Jowett Equation (80)</u>		<u>Equation (82)</u>	
	<u>$(n_1^s)_{\text{max}} \times 10^4 / \text{moles}$</u>	<u>A_m / nm^2</u>	<u>$(n_1^s)_{\text{max}} \times 10^4 / \text{moles}$</u>	<u>A_m / nm^2</u>
$(\text{CH}_3)_3\text{C}-$	1.295	1.332	1.365	1.263
$\text{CH}_3 -$	1.575	1.095	1.639	1.052
H -	1.671	1.028	1.744	0.985
Cl -	1.803	0.956	1.823	0.946
Br -	1.841	0.937	1.896	0.910
CN -	2.376	0.726	2.382	0.724
$\text{NO}_2 -$	2.611	0.661	2.626	0.657

Following the conclusions reached previously for 1-naphthol from dioxan it is reasonable to suppose that the mechanism of sorption is by cleavage of a hydrogen bond between solute and solvent molecules in the liquid phase accompanied by simultaneous formation of a hydrogen bond between the sorptive molecule and a surface hydroxyl group. The adsorption of a solute-solvent complex molecule is most unlikely for the reasons discussed earlier; solute and solvent molecules are adsorbed discretely. The area requirement per molecule quoted in Table 43 are once again far in excess of those demanded by perpendicularly orientated molecules in a close-packed monolayer of the naphthols. In accounting for these large A_m values a parallel orientation might be proposed, but it would be difficult to put forward a convincing explanation for such a sudden change in behaviour. A much more rational interpretation would be that the naphthol molecules are still aligned perpendicularly to the surface but the solvent is strongly adsorbed too. Nonetheless, in the cases of 4-cyano- and 4-nitro-1-naphthols it is interesting to note that additional hydrogen bond formation by the 4-substituent with the surface is feasible. In weighing this possibility it might be noted that a perpendicular orientation of 4-nitrophenol when sorbed on alumina has been reported¹¹⁵ and the author in an earlier study³² concluded that sorption of 4-nitrophenol onto alumina from dioxan also produced a perpendicular alignment, and further, the area requirements in Table 43 do not support such a discontinuity in orientation.

In the sorption of 1-naphthol from non-hydrogen bonding solvents the naphthol molecules experience very little effective competition for the surface and are not involved in strong liquid

phase interactions and so the adsorption process quickly comes to virtual completion, i. e. the formation of a close-packed monolayer of naphthol molecules. Had the sorption of the series of 4-substituted-1-naphthols from cyclohexane or decalin been possible (solubility limitations preclude this in practice) the chemical nature of the 4-substituent might be expected to be irrelevant to the limiting sorption uptakes on alumina since close-packed naphthol monolayers would be formed each time and the only variation would result from the physical size of the 4-substituent. The findings of Deuchar⁹⁹ lend substance to this hypothesis: limiting sorption values of a series of 4-substituted phenols from benzene onto alumina reflected the size of the para group rather than its chemical nature. However, the chemical nature of the 4-substituent might be manifested in the curvature of the isotherm at low equilibrium mole fractions of the solute. In this region solvent molecules are able to compete for surface sites, albeit rather feebly, but unfortunately accurate data at such low concentrations are not easy to obtain. Certainly, the 'plateau' n_1^s values are insensitive to the effect of the para group upon the strength of the hydrogen bond formed by the phenolic or naphtholic OH group. In effect, with non-hydrogen bonding solvents, the exchange equilibrium:



tends to proceed towards completion.

In contrast, when dioxan is used as a solvent the above equilibrium lies far from completion and rarely reaches a 50% exchange. In consequent, the equilibrium can shift easily and

extensively in either direction and the position is now sensitive to the transmitted influence of the 4-substituent and not merely to its bulk. Again, with dioxan as solvent, interactions at the surface and in solution at once become similar in nature and magnitude; the overall equilibrium state of the solution-adsorbent system rests on a compromise between affinities of comparable effect.

If changes in hydrogen bond strength (with change of 4-substituent) to dioxan and to surface OH groups were exactly parallel, it might be expected that sorption 'plateau' values would reflect only changes in the size of the substituent. That the limiting sorption values steadily increase with increasing electron withdrawing power of the 4-substituent (Table 43) suggest that, although hydrogen bonding in solution is also increasing in strength (Table 15), the strength of hydrogen bonding to the surface is increasing at a greater rate. The data of Table 43 thus point to a 'differential' increase in hydrogen bond strength since before an attachment to the surface can be made a union in the liquid phase has to be destroyed. Thus when a naphthol-dioxan-alumina system is in thermodynamic equilibrium, three independent equilibria simultaneously operate :-

- (a) liquid phase: naphthol molecules + dioxan molecules \rightleftharpoons
complex molecules
- (b) surface phase: naphthol molecules + surface hydroxyls \rightleftharpoons
adsorbed naphthol molecules
- (c) surface phase: dioxan molecules + surface hydroxyls \rightleftharpoons
adsorbed dioxan molecules.

A measure of (a) has already been discussed in evaluating hydrogen bonding association constants in solution, the effectiveness of (c) has been demonstrated by the adsorption of dioxan vapour, it remains to evaluate (b).

The Applicability of Everett's Theory

The remarks made earlier during the discussion of the adsorption of the parent 1-naphthol apply equally well to the adsorption of the 4-substituted derivatives. Everett's stipulation that the molar capacity of the first adsorbed layer should remain constant cannot be exactly met, nor can his condition of a perfectly uniform surface: the spacing of the surface hydroxyl groups may well influence packing to an extent impossible to assess accurately. Lastly, ideal behaviour in the solution and sorbed phases can scarcely be realised in the presence of interactions so specific and strong. In spite of these obvious failures to meet the specified conditions precisely, Fig. 63 shows good straight lines produced by application of the linear form of Everett's equation and values of n^s and K are once again easily calculated.

The values of n^s , the molar capacity of the adsorbed monolayer, does not show the required constancy but varies between 1.4×10^{-4} mol and 2.7×10^{-4} mol and is thus less than half the predictable value of around 5×10^{-4} mol. Further, the values of n^s are in every case only slightly higher than the limiting sorption values for the solute molecules which is inconsistent with the considerable presence of dioxan in the adsorbed layer.

The values derived for the equilibrium constant, K , cannot represent the simple exchange equilibrium used by Everett in view of the non-ideality of the liquid and sorbed phases. In the systems studied the precise physical significance of the K values is not clear; possibly they refer to a combination of equilibria (a)

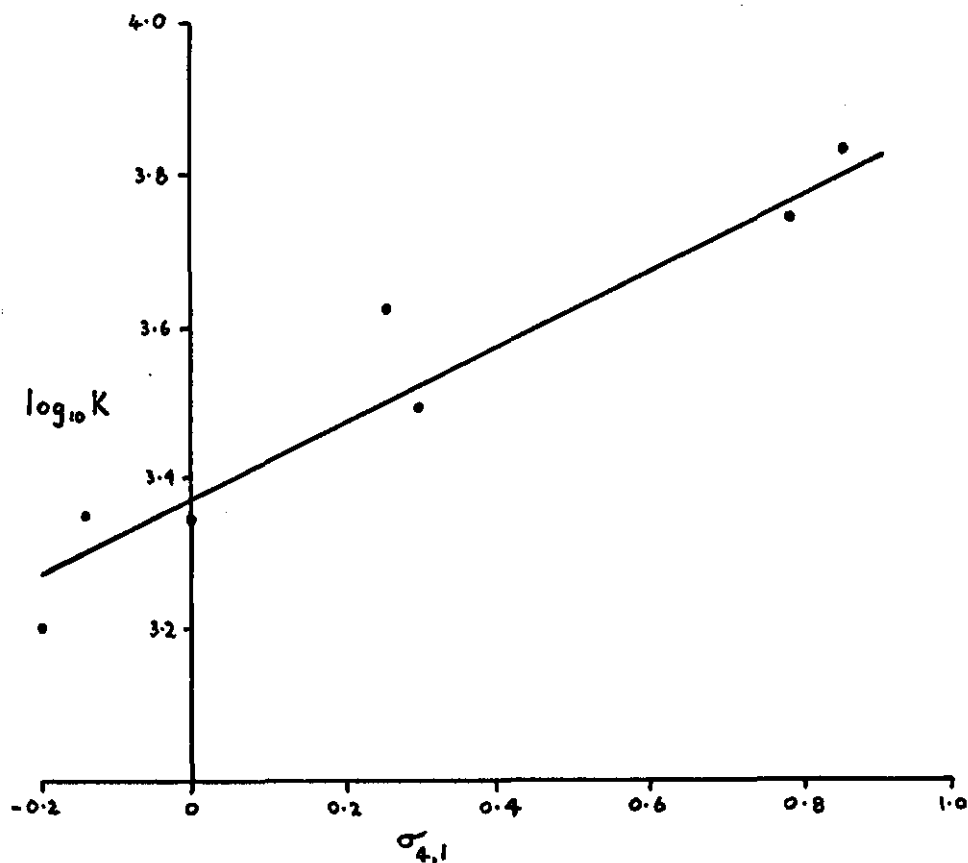
and (b) mentioned earlier: a more sophisticated theory of adsorption, taking into account the specific interactions at the outset, is required to adequately interpret the sorption data and derive physically meaningful quantities.

Whilst a quantitative significance cannot be given to the experimental K values, they show an interesting trend qualitatively. Fig. 64 is a plot of data recorded in Table 44 and demonstrates a correlation between the transmitted effect of the substituent, represented once again by $\sigma_{4,1}$ values, and log K. The relationship is essentially linear and shows that the 4-substituent is influential in the adsorption process, although it would be misguided to adopt this as evidence for the applicability of Everett's treatment of adsorption to the systems studied or for the validity of the K values.

TABLE 44

<u>4-Substituent</u>	<u>$\sigma_{4,1}$</u>	<u>K</u>	<u>log K</u>
(CH ₃) ₃ C-	- 0.20	1633	3.213
CH ₃ -	- 0.14	2231	3.349
H -	0	2201	3.343
Cl -	0.26	4155	3.619
BR -	0.30	3084	3.489
CN -	0.79	5505	3.741
NO ₂ -	0.86	6756	3.830

Fig. 64



In conclusion, it would seem that the systems in which solvent-solute and solvent-surface interactions are low probably approximate to Everett's stipulations: the adsorbed phase consists mainly of naphthol molecules and this would seem to determine the closeness of approach of these systems to Everett's ideal model. When adsorption of an interacting solvent is appreciable the systems deviate widely from ideal behaviour and Everett's treatment is no longer valid, and although derived quantities can still be used to demonstrate trends qualitatively, to attribute precise thermodynamic definitions to parameters in his equation proves a supine pursuit.

APPENDIX

PREPARATION AND PURIFICATION OF SOLVENTS AND SOLUTES

The Solvents

- (a) Cyclohexane was dried over phosphorus pentoxide and fractionally distilled over sodium wire immediately before use (80.8°C at $101\,325\text{ Nm}^{-2}$). As a precaution cyclohexane used for sorption studies was allowed to run slowly down a column of the pretreated sorption alumina, prior to final drying and distillation, until no traces of aromatics could be detected in the ultraviolet spectrum.
- (b) Dioxan was boiled under reflux with molten sodium for several days, distilled and then heated under reflux again until the beads of sodium presented a mercury-bright surface. Finally the dioxan was fractionally distilled immediately before use through a one metre column of Fenske helices, the fraction coming over at 101.4°C ($101\,325\text{ Nm}^{-2}$) being collected under anhydrous conditions.
- (c) Decalin was pretreated by shaking with concentrated sulphuric acid and by elution down a column of the sorption alumina until no trace of aromatic absorption bands could be detected in the ultraviolet spectrum. The solvent was then heated under reflux in the presence of molten sodium and finally distilled, collecting the fraction between 188 and 192°C at ambient pressure, being a mixture of the cis-form ($194.6^{\circ}\text{C}/101\,325\text{ Nm}^{-2}$) and the trans-form ($185.8^{\circ}\text{C}/101\,325\text{ Nm}^{-2}$).
- (d) Tetralin was heated under reflux with sodium followed by distillation, collecting the fraction at 207.6°C at $101\,325\text{ Nm}^{-2}$.

- (e) Commercial 1-methylnaphthalene was decolourised by elution down an activated charcoal column, heated under reflux over molten sodium and finally distilled, collecting the fraction at $244 - 245^{\circ}\text{C}/101\ 325\ \text{Nm}^{-2}$.

The Solutes

Samples of the parent 1-naphthol purified as described below were used to prepare some of the 4-substituted-1-naphthols. Each sample was carefully screened by means of its infrared spectrum to ensure freedom from 2-naphthol and to avoid in consequence the formation of dangerous 2-derivatives. The preparations were largely extracted from the literature^{117, 118} and so outline procedures only are given. All the solutes were recrystallised before use and stored over phosphorus pentoxide in an atmosphere of nitrogen.

- (a) 1-Naphthol, of analytical reagent grade, was first crystallised from water containing a little hydrochloric acid and then from 60-80 petroleum spirit (m.p. 95.6°C).
- (b) 4-Chloro-1-naphthol (m.p. 121°C) was prepared by the chlorination of 1-naphthol by sulphuryl chloride in chloroform. The reagents were mixed, allowed to stand overnight at 20°C , raised to 80°C over four hours, held at 80°C for one hour, distilled in vacuo and finally crystallised from petroleum spirit.¹¹⁹
- (c) 4-Bromo-1-naphthol (m.p. 129°C) was prepared by the bromination of 1-naphthol with iodine monobromide in glacial acetic acid at 10°C , followed by crystallisation from petroleum spirit.^{120, 121}

- (d) 4-Nitro-1-naphthol (m.p. 166°C): 1-naphthylamine was acetylated in glacial acetic acid with acetic anhydride and sodium acetate. The N-acetyl-1-naphthylamine was then nitrated with a mixture of concentrated nitric and sulphuric acids at 15°C in glacial acetic acid, and the mixture of 2- and 4-nitro-N-acetyl-1-naphthylamines was hydrolysed either by reflux with hydrogen chloride in methanol¹²² or by boiling with 5% sodium hydroxide solution. The 2-isomer (unlike the 4-derivative) is steam volatile and was thus removed.^{123, 124} Finally the 4-nitro-1-naphthol was crystallised from ethanol.
- (e) 4-Cyano-1-naphthol (m.p. 170°C): hydrogen chloride was bubbled through 1-naphthol and zinc cyanide in dry ether for two hours. The resulting imide hydrochloride was boiled with 30% ethanol, yielding 4-hydroxy-1-naphthaldehyde upon cooling.^{125, 126} The latter was heated with acetic anhydride, acetic acid and sodium acetate to give 4-acetoxy-1-naphthaldehyde¹²⁷ which was then boiled with hydroxylamine hydrochloride, sodium acetate and sodium hydrogen carbonate in aqueous methanol producing 4-hydroxy-1-naphthaldoxime.¹²⁷ With acetic anhydride and glacial acetic acid this gave 4-hydroxy-1-naphthaldoxime acetate which upon heating with ethanol in pyridine¹²⁷ gave 4-cyano-1-naphthol.
- (f) 4-t-Butyl-1-naphthol (m.p. 152°C): 1-naphthol and t-butyl chloride were heated under reflux in ether in the presence of aluminium chloride when some 4-t-butyl-1-naphthol was

formed, ¹²⁸ Isolation was achieved by distillation in vacuo, followed by crystallisation from petroleum spirit.

- (g) 4-Methyl-1-naphthol (m.p. 85°C): sulphonation of 1-naphthol at room temperature by concentrated sulphuric acid yielded 4-methyl-1-naphthalene sulphonic acid which was fused in potassium hydroxide at 250-265°C. The sodium naphthoxide salt was precipitated from an aqueous solution of the residue by addition of sodium chloride; acidification gave 4-methyl-1-naphthol which was extracted with ether and crystallised from petroleum spirit.

REFERENCES

1. Hammett,
J. Amer. Chem. Soc., 1937 59 96.
2. Hammett,
Trans. Far. Soc., 1938 34 156.
3. Dewar,
J. Amer. Chem. Soc., 1952 74 3351.
4. Yukawa, Tsuno,
Bull. Chem. Soc. Japan, 1959 32 971.
5. Taft, Lewis,
J. Amer. Chem. Soc., 1959 81 5343.
6. Taft, Ehrenson, Lewis, Glick,
J. Amer. Chem. Soc., 1959 81 5352.
7. Brown, Dewar,
J. Chem. Soc., 1953 2406.
8. Jaffé,
J. Chem. Phys., 1952 20 279, 778
J. Amer. Chem. Soc., 1954 76 4261
ibid 1955 77 274.
9. Dewar, Grisdale,
J. Amer. Chem. Soc., 1962 84 3539, 3541, 3546, 3548.
10. Jaffé,
Chem. Rev., 1953 53 241.
11. Longuet-Higgins,
J. Chem. Phys., 1950 18 265, 275, 283.
12. Coulson, Daudel,
'Dictionary of Values of Molecular Constants', Centre
National de la Recherche Scientifique, Paris.
13. Dimroth, Reichardt, Siepmann, Bohlmann,
Justus Liebigs Ann In. Chem., 1963 661 1.
14. Kagiya, Sumida, Inoue,
Bull. Chem. Soc. Japan, 1968 41 767.
15. Benesi, Hildebrand,
J. Amer. Chem. Soc., 1949 71 2703.
16. Mulliken,
J. Phys. Chem., 1952 56 801.
17. Coulson, Danielsson,
Arkiv. f. Fys., 1954 8 239, 345.
18. Pimentel, McClellan,
'The Hydrogen Bond', Freeman and Co., 1960 p.158.

19. Pimentel,
J. Amer. Chem. Soc., 1957 79 3323.
20. Bayliss, McRae
J. Phys. Chem., 1954, 58 1002.
21. Brealey, Kasha,
J. Amer. Chem. Soc., 1955 77 4462
22. Nagakura, Baba,
J. Amer. Chem. Soc., 1952 74 5693.
23. Ketelaar, van de Stope, Goudsmit, Dzcubas,
Rec. Trav. Chim., 1952 71 1104.
24. Nagakura, Baba,
J. Amer. Chem. Soc., 1952 74 5693.
25. Baba, Suzuki,
J. Chem. Phys., 1961 35 1118.
26. Nagakura,
J. Amer. Chem. Soc., 1958 80 520.
27. Andrews, Keefer,
J. Amer. Chem. Soc., 1952 74 4500.
28. Andrews, Keefer,
J. Amer. Chem. Soc., 1953 75 543.
29. Rose, Drago,
J. Amer. Chem. Soc., 1959 81 6138.
30. Nagakura,
J. Amer. Chem. Soc., 1954 76 3070.
31. Nagakura, Gouterman,
J. Chem. Phys., 1957, 26 881.
32. Hawley,
M.Sc. Thesis, University of Durham, 1968.
33. Jaffe,
Chem. Revs, 1953 53 199.
34. Vallance,
Ph.D. Thesis, University of Loughborough, 1969.
35. Bartell, Scheffer, Sloan,
J. Amer. Chem. Soc., 1931 53 2510.
36. Jones, Outridge,
J. Chem. Soc., 1930 1574.
37. Bartell, Scheffer,
J. Amer. Chem. Soc., 1931 53 2507.

38. Kipling,
'Proceedings of the Second International Congress of
Surface Activity', Butterworth, London, 1957 3 463.
39. Claesson,
Rec. Trav. Chim., 1946 65 571.
40. Kiselev,
'Structure and Properties of Porous Materials',
Academic Press, New York, 1958, p.195.
41. Snyder, Ward,
J. Phys. Chem., 1966 70 3941.
42. Cusamo, Low,
J. Catalysis, 1971 23 214.
43. Hudson,
M.Sc. Thesis, London University, 1969.
44. Puranik, Kumar,
Proc. Indian Acad. Sci., 1963 A58 327.
45. King, Benson,
Anal. Chem., 1966 38 261.
46. King, Benson,
J. Chem. Phys., 1966 44 1007.
47. Bark, Graham,
Talanta, 1964 11 839.
48. Giles,
'Chromatography', E. Heftmann ed., Reinhold, 1961
Chap. 4.
49. Naccache, Kodratoff, Pink, Imelik,
J. Chim. Phys., 1966 63 341.
50. Ibbitson, Jackson, McCarthy, Stone,
J. Chem. Soc., 1960 5127.
51. Eric, Goode, Ibbitson,
J. Chem. Soc., 1960 55.
52. Kipling,
Quart. Rev., 1951 5 60.
53. Elton,
J. Chem. Soc., 1951 2958.
54. Kipling, Tester,
J. Chem. Soc., 1952 4123.
55. Kipling, Wright,
J. Chem. Soc., 1962 855.
56. Day, Parfitt,
J. Phys. Chem., 1967 71 3073.

57. Everett,
Trans. Far. Soc., 1964 60 1803.
58. Schuchowitzsky,
Acta physio chim., 1944 19 176, 508.
59. Belton, Evans,
Trans. Far. Soc., 1945 41 1.
60. Elton,
J. Chem. Soc., 1954 3813.
61. Patterson, Delmas,
J. Phys. Chem., 1960 64 1827.
62. Wright,
Trans. Far. Soc., 1966 62 1275.
63. Kagiya, Sumida, Tachi,
Bull. Chem. Soc. Japan, 1971 44 1219.
64. Everett,
Trans. Far. Soc., 1965, 61 2478.
65. Guggenheim,
'Mixtures', Oxford Press, 1952, Chap. 9.
66. Day, Eltekov, Parfitt, Thompson,
Trans. Far. Soc., 1969 65 226.
67. I.U.P.A.C.,
'Tables of Wavenumbers for Calibration of Infrared Spectrophotometers', Butterworths, London, 1961.
68. Deuchar
M.Sc. Thesis, University of Durham, 1970.
69. Stumpf, Russell, Newsome, Tucker,
Ind. and Eng. Chem., 1950 42 1398.
70. Brown, Clark, Elliot,
J. Chem. Soc., 1953 84.
71. Day, Hill,
J. Phys. Chem., 1963 57 946.
72. de Boer, Hauben, Lippens, Meys, Walrave,
J. Catalysis, 1962 1 1.
73. Evans,
'An Introduction to Crystal Chemistry', Cambridge University Press, 2nd ed., 1964.
74. Peri,
J. Phys. Chem., 1965 69 220.

75. Cornelius, Milliken, Mills, Oblad,
J. Phys. Chem., 1955 59 809.
76. Sheppard,
'Hydrogen Bonding' Pergamon Press, London, 1957.
77. Folman, Yates,
Proc. Roy. Soc., 1958 A246 32.
78. Peri, Hannan,
J. Phys. Chem., 1960 64 1526.
79. Bersohn,
J. Phys. Chem., 1958 29 326.
80. Peri,
J. Phys. Chem., 1965 69 211.
81. Uvarov,
Zh. Fiz. Khim., 1962 36 1346.
82. Kipling, Peakall,
J. Chem. Soc., 1957 834.
83. Brunauer, Emmett, Teller,
J. Amer. Chem. Soc., 1938 60 309.
84. Brunauer, Deming, Deming, Teller,
J. Amer. Chem. Soc., 1940 62 1723.
85. Brunauer, Emmett,
J. Amer. Chem. Soc., 1937 59 1553.
86. Lippens, de Boer,
J. Catalysis, 1965 4 319.
87. Schull,
J. Amer. Chem. Soc., 1948 70 1405.
88. Cranston, Inkley,
Adv. in Catalysis, 1957 9 143.
89. Harris, Sing,
Chem. and Ind., 1959 487.
90. de Boer, Linsen, Osinga,
J. Catalysis, 1965 4 643.
91. Lippens, Linsen, de Boer,
J. Catalysis, 1964 3 32.
92. Sing,
'Proceedings of the International Symposium on Surface
Area Determination', Butterworths, London, 1970, P.25.

93. Wheeler,
Adv. in Catalysis, 1951 3 250.
94. Gregg, Sing,
'Adsorption, Surface Area and Porosity', Academic
Press, 1967, Chap.2.
95. Barlin, Perkin,
Quart. Rev., 1966 XX 1 75.
96. Joesten, Drago,
J. Amer. Chem. Soc. 1962 84 3187.
97. Trotter, Hanna,
J. Amer. Chem. Soc., 1966 88 3724.
98. Kunz, Gasparro, Johnston, Taylor.
J. Amer. Chem. Soc., 1968 90 4778.
99. Deuchar,
Ph.D. Thesis, University of Leicester, 1973.
100. Davis, de Witt, Emmett,
J. Phys. Chem. 1947 51 1232.
101. Brunauer, Emmett,
J. Amer. Chem. Soc., 1937 59 2682.
102. Kōdera, Onishi,
J. Chem. Soc. Japan, 1959 32 356.
103. Corrin,
J. Amer. Chem. Soc. 1951 73 4061.
104. Bowers,
Phil. Mag., 1953 44 467.
105. Aristov, Kiselev,
Russ. J. Phys. Chem., 1963 37 1359.
ibid 1964 38 1077.
106. Lippens,
'Structure and Texture of Aluminas', Thesis,
Technische Hogeschool of Delft, Netherlands, 1961.
107. Deer, Howie, Zussman,
'Rock Forming Minerals! Longmans, 1963, Vol.5, p.111
et seq.
108. de Boer, Fortuin, Lippens, Meijs,
J. Catalysis, 1963 2 1.
109. Frangiskos, Harris, Jowett,
'The Third International Congress of Surface Activity',
verlag. der Universitätsdruckerei, Mainz, 1961 4 404.

110. McDonald,
J. Amer. Chem. Soc., 1957 79 850.
111. Frohnsdorff, Kington,
Trans. Far. Soc. 1959 55 1173.
112. Kiselev, Khrapova,
Kolloid Zh., 1957 19 572.
113. Kipling, Wright,
J. Chem. Soc., 1964 683, 3535.
114. Smith, Pierce, Cordes,
J. Amer. Chem. Soc., 1950 72 5595.
115. Giles, Nakhwa,
J. Appl. Chem., 1962 12 266.
116. Adam,
'The Physics and Chemistry of Surfaces,' Oxford
University Press, 1941.
117. Elsevier's Encyclopaedia of Organic Chemistry,
ed. F. Radt, Vol. 12B, Elsevier Pub. Co., 1950.
118. The Chemistry and Technology of Naphthalene Compounds,
N. Donaldson, Arnold Ltd., 1958.
119. Lesser, Gad,
Ber., 1923 56 963, 971, 972.
120. Militzer,
J. Amer. Chem. Soc., 1938 60 256.
121. Fieser, Desreux,
J. Amer. Chem. Soc., 1938 60 2255, 2260.
122. B.D. Pearson, Private Communication.
123. Hodgson, Kilner,
J. Chem. Soc., 1924 807.
124. Burkhardt, Wood,
J. Chem. Soc., 1929 141, 143, 145.
125. Adams, Levine,
J. Amer. Chem. Soc., 1923 45 2373.
126. Arnold, Sprung,
J. Amer. Chem. Soc., 1938 60 1699.
127. Arnold, Sprung,
J. Amer. Chem. Soc., 1939 61 2475.
128. Contractor, Peters, Rowe,
J. Chem. Soc., 1949 1993, 1995.

